A prevalence of *Arthropterygius* (Ichthyosauria: Ophthalmosauridae) in the Late Jurassic – earliest Cretaceous of the Boreal Realm (#33148)

First submission

Editor guidance

Please submit by **4 Jan 2019** for the benefit of the authors (and your $200 publishing discount).

Structure and Criteria
Please read the 'Structure and Criteria' page for general guidance.

Author notes
Have you read the author notes on the guidance page?

Raw data check
Review the raw data. Download from the location described by the author.

Image check
Check that figures and images have not been inappropriately manipulated.

Privacy reminder: If uploading an annotated PDF, remove identifiable information to remain anonymous.

Files
Download and review all files from the materials page.

23 Figure file(s)
1 Table file(s)
1 Raw data file(s)

Structure and Criteria

Structure your review

The review form is divided into 5 sections. Please consider these when composing your review:

1. **BASIC REPORTING**
2. **EXPERIMENTAL DESIGN**
3. **VALIDITY OF THE FINDINGS**
4. General comments
5. Confidential notes to the editor

You can also annotate this PDF and upload it as part of your review

When ready submit online.

Editorial Criteria

Use these criteria points to structure your review. The full detailed editorial criteria is on your guidance page.

BASIC REPORTING

- Clear, unambiguous, professional English language used throughout.
- Intro & background to show context. Literature well referenced & relevant.
- Structure conforms to PeerJ standards, discipline norm, or improved for clarity.
- Figures are relevant, high quality, well labelled & described.
- Raw data supplied (see PeerJ policy).

EXPERIMENTAL DESIGN

- Original primary research within Scope of the journal.
- Research question well defined, relevant & meaningful. It is stated how the research fills an identified knowledge gap.
- Rigorous investigation performed to a high technical & ethical standard.
- Methods described with sufficient detail & information to replicate.

VALIDITY OF THE FINDINGS

- Impact and novelty not assessed. Negative/inconclusive results accepted. *Meaningful* replication encouraged where rationale & benefit to literature is clearly stated.
- Data is robust, statistically sound, & controlled.
- Speculation is welcome, but should be identified as such.
- Conclusions are well stated, linked to original research question & limited to supporting results.

Standout reviewing tips

The best reviewers use these techniques

Tip	*Example*
Support criticisms with evidence from the text or from other sources	*Smith et al (J of Methodology, 2005, V3, pp 123) have shown that the analysis you use in Lines 241-250 is not the most appropriate for this situation. Please explain why you used this method.*
Give specific suggestions on how to improve the manuscript	*Your introduction needs more detail. I suggest that you improve the description at lines 57- 86 to provide more justification for your study (specifically, you should expand upon the knowledge gap being filled).*
Comment on language and grammar issues	*The English language should be improved to ensure that an international audience can clearly understand your text. Some examples where the language could be improved include lines 23, 77, 121, 128 – the current phrasing makes comprehension difficult.*
Organize by importance of the issues, and number your points	*1. Your most important issue* *2. The next most important item* *3. …* *4. The least important points*
Please provide constructive criticism, and avoid personal opinions	*I thank you for providing the raw data, however your supplemental files need more descriptive metadata identifiers to be useful to future readers. Although your results are compelling, the data analysis should be improved in the following ways: AA, BB, CC*
Comment on strengths (as well as weaknesses) of the manuscript	*I commend the authors for their extensive data set, compiled over many years of detailed fieldwork. In addition, the manuscript is clearly written in professional, unambiguous language. If there is a weakness, it is in the statistical analysis (as I have noted above) which should be improved upon before Acceptance.*

A prevalence of *Arthropterygius* (Ichthyosauria: Ophthalmosauridae) in the Late Jurassic – earliest Cretaceous of the Boreal Realm

Nikolay Zverkov Corresp., ,

Corresponding Author: Nikolay Zverkov
Email address: zverkovnik@mail.ru

The ichthyosaur genus *Arthropterygius* Maxwell, 2010 has heretofore been considered as rare and poorly known, although it is among the key taxa for understanding the evolution of derived Late Jurassic and Early Cretaceous ichthyosaurs. Recently excavated unique material from the Berriassian of Franz Josef Land (Russian Extreme North) and examination of historical collections in Russian museums provided numerous specimens referable to *Arthropterygius*. New data on *Arthropterygius* combined with personal examination of ichthyosaurs *Palvennia*, *Janusaurus* and *Keilhauia* from Svalbard give us reasons to refer all these taxa to *Arthropterygius.* Therefore we recognize four valid species within the genus: *Arthropterigius chrisorum* (Russell, 1994), *A. volgensis* (Kasansky, 1903) comb. nov., *A. hoybergeti* (Druckenmiller, Hurum, Knutsen & Narkem, 2012) comb. nov*.,* and *A. lundi* (Roberts, Druckenmiller, Sætre & Hurum, 2014) comb. nov. Three of the species are present both in the Arctic and in the European Russia. This allows us to suggest that *Arthropterygius* was common and widespread in the Boreal Realm during the Late Jurassic and earliest Cretaceous. The results of our multivariate analysis of ophthalmosaurid humeral morphology indicate that at least some ophthalmosaurid genera and species, including *Arthropterygius*, could be easily recognized based solely on humeral morphology. Our phylogenetic analyses place the clade of *Arthropterygius* close to the base of Ophthalmosauria as a sister group either to ophthalmosaurines or to platypterygiines. Although its position is still uncertain, this is the most well-supported clade of ophthalmosaurids (Bremer support value of 5, Bootstrap and Jackknife values exceeding 80). This provides a further argument for the reliability of our taxonomic decision.

A prevalence of *Arthropterygius* (Ichthyosauria: Ophthalmosauridae) in the Late Jurassic – earliest Cretaceous of the Boreal Realm

Nikolay G. Zverkov[1,2,3] and Natalya E. Prilepskaya[1]

[1]Geological Faculty, Lomonosov Moscow State University, Leninskie Gory 1, Moscow 119991, Russia
[2]Geological Institute of the Russian Academy of Sciences, Pyzhevsky lane 7, Moscow 119017, Russia
[3]Borissiak Paleontological Institute of the Russian Academy of Sciences, Profsoyuznaya st., 123, Moscow 117997, Russia

Corresponding Author:
Nikolay G. Zverkov
Email address: zverkovnik@mail.ru

Abstract

The ichthyosaur genus *Arthropterygius* Maxwell, 2010 has heretofore been considered as rare and poorly known, although it is among the key taxa for understanding the evolution of derived Late Jurassic and Early Cretaceous ichthyosaurs. Recently excavated unique material from the Berriassian of Franz Josef Land (Russian Extreme North) and examination of historical collections in Russian museums provided numerous specimens referable to *Arthropterygius*. New data on *Arthropterygius* combined with personal examination of ichthyosaurs *Palvennia*, *Janusaurus* and *Keilhauia* from Svalbard give us reasons to refer all these taxa to *Arthropterygius.* Therefore we recognize four valid species within the genus: *Arthropterigius chrisorum* (Russell, 1994), *A. volgensis* (Kasansky, 1903) comb. nov., *A. hoybergeti* (Druckenmiller, Hurum, Knutsen & Narkem, 2012) comb. nov., and *A. lundi* (Roberts, Druckenmiller, Sætre & Hurum, 2014) comb. nov. Three of the species are present both in the Arctic and in the European Russia. This allows us to suggest that *Arthropterygius* was common and widespread in the Boreal Realm during the Late Jurassic and earliest Cretaceous. The results of our multivariate analysis of ophthalmosaurid humeral morphology indicate that at least some ophthalmosaurid genera and species, including *Arthropterygius*, could be easily recognized based solely on humeral morphology. Our phylogenetic analyses place the clade of *Arthropterygius* close to the base of Ophthalmosauria as a sister group either to ophthalmosaurines or to platypterygiines. Although its position is still uncertain, this is the most well-supported clade of ophthalmosaurids (Bremer support value of 5, Bootstrap and Jackknife

values exceeding 80). This provides a further argument for the reliability of our taxonomic decision.

Introduction

Ichthyosaurs were common components of marine herpetofauna in the Late Jurassic. We know this thanks to several Late Jurassic formations that yielded significant ichthyosaur materials. These are primarily Kimmeridge Clay Formation of England and France (Hulke, 1871; Mansell-Pleydell,1890; Sauvage, 1911; Delair, 1960, 1986; McGowan, 1976, 1997; Grange *et al*., 1996; Etches & Clarke, 1999; Moon & Kirton, 2016), the Solnhofen Formation of Germany (Wagner, 1852, 1853; Meyer, 1864; Bauer, 1898; Bardet & Fernández, 2000), the Vaca Muerta Formation of Argentina (Fernández, 1997, 2000, 2007a,b; Gasparini et al., 1997, 2015), the Agardhfjellet Formation of Svalbard, Norway (Angst et al., 2010; Druckenmiller *et al*., 2012; Roberts *et al*., 2014; Delsett *et al*., 2016, 2017) and a number of formations of the Volgian (Tithonian) age in European Russia (Kabanov, 1958; Efimov, 1998-1999*b*; Arkhangelsky, 1997-2001; Zverkov, Arkhangelsky & Stenshin, 2015; Zverkov *et al*., 2015; Zverkov & Efimov, in press). Still our knowledge of the Late Jurassic ichthyosaurs is non-uniform: some taxa are well known thanks to complete and well-preserved specimens (*Grendelius* McGowan, 1976; *Caypullisaurus* Fernández, 1997; *Aegirosaurus* Bardet et Fernández, 2000; *Undorosaurus* Efimov, 1999*b*), whereas others are poorly known from only a small number of largely incomplete and/or poorly preserved specimens (e.g. *Nannopterygius* Huene, 1922, *Brachypterygius* Huene, 1922 and *Arthropterygius* Maxwell, 2010). Being in the list of these puzzling ichthyosaurs, *Arthropterygius* was heretofore supposed to be known by only fragmentary remains: its type and the only hitherto identified species is represented only by the holotype, an incomplete skeleton from Arctic Canada (Maxwell, 2010). Two more fragmentary specimens were subsequently referred to as *Arthropterygius*: one from Argentina (Fernández & Maxwell, 2012) and another from the Russian North (Zverkov *et al*., 2015), however, both of them were described in open nomenclature. Thereby the genus remained poorly known that hampered detailed comparisons with other Late Jurassic taxa and affected taxonomic decisions in a number of subsequent contributions.

In recent years, the Slottsmøya Member of the Agardhfjellet Formation of Svalbard has yielded numerous marine reptile specimens including four monotypic ichthyosaur genera, for most of which only one specimen is known (Druckenmiller *et al*., 2012; Roberts *et al*., 2014; Delsett *et al*., 2017). However, most of the characters used to distinguish the new taxa from Svalbard were based on skeletal regions poorly known for other ophthalmosaurids, which combined with misinterpretations resulted in an alleged diversity and endemism of Svalbard ichthyosaurs (Roberts *et al*., 2014; Delsett *et al*., 2016, 2017). It has already been demonstrated that one of the ichthyosaur genera from Svalbard, '*Cryopterygius*', is a junior subjective synonym of *Undorosaurus* Efimov, 1999b (Zverkov & Efimov, in press). The other three genera are subjects of current revision and are all considered herein as junior subjective synonyms of *Arthropterygius.* Study of newly discovered materials from Franz-Josef Land (Russian Extreme North) combined with examination of ichthyosaurs in historical collections of several museums in Russia and in the Natural History Museum at the University of Oslo allow us substantially expand the knowledge of *Arthropterygius*.

This research continues an ongoing project of taxonomic and phylogenetic revision of the Late Jurassic ichthyosaurs of the Boreal Realm. Here we focus on ichthyosaurs of *Arthropterygius* clade (Zverkov & Efimov, in press), their taxonomy, ontogenetic, intra- and interspecific variation along with their phylogenetic relations to other ophthalmosaurids.

Materials

During the fieldwork of A.P. Karpinsky Russian Geological Research Institute (VSEGEI) in Franz Josef Land, several ichthyosaur specimens were collected from the black shales of the Hofer Formation (Upper Jurassic to lowermost Cretaceous; Kosteva, 2005; Rogov *et al*., 2016). The first specimen represented by a medial fragment of the left scapula and proximal fragment of the right humerus of a big ichthyosaur was found by S. Yudin and P. Rekant in a scree of a slope formed by Kimmeridgian and Volgian sediments at Wilczek Land (Fig. 1A). NGZ had excavated two more relatively complete specimens at Berghaus Island (Fig. 1A): one skeleton of a juvenile, near 2.5 m long, and one skeleton of a young adult *c.* 3.5 m at estimated length. Both of them are referable to *Arthropterygius chrisorum* (see descriptive part). When found, skulls and some

portions of postcranial skeleton of both CMGE 3-16/13328 and CMGE 17-44/13328 were already exposed and weathered, thereby a number of cranial elements are too fragmental for description and even more parts are missing, nevertheless, these specimens provide new data on the cranial morphology of *A. chrisorum*. The specimens were collected and prepared by NGZ, and scanned by NEP using Artec Spider 3D scanner.

Furthermore, studying the collections in museums of Russia, we found out several specimens referable to *Arthropterygius.* Four of them are from the Middle Volgian of the Volga Region (Ulyanovsk and Samara regions), the fifth, originating from the Russian North, was described earlier (Zverkov, *et al*. 2015). Two of the specimens, deposited in Vernadsky State Geological Museum (SGM, Moscow), were excavated at the beginning of the last century. One (SGM 1573) was discovered by outstanding Russian geologist and palaeontologist A.P. Pavlov and subsequently described by N.N. Bogolubov (1910) as *Ophthalmosaurus* cf. *thyreospondylus*, another specimen (SGM 1731-01–15), found in 1937 by an unknown collector, remained hitherto undescribed. A partial skeleton of a juvenile (KSU 982/P-213), described by P.A. Kasansky in 1903 as a new species, *Ichthyosaurus volgensis*, is deposited in the Museum of Geology and Mineralogy of Kazan State University (KSU). During its further studying history this specimen was referred to as *Ophthalmosaurus* Seeley, 1874, *Undorosaurus* and *Otschevia* Efimov, 1998 (Bogolubov, 1910; Arkhangelsky, 2000; Storrs *et al*., 2000; Arkhangelsky, 2008), and even considered as undiagnostic (McGowan & Motani, 2003: 134). A series of dramatic events in Russian history happened since the original descriptions of SGM 1573 and KSU 982/P-213 left a partial missing of the bones as a legacy. The vertebral column (except for several small tailfin centra) is now lost in KSU 982/P-213. Initially, the specimen excavated by A.P. Pavlov (SGM 1573) included 13 vertebrae, several neural arches, rib fragments, left coracoid, complete right scapula, interclavicle, left humerus, anterior accessory epipodial and several autopodial elements (Bogolubov, 1910). Currently, ten vertebrae, interclavicle, broken distal portion of the scapula and left humerus are deposited in SGM, the rest of originally described elements were possibly decayed or missed (I.A. Starodubtseva pers. comm.). However, the available remains are sufficient for attributing SGM 1573 to *Arthropterygius chrisorum* and ~~give an~~ additional information on the morphology of the interclavicle, which is unknown for the holotype (CMN 40608) and most of the other specimens.

Thee more specimens referable to *Arthropterygius* were found in Ulyanovsk Region in recent decades. Incomplete postcranial skeleton YKM 63548 was found by V. M. Efimov at the bank of the Volga River near Gorodischi Village and donated to YKM; an isolated humerus UPM 2442 was found by I.M. Stenshin (UPM); an isolated basisphenoid referable to as *Arthropterygius* cf. *chrisorum* from the Middle Volgian of Gorodischi locality was obtained by NGZ from an anonymous fossil dealer and donated to SGM, where it deposited now under the number SGM 1743-2.

Geological Setting

Stratigraphic position of specimens from European Russia. All *Arthropterygius* specimens from European Russia originate from black shales of the Upper Jurassic (Middle Volgian) formations: Paromes Formation of the Timan-Pechora Basin (Kravets, Mesezhnikov, Slonimsky, 1976) and Promza Formation of the Volga Region (Yakovleva, 1993; Mitta *et al*., 2012). These formations are corresponding to *Dorsoplanites panderi* Ammonite Biozone.

Stratigraphic position of specimens from Franz-Josef Land. Two ichthyosaur skeletons were found very close to each other, on the northeast slope of Berghaus Island, 150 m above sea level, in the uppermost part of a sequence of black shale and siltstone of the Hofer Formation (Kosteva, 2005). CCMGE 3-16/13328 was collected 5 m higher stratigraphically than CCMGE 17-44/13328. The layers with ichthyosaurs were filled with bivalves *Buchia unschensis*, *Buchia fischeriana* and *B.* cf. *volgensis* (identifications are made by V. A. Zakharov, GIN) characteristic of the Jurassic/Cretaceous transitional interval of the Boreal Realm (Zakharov, 1987). On the adjacent slope, at a slightly higher level, ammonites *Surites* cf. *praeanalogus* were collected, indicating *Hecteroceras kochi* Ammonite Biozone of the Ryazanian age (this and all subsequent ammonite identifications are made by M. A. Rogov, GIN); 20 m below, ammonites *Chetaites chetae,* index of the uppermost Ammonite Biozone of the Volgian of Arctic were collected; and finally, 50 m below the level of CCMGE 17-44/13328 on the same slope *Laugeites lambecki* and *Praechetaites* cf. *exoticus* were collected, indicating *Laugeites groenlandicus* Ammonite Biozone of the upper Middle Volgian (Rogov & Zakharov, 2009; Rogov *et al*., 2016). Absence of ammonite finds in the layers with ichthyosaurs do not allow to conclude with confidence

whether they are from the uppermost Volgian or whether Ryazanian part of the section; however, it is almost unambiguous that the ichthyosaurs are of early Berriassian age (for comments on Jurassic–Cretaceous Boreal–Tethyan correlation see e.g. geological setting section of our previous paper, Zverkov & Efimov, in press).

Comment on stratigraphic position of CMN 40608. In the locality, Cape Grassy, Melville Island, shale and siltstone of the Ringnes Formation are conformably overlain by soft, clay shales of the Deer Bay Formation (Embry, 1994). Elsewhere these lithologically similar formations are separated by sandstones of the Awingak Formation (Embry, 1994; Poulton, 1994). According to Embry (1994) the thickness of the Ringnes Formation in Cape Grassy is *c.* 20 m (Embry, 1994: fig. 6). Taking this into consideration, the fact that CMN 40608 was found 51 m above the base of the Ringnes Formation, withal weathered out on the surface of the outcrop and slightly scattered (Russell, 1994), indicates that CMN 40608 was actually found within the Deer Bay Formation, but not Ringnes Formation as indicated by Russell (1994). Considering that not much data is published on Late Jurassic invertebrates and biostratigraphy of Cape Grassy, it could not be said with certainty what is the stratigraphic volume of the Ringnes and Deer Bay formations in this locality. In general, the age of the Ringnes Formation is considered as Oxfordian to Kimmeridgian and the age of the Deer Bay Formation is considered as Volgian to Valanginian (Jeletzky, 1965, 1973; Embry, 1994; Poulton, 1994), thereby CMN 40608 is most likely Volgian or Ryazanian (Tithonian or Berriassian) in age.

Institutional abbreviations. CCMGE, Chernyshev's Central Museum of Geological Exploration, Saint Petersburg, Russia; CMN, Canadian Museum of Nature, Ottawa, Canada; GIN, Geological Institute of the Russian Academy of Sciences, Moscow, Russia; KSU, A.A. Shtukenberg Museum of Geology and Mineralogy of Kazan State University, Kazan, Russia; MOZ, Museo Prof. J. Olsacher, Dirección Provincial de Minería, Zapala, Argentina; PMO, Natural History Museum, University of Oslo (Palaeontological collection), Oslo, Norway; SGM, V.I. Vernadsky State Geological Museum of the Russian Academy of Sciences, Moscow, Russia; SVB, Svalbard Museum, Longyearbyen, Norway; UPM, Undory Palaeontological museum, Undory, Ulyanovsk Region, Russia; VSEGEI, A.P. Karpinsky Russian Geological Research Institute, St. Petersburg, Russia; YKM, I.A. Goncharov Ulyanovsk Regional Museum, Ulyanovsk, Russia.

Systematic Palaeontology

Ichthyosauria de Blainville, 1835

Ophthalmosauridae Baur, 1887

Arthropterygius Maxwell, 2010

2010 *Arthropterygius* Maxwell: 403

2012 *Palvennia* Druckenmiller, Hurum, Knutsen, Narkem: 326

2014 *Janusaurus* Roberts, Druckenmiller, Sætre & Hurum: 4

2017 *Keilhauia* Delsett, Roberts, Druckenmiller & Hurum: 7

2018 *Palvennia* Druckenmiller, Hurum, Knutsen, Narkem 2012; Delsett, Druckenmiller, Roberts, Hurum: 8

Type species: *Ophthalmosaurus chrisorum* Russell, 1994

Other valid species: *Arthropterygius volgensis* (Kasansky, 1903) comb. nov., *A. hoybergeti* (Druckenmiller, Hurum, Knutsen & Narkem, 2012) comb. nov., *A. lundi* (Roberts, Druckenmiller, Sætre & Hurum, 2014) comb. nov.

Emended diagnosis: Moderate to large (3-5 m) ichthyosaurs with following unique combination of features (synapomorphies are marked with '*'): relatively short and anteriorly pointed snout, strongly ventrally bowed jugal; wide supratemporal anteromedial tongue covering the postfrontal (shared with *Athabascasaurus* Druckenmiller & Maxwell, 2010); extremely anteroposteriorly shortened medial symphysis of parietals posteriorly restricted by a pronounced excavation and notch*; large parietal foramen; gracile quadrate with poorly developed 'weak' condyle*; basioccipital with extracondylar area wide in lateral view and practically unseen in posterior view; stapedial and opisthotic facets of the basioccipital shifted anteriorly and poorly visible in lateral view* (laterally exposed in other known ophthalmosaurids); basisphenoid with foramen for the internal carotid arteries opening posteriorly*; basioccipital facet of the basisphenoid

facing posterodorsally, occupying in dorsal view area equal or even larger than that of dorsal plateau*; stapes with extremely gracile shaft (shared with *Acamptonectes* Fischer *et al.*, 2012); short and robust paraoccipital process of the opisthotic; wide and extremely robust clavicles; bulge in the middle of the interclavicle posterior median stem*; large coracoids (proximodistal length of the scapula reduced in comparison to coracoid length); pronounced angle close to 90-100 degrees between the articulated coracoids*; ventral skew between the radial and ulnar facets of the humerus (ulnar facet:radial facet dorsoventral width ratio less than 0.8; as in *Sisteronia* Fischer *et al.,* 2014); three concave distal articular facets on humerus for a preaxial accessory element, radius and ulna; ulna larger than the radius in dorsal view and lacking posterior perichondral ossification (uncommon for ophthalmosaurines *sensu* Fischer *et al*., 2012); 'latipinnate' forefin architecture with two distal carpals (4 and 3) contacting the intermedium, and distal ulnare/metacarpal 5 contact (among ophthalmosaurids shared with *Ophthalmosaurus* Seeley, 1874*, Brachypterygius* Huene, 1922 and *Aegirosaurus* Bardet & Fernández, 2000); autopodial elements circular in outline and loosely arranged (shared with *Ophthalmosaurus* Seeley, 1874); plate-like ishiopubis, lacking the obturator foramen (shared with derived platypterygiines); ?ilium anteroposteriorly expanded at the dorsal end.

Occurrence: Arctic Canada, Russian Extreme North (Franz Josef Land) and the European part of Russia, Norway (Svalbard) and Argentina (Neuquen Basin). Middle to Upper Volgian–Ryazanian (Tithonian–Berriassian) (see Maxwell, 2010; Fernández & Maxwell, 2012; Druckenmiller *et al*., 2012; Roberts *et al*., 2014; Zverkov *et al*., 2015; Delsett *et al*., 2016, 2017).

Remarks: Based on the type specimen solely, the characteristic features of *Arthropterygius* are: basisphenoid with foramen for the internal carotid arteries opening posteriorly; basioccipital facet of the basisphenoid facing posterodorsally and occupying a half of the element in dorsal view; basioccipital with extracondylar area wide in lateral view and practically unseen in posterior view; shifted anteriorly stapedial and opisthotic facets of the basioccipital; presence of 'ulnar torsion', with ulnar facet not as dorsoventrally wide as the radial facet, forming a distal skew of the humeral ventral surface (Maxwell, 2010; Zverkov *et al*., 2015). All these features could be observed in the type specimens of genera that are here synonymized with *Arthropterygius*, except for cases where an element is unknown or obscured from observation: basisphenoid is mostly hidden in the holotype of *Janusaurus lundi*; humerus is incomplete in the

holotype of *Palvennia hoybergeti* and both basioccipital and humerus are absent in the holotype of *Ichthyosaurus volgensis*. Additional specimens of *Arthropterygius chrisorum* provided a number of other overlapping elements that bear diagnostic traits; these are postfrontal, jugal, quadrate, opisthotic, stapes, interclavicle, clavicle and scapula. ~~We believe that this all makes our taxonomic decisions clear and convincing.~~

Recently erected from the Berriassian of Svalbard *Keilhauia nui* is also referable to *Arthropterygius*, however, only in open nomenclature. The holotype and only known specimen of this taxon is poorly preserved skeleton of a small individual that was considered to be of 'late juvenile to adult ontogenetic stage' (Delsett *et al*., 2017: 14). Our personal observations of the holotype (PMO 222.655) allow to conclude that ~~in fact,~~ all the evidences proposed by Delsett *et al.* (2017) ~~as~~ supporting maturity of PMO 222.655 are misleading: the proximal portion of the humerus of PMO 222.655 is heavily weathered and its posterior portion is broken so that it is impossible to say something regarding its natural shape and its value for identification of maturity; the same concerns a texture of the humeral shaft, which along with other skeletal elements of PMO 222.655 is poorly preserved, weathered, and partially covered by matrix along with products of pyrite decay. It is unclear what Delsett *et al*. 2017 meant under the degree of ossification that '(when it is possible to observe) resembles mature finished bone', because all the available articular surfaces demonstrate markedly unfinished ossification: the facets of appendicular elements are poorly demarcated from each other, the ventral margin of the ischiopubis bears an excavation along its ventral margin which indicates a presence of extensive cartilaginous continuation of the element. Furthermore, a natural shape of the ischiopubis is unclear because its proximal portion is partially eroded and unnaturally compressed. PMO 222.655 is generally similar to CCMGE 3-16/13328, and it demonstrates a number of features that are diagnostic of *Arthropterygius*: the humerus of PMO 222.655 has ventral skew between the radial and ulnar facets, its ulnar facet:radial facet dorsoventral width ratio is less than 0.8; the facet for anterior accessory element is nearly as large as the radial facet (a diagnostic feature of *A, chrisorum*); the clavicle of PMO 222.655 is relatively large and robust; judging from the field photographs (J. Hurum pers. comm. Sept. 2017), the coracoid was originally longer anteroposteriorly than mediolaterally wide and extremely similar to that of CCMGE 3-16/13328, thus its current 'shape' is a result of unsuccessful conservation; the ischiopubis of PMO 222.655 is plate-like and lacks obturator foramen. What concerns the ilium of 222.655, its expanded

dorsal portion is an important character that probably demonstrates a juvenile condition of what in *A. lundi* (PMO 222.654) developed in an 'anteromedial process' and posteriorly curved end. Thus, expanded dorsal portion of the ilium could also be a generic feature of *Arthropterygius*. Taking into account all the arguments above, we consider *'Keilhauia nui'* as a *nomen dubium* and identify its type specimen as *Arthropterygius* sp. juv. cf. *A. chrisorum*.

***Arthropterygius chrisorum* (Russell, 1994)**

(Figs 2–10, 20A, B, D, S2)

v.1910 ?*Ophthalmosaurus thyreospondylus* Owen; Bogolubov: 474

*1994 *Ophthalmosaurus chrisorum* Russell: 198, fig. 3

2010 *Arthropterygius chrisorum* (Russell, 1993); Maxwell: 404, figs 2–5

v.2018 *Palvennia hoybergeti* Druckenmiller *et al.,* 2012; Delsett, Druckenmiller, Roberts, Hurum: 8, figs 5–13

Holotype: CMN 40608, fragmentary skeleton of a large mature individual (for details see Maxwell, 2010).

Referred specimens: SGM 1573, fragments of the skeleton of a large mature individual: ten vertebrae, interclavicle, broken distal part of the scapula, left humerus. CCMGE 3-16/13328, incomplete skeleton of a juvenile individual: left quadrate, partial basisphenoid, incomplete supratemporals, fragmentary parietal, and several other indeterminate cranial fragments, incomplete vertebral column (69 vertebrae from anterior dorsal to tailfin centra); rib fragments, right forefin, right scapula, coracoids. CCMGE 17-44/13328, incomplete skeleton of a young adult individual: right nasal, prefrontals, right postfrontal, fragmentary parietal, basisphenoid, left quadrate; fragments of palate bones and other indeterminate cranial remains; mandible, including articulated left surangular, angular, splenial and prearticular, isolated presacral and anterior caudal centra (31 fragment), multiple rib fragments, fragments of pectoral girdle (coracoids, scapulae, interclavicle and clavicle), incomplete right forefin, proximal part of the left humerus, left radius,

partial ischiopubis, left femur. PMO 224.250, a partially articulated and almost complete anterior half of the skeleton of a moderately large ichthyosaur (for details see Delsett *et al.,* 2018).

Emended diagnosis: ~~A~~ moderately large (4–5 m) ichthyosaur, diagnosed relative to other species of *Arthropterygius* by the following unique characters: quadrate with strongly ventrally shifted articular boss, V-shaped in posteromedial view; absence of pronounced angular protrusion of the quadrate; basisphenoid trapezoidal in outline with maximum mediolateral width in its anterior part; posterior foramen for the internal carotid arteries not visible in ventral view in adults, separated from the ventral surface by a thin shelf; dorsoventrally high opisthotic with extremely reduced and robust paraoccipital process (hitherto found only in PMO 222.669); blunt termination of the lateral extremities of the interclavicle; strongly anteroposteriorly elongated proximal end of the humerus with reduced deltopectoral crest shifted to its anterior edge; extremely pronounced ventral skew between the ulnar and radial facets of the humerus; facet for the anterior accessory epipodial element of the humerus as wide as, and equal in size to the radial facet.

Occurrence: Upper Jurassic, Deer Bay Formation (Volgian) of Melville Island, Northwest Territories, Canada (type locality); Middle Volgian Promza Formation (*Dorsoplanites panderi* Ammonite Biozone) of Ulyanovsk Region, Russia; upper part of the Hofer Formation (uppermost Volgian to lowermost Ryazanian, Berriassian) of Franz-Josef Land, Russian Extreme North; Slottsmøya Member of the Agardhfjellet Formation (Middle Volgian part of the section) of Svalbard, Norway.

Remarks: Recently referred to as *Palvennia hoybergeti* PMO 222.669 shares all diagnostic features of *A. chrisorum*, but differs from *A. hoybergeti* in extremely shortened and robust paraoccipital process of the opisthotic (relatively elongated and dorsoventrally compressed in *A. hoybergeti*; see description of *A. hoybergeti* below); reduced deltopectoral crest of the humerus shifted to its anterior edge (well pronounced, plate-like, in *A. hoybergeti*); prominent ventral skew between the ulnar and radial facets of the humerus (cannot be observed in the holotype of *A. hoybergeti*, SVB 1451, but see description and discussion sections); facet for the anterior accessory epipodial element of the humerus semicircular in outline and comparable in size to the radial facet (comparatively small and anteriorly tapered in *A. hoybergeti*; Fig. S7 in Zverkov & Prilepskaya, documents); large and rounded in outline anterior accessory epipodial element (aae of *A.*

hoybergeti SVB 1451 is relatively small, semicircular in outline, with nearly straight anterior margin).

Delsett *et al.* (2018) provided a ~~very restricted~~ comparison of PMO 222.669 and *A. chrisorum* (holotype CMN 40608). According to that comparison, PMO 222.669 differs from *A. chrisorum* in the following features: anterior face of basioccipital lacks notochordal pit and basioccipital peg (not supported by our observations because of poor preservation of this region in PMO 222.669); dorsal margin of the articular is slightly concave in medial view (unclear degree of difference; this also could be ontogenetic and interspecific variation); the anterior notch of the coracoid is longer and narrower (the actual difference of the two is minute and easily explained by ontogenetic variation; see discussion); proximodistally shorter dorsal process of the humerus (ontogenetic variation, see discussion); not as convex articular faces of epipodial elements (ontogenetic and intercpecific variation; see discussion). In fact, none of these 'differences' is sufficient to distinguish the species. From our personal observations on PMO 222.669 (NGZ) we have not found any additional differences, thereby PMO 222.669 is referred herein to as *Arthropteryguis chrisorum*.

Description

Skull

The skull of *A. chrisorum* is now well-known thanks to a new find from Svalbard (PMO 222.669; Delsett *et al*., 2018). Thereby here we provide only some additional observations on the referred specimens, with special reference to new specimens from Franz Joseph Land. For more details on cranial morphology of *A. chrisorum* see the description of PMO 222.669 in Delsett *et al*. (2018).

Nasal. ~~A~~ supranarial portion of the right nasal is preserved in CCMGE 17-44/13328 (Fig. 2C, G, H). It is too fragmentary for substantial description, however, ~~from this fragment it could be said that~~ the nasal lamella is well developed and forms a lateral 'wing' overhanging the dorsal border of the external naris (Fig. 2G, H). In PMO 222.669 both nasals are preserved in articulation. To

the description of these elements provided by Delsett *et al*. (2018), we could add that the nasal bears a pronounced lateral 'wings' over the external naris (Fig. 2L, M). The posterior portion of the nasal articulates with the postfrontal and frontal in a complex interdigitating suture, covering most of the frontal anteriorly (Fig. 2M). Posteriorly, the dorsal surface of the nasal is shallowly concave, forming an excavatio internasalis that is constricted laterally and medially by a raised areas.

Prefrontal. Although incomplete, both prefrontals are preserved in CCMGE 17-44/13328 (Fig. 2D–F). These elements are composed of a dorsal sheet and robust, anteroventrally directed strut, forming the anterodorsal margin of the orbit (Fig. 2C, K). A straight ridge along the medial edge of the dorsal sheet meets a deep groove in the lateral margin of the overlapping nasal (Fig. 2D, E). Anterior to it, there is a facet for articulation with the frontal. When articulated with other elements, prefrontal had little dorsal exposure, being covered by the anterior plate of the postfrontal posteriorly and by the nasal anteromedially. In PMO 222.669, prefrontals are practically unseen dorsally, being covered by postfrontals and nasals (Fig. 2L, M).

Parietal. Only posterolateral processes of the parietal are preserved in both CCMGE 3-16/13328 and 17-44/13328, thereby the only observation that could be made on their morphology is that the process was slender but not robust as in *Undorosaurus* and some other platypterygiines (for comments on this character see Zverkov & Efimov, in press). The parietals of PMO 222.669 are complete and articulated. In the original description (Delsett *et al.,* 2018), the skull was not completely prepared of embedded rock, so that the posteromedial excavation and notch of the parietals were not ~~seen~~. ~~In general, the~~ parietal of PMO 222.669 ~~demonstrates characteristic morphology with the~~ relatively slender posterolateral process and short but robust medial symphysis restricted posteriorly by a pronounced notch (Fig. 2L, M).

Postfrontal. The partial right postfrontal is preserved in CCMGE 17-44/13328. An extensive facet of the supratemporal anteromedial tongue occupy nearly a half of the element mediolateral width dorsally and terminates right before the expansion of the anterior plate in an interdigitating suture (Fig. 2B, L, M). This condition is similar to that of *A. hoybergeti* (SVB 1451) and *A. lundi* (see descriptions below), and among other ophthalmosaurids, it occurs only in not closely related *Athabascasaurus* (Druckenmiller & Maxwell, 2010); thus it could likely be considered as a non-unique synapomorphy of *Arthropterygius*. Delsett *et al.* (2018) described more short and gracile

'supratemporal finger' = supratemporal anteromedial tongue, however, this is due to incorrect identification of sutures (see reinterpretation on Fig. 2L, M).

Supratemporal. Medial rami of both supratemporals are preserved in CCMGE 3-16/13328. These portions are massive and quite short mediolaterally bearing triangular and excavated medial facets for articulation with the parietal (Fig. 3S–U). Ventrolaterally to this facet, there is a small depression of the facet for the paroccipital process of the opisthotic (Fig. 3S–V).

Jugal. The jugal is a slender, strongly bowed J-shaped element (Fig. 2I, J). Its posterior part is mediolaterally compressed, ascending dorsally as a slender process and forming the posterior part of the orbit (Fig. 2K). On its medial surface, the process bears facets for the postorbital and quadratojugal (Fig. 2I). The suborbital portion of the jugal is strongly bowed, ~~greater~~ than that of *Ophthalmosaurus icenicus* (Moon & Kirton, 2016) but in similar degree to those of *Arthropterygius hoybergeti* and *A. lundi*.

Quadrate. The quadrate is known for both CCMGE 3-16/13328 and 17-44/13328 (strongly compressed). It is a relatively gracile ear-shaped element. The posterodorsal part of the occipital lamella is broken in both CCMGE specimens so it is hard to say anything regarding its natural shape. Thanks to its complete preservation in PMO 222.669, we know that the occipital lamella is well developed. A shallow notch of the quadrate foramen restricts the posterolateral edge of the quadrate. The anterior edge of the pterygoid lamella is convex (Fig. 3J, K, O, Q). There is no marked angular protrusion ('antero-internal angle' of Andrews, 1910) on the quadrate. The articular condyle is weak and mediolaterally compressed. Its ventral surface is divided by the smooth groove into two bosses: large ventrally protruding medial boss for the articulation with the articular and reduced anteriorly shifted lateral boss for the articulation with the surangular (Fig. 3L–N). The ventral edge of the articular boss is somewhat V-shaped (Fig. 3J). Above the condyle, there is a pronounced circular depression – a facet for the quadratojugal (Fig. 3L, O, P). The stapedial facet, situated in the middle of the medial surface of the quadrate, is circular in outline (Fig. 3J, O).

Basioccipital. The basioccipital is hitherto known for the holotype, CMN 40608, and for PMO 222.669. Although it was already described, we feel it necessary to add some remarks to the original description of Maxwell (2010). The extracondylar area is extremely reduced and

completely unseen in posterior view, as in *A. hoybergeti* and *A. lundi* (Druckenmiller *et al*., 2012; Roberts *et al*., 2014). However, it is relatively anteroposteriorly wide in lateral view, unlike that of *Grendelius* spp. (McGowan, 1976; Zverkov, Arkhangelsky & Stenshin, 2015). Maxwell (2010) has misinterpreted a part of the extracondylar area as a stapedial facet, probably due to poor preservation of CMN 40608. The true stapedial facet faces anteriorly and is practically unseen in lateral view. An anterior protrusion of the basioccipital under the floor of the foramen magnum interpreted by Maxwell (2010) as an 'incipient basioccipital peg', is also present in *A. hoybergeti* and *A. lundi* (NGZ pers. obs.) and was reported for some other ophthalmosaurids (e.g. Moon & Kirton 2016). Although this structure is a vestige of a basioccipital peg, the condition observed in *Arthropterygius* could not be considered as a plesiomorphic state (i. e. the presence of a basioccipital peg), as was supposed and coded in some previous works (e.g. Fischer *et al*., 2011, 2012). In PMO 222.669 the anterior surface of the basioccipital is too badly preserved for any observations.

Basisphenoid. The basisphenoid is the most peculiar element in basicranium of *Arthropterygius* due to an uncommon position of the posterior opening for the internal carotid arteries, which pierce the basisphenoid at its posterior edge (in most ophthalmosaurids this foramen situated close to the middle of the ventral surface). The ventral surface of the basisphenoid is trapezoid in outline (Fig. 3A, E). It is longer anteroposteriorly than mediolaterally wide, having the width to length ratio of 1.33 (see Tab. S5 in Zverkov & Prilepskaya, documents). The mediolateral width of the anterior part is greater than the width of the posterior part. The basipterygoid processes are relatively reduced in comparison to *Undorosaurus*, *Grendelius* and most of platypterygiines (see Zverkov & Efimov, in press). The lateral facet of the basipterygoid processes is elongated-oval, lenticular in outline (Fig. 3D, G). The dorsal surface of the basisphenoid is divided into two surfaces – square posterodorsally faced basioccipital facet and pentagonal dorsally faced dorsal plateau (Fig. 3B, F). A median groove bisects the dorsal surface over the entire length. The high anterior wall is vertical, slightly curving posterodorsally on its lateral sides, lining the cranioquadrate passage. It raises the dorsum sellae in the middle, which is ventrally bounded by the funnel-like anterior foramen for the internal carotid arteries (Fig. 3C, H). Laterally the dorsum sellae is bounded by the ridges (crista trabeculares), which ventrally form the surfaces for their cartilaginous continuation; these surfaces are poorly pronounced in all specimens referred to *A. chrisorum* (Fig. 3C, H). Lateral to the crista trabeculares deep pits for attachment

of the ocular musculature (likely retractor bulbi group) are situated. The posterior foramen for the internal carotid arteries opens posteroventrally in juvenile specimen CCMGE 3-16/13328, and posteriorly in mature individuals CCMGE 17-44/13328 and CMN 40608.

Opisthotic and stapes. The opisthotic and stapes are known only for PMO 222.669 (Fig. 4). Compared to other species of *Arthropterygius*, in *A. chrisorum* opisthotic is markedly higher dorsoventrally, and has more short and robust paraoccipital process (Fig. 4A, B). The medial head of the stapes is more massive than in *A. hoybergeti* and *A. lundi* and the lateral extremity of the stapedial process is more straight and somewhat dorsoventrally compressed (Fig. 4D, E, F): in other species, it is dorsoventrally expanded.

Mandible. In general, the mandible was well characterized for PMO 222.669 by Delsett *et al.* (2018). ~~From other specimens, it~~ is well ~~enough~~ preserved only in CCMGE 17-44/13328, however, lacking anterior and posterior portions, including the whole dentary and articular. Judging from its general proportions, ~~it could be concluded that~~ the whole jaw of CCMGE 17-44/13328 was relatively short anteroposteriorly (*c.* 65-70 cm at an estimated length).

Splenial. The splenial is an elongated and strongly mediolaterally compressed bone that covers most of the medial surface of the mandible (Fig. 5B, C).The dorsal ramus of the anterior forked part of the splenial is preserved, its medial surface is rugose forming a contribution to the mandibular symphysis. The ramus is thickened while the rest of the bone is a thin sheet that is slightly S-shape curved forming a medial wall of the Meckelian canal. The medial surface of the bone is pierced by a series of small foramina (Fig. 5B, C).

Surangular. The surangular of CCMGE 17-44/13328 is broken at its anterior and posterior ends. It is an elongate plate-like element, thickened along the dorsal margin; the medial and lateral surfaces of the surangular bear longitudinal grooves. The medial concavity comprises the lateral wall of the Meckelian canal. The lateral groove, fossa surangularis, runs along the lateral surface of the surangular. Posteriorly, before the paracoronoid eminence, it is pierced by an oval surangular foramen. The paracoronoid process is well pronounced and somewhat tapered, posterior to it, the lateral margin of the surangular forms a pronounced dorsally directed ridge, which probably functioned as attachment point of the *Musculus adductor mandibulae externus* (according to Moon

& Kirton, 2016) (Fig. 5C). The surfaces of both these processes are rugose for attachment of jaw muscles.

Angular. The angular forms most of the ventral margin of the mandible. Its dorsal surface bears ~~a~~ floor of the Meckelian canal and several longitudinal grooves for articulation with other jaw elements. The more laterally situated groove is for the surangular. In lateral view, the angular forms a high sheet that covers the surangular and composes more than a half of the dorsoventral height at the posterior end of the mandible (Fig. 5A). The medial exposure of the angular is not as high. Medial to the ventral floor of the Meckelian canal a thin furrow for the articulation with the prearticular is placed.

Prearticular. The prearticular is an extremely thin sheet of a bone that form the medial wall of the Meckelian canal at its posterior part. Only a small portion of this element is preserved, so little can be said regarding its morphology.

Axial skeleton. A continuous series of 69 vertebral centra is preserved in CCMGE 3-16/13328, only a few fragmentary, severely deformed and weathered vertebrae are collected for CCMGE 3-16/13328, and ten vertebrae including atlas-axis complex are available for SGM 1573. This provides additional information to that published by Maxwell for the holotype (Maxwell, 2010).

The atlas-axis complex preserved in SGM 1573 is very similar to that of the holotype, however, diapophyses and parapophyses are relatively more protruding (Fig. 6A, C)**.** The vertebrae of *Arthropterygius chrisorum*~~, in general,~~ are similar to those of *Ophthalmosaurus icenicus* (see Moon & Kirton, 2016). The middle and posterior dorsal vertebrae of the large mature specimen, SGM 1573, are characterized by strongly protruding diapophyses and parapophyses (Fig. 6F–I), whereas in juvenile CCMGE 3-16/13328 these apophyses are less well pronounced (Fig. 6L–S). ~~A~~ continuous vertebral series of CCMGE 3-16/13328 allows making some observations on vertebral count (Fig. S2 in Zverkov & Prilepskaya, documents). As anteriormost presacral centra are missing it is hard to ~~say~~ about the number of presacral vertebrae. Only thirteen anterior presacral vertebrae, in which diapophyses are fused with neural arch facets, are present in CCMGE 3-16/13328. A count of posterior presacral vertebrae is 17. Six anteriormost caudal vertebrae bear characteristic 8-shaped synapophyses that commonly mark ~~a~~ ‘sacral’ region (Fig. 6W). The rest preflexural caudal centra bear typical oval to circular rib facets (Fig. 6Y, A’). The

shape of articular surfaces in caudal vertebrae is circular with the height slightly exceeding width in some anteriormost caudal vertebrae (Figs 6V, X; S2 in Zverkov & Prilepskaya, documents); in posterior caudal vertebrae, width markedly exceeds the~~ir~~ height (Figs 6Z; S2 in Zverkov & Prilepskaya, documents). Several fluke centra preserved in CCMGE 3-16/13328 have circular articular surfaces with nearly equal width and length.

Both mature SGM 1573 and juvenile CCMGE 3-16/13328 individuals do not ~~demonstrate~~ such a high degree of regionalization in posterior dorsal to anterior caudal centra, which was observed by Maxwell (2010). It is possible that this condition is quite variable both in ontogeny and intraspecifically, thereby it is hard to assess its potential taxonomic ~~value to the moment~~.

Numerous rib fragments were collected for CCMGE 17-44/13328. The longest but incomplete rib is near 70 cm in preserved lengths. The ribs are from T-shaped to 8-shaped in cross-section in ~~a~~ proximal part of their length and ~~becoming~~ circular in cross-section distally.

Appendicular skeleton

Scapula. The left scapula is completely preserved in CCMGE 17-44/13328 (Fig. 7J–M). The element is robust: its proximodistal length is shorter than coracoid anteroposterior length. It is similar to that of *Ophthalmosaurus* icenicus in general morphology (Seeley, 1984; Andrews, 1910; Moon & Kirton, 2016). The scapular shaft is mediolaterally flattened and elongated-oval in cross-section. The glenoid contribution is well developed and equal in length to the coracoid facet. The acromial process is massive and well-prominent; it curves ventrolaterally, forming a nearly right angle with the lateral surface of the scapula (Fig. 7N).

Coracoid. The coracoid is slightly longer anteroposteriorly than wide mediolaterally (Fig. 7P). It is similar to that of *Ophthalmosaurus icenicus* and *Undorosaurus gorodischensis* (Andrews, 1910; Moon & Kirton, 2016; Zverkov & Efimov, in press), but differs in relative size, being anteroposteriorly longer than scapular proximodistal length. The medial symphysis is lenticular in outline; it occupies anterior two-thirds of the medial surface. The anteromedial process is prominent, laterally limited by an extensive anterior notch (anterior notch is relatively smaller in CCMGE 3-16/13328 than in the holotype, most likely as a reason of immaturity). The posterior portion of the coracoid is strongly compressed and convex posteriorly (Fig. 7P). The most interesting trait is that articulated coracoids form a pronounced angle of 100 degrees (Fig. 7O);

this condition is unique for *Arthropterigius.* The scapular facet and glenoid contribution are offset by an angle of *c.* 140 degrees. Their surfaces are slightly convex and tuberous. The glenoid contribution surface is parallel to the medial symphysis of the coracoid, thus coracoid mediolateral length is constant, unlike caudally constricting coracoids of *Sveltonectes* (Fischer *et al.,* 2011), *Nannopterygius* (Hulke, 1871; Kirton, 1983) and '*Paraophthalmosaurus*' (Arkhangelsky 1997; Efimov 1999a) and caudally expanding coracoids of *Undorosaurus* (Efimov 1999b).

Clavicle. The clavicle (Fig. 7X–Z) is a large and robust element. It is very similar to that of *A. lundi*, being dorsoventrally high and anteroposteriorly thick, compared to other known ophthalmosaurids. On its medial surface, there is a rugose circular facet for articulation with the acromial process of the scapula (Fig. 7Y). This facet is pronounced, but not as well developed as in *A. lundi* (see below).

Interclavicle. The interclavicle of SGM 1573 is a large and slender T-shaped element. The anterior transverse bar of the interclavicle is straight, with a high dorsally rising wall; its lateral extremities extend far laterally, and their ends are rounded (Fig. 7C', D'). There is no ventral knob observed in *Undorosaurus gorodischensis* and *Grendelius alekseevi* (Zverkov, Arkhangelsky & Stenshin, 2015; Zverkov & Efimov, in press). The posterior median stem is slender and bears a shallow trough along its dorsal surface. There is a prominent bulge in the middle of the ventral surface of the stem (Fig. 7C', D'). In PMO 222.669 a displaced portion of the clavicle was erroneously interpreted as a wide interclavicle posterior median stem (Delsett *et al.* 2018). In fact, the interclavicle of PMO 222.669 is heavily distorted and broken into several disarticulated pieces due to a collapsing of pectoral girdle during the taphonomic process, but judging from the preserved fragments, its posterior median stem was quite slender.

Humerus. The humerus is a large and robust bone with wide and dorsoventrally compressed midshaft. The humeral 'torsion' (angle between the long axes of the proximal and distal ends of the humerus) is *c*. 70 degrees. The dorsal process is prominent and plate-like, extending up to the half of the humeral midshaft (Fig. 7C, F, S). The deltopectoral crest is poorly developed and shifted to the anterior border of the humerus (Fig. 7A, E, G, I, T, W). The proximal end is semi-rectangular in outline, being anteroposteriorly longer than dorsoventrally thick (Fig. 7E, I, W). There are three distal concave facets for the preaxial accessory element, radius and ulna. The facet for the preaxial accessory element is large and semicircular in outline; it occupies nearly

equal space as the radial facet. The radial facet is irregularly pentagonal in outline; its ventral edge is angular, forming in posterior half an abrupt skew to the ulnar facet (Fig. 7D, H, V). A ratio of the dorsoventral width of the radial facet to ulnar facet is 0.7–0.78 (see Tab. S1 in Zverkov & Prilepskaya, documents).

Epipodial elements. The articular surfaces of the epipodial elements are convex for a peg-and-socket articulation with concave distal humeral facets; however, this condition varies even in mature specimens from extremely deep in CMN 40608 to more shallow in SGM 1573. The anterior accessory epipodial element is circular in dorsal view; its anterior edge lacks perichondral ossification as in *Ophthalmosaurus icenicus* (Andrews, 1910; Moon & Kirton, 2016). This element rapidly tapers anteriorly. The radius is pentagonal in dorsal and ventral views (Fig. 6A, F). The ulna is the largest element in the epipodial row, its dorsal and ventral cortical parts are roughly hexagonal in outline. The element gradually constricts in dorsoventral width posteriorly. A perichondral ossification of the posterior edge of the ulna is absent (Fig. 6A). The intermedium wedges between the radius and ulna, but not reach the humerus, however, a distance between the humerus and intermedium varies from relatively short in CCMGE 3-16/13328 and CMN 40608 to relatively long in CCMGE 17-44/13328. Distally intermedium bears two slightly demarcated facets for distal carpals three and four, indicating a 'latipinnate' forefin architecture. A statement of Maxwell that 'the distal edge of the intermedium forms a surface for the articulation of a single distal carpal in the forefin of *Arthropterygius chrisorum*' (Maxwell, 2010: 411) is likely a misinterpretation. Maxwell described the distal margin of the intermedium of CMN 40608 as 'gently curved'(Maxwell, 2010: 410), so there are more likely two poorly demarcated facets for distal carpals three and four rather than a single convex 'facet'. This becomes clear when other specimens with better-demarcated facets are considered (CCMGE 3-16/13328, CCMGE 17-44/13328, PMO 222.669).

Distal limb elements. All the mesopodial and autopodial elements are strongly dorsoventrally thickened, circular in outline and loosely packed, indicating a large amount of cartilage in forefin, which is most similar to the condition observed in *Ophthalmosaurus icenicus* (Andrews, 1910; Moon & Kirton, 2016). One of the elements in CCMGE 17-44/13328 has a semicircular outline in dorsal view and bears a perichondral ossification along one of its edges, this probably

represents a pisiform (Fig. 6A). The pisiform of exact same morphology is present in the left limb of PMO 222.669 (NGZ pers. obs.).

Pelvic girdle. The only central portion of the ischiopubis has been collected for CCMGE 17-44/13328, which complicates the description of the element. The ischiopubis is plate-like, mediolaterally compressed (8 mm at its thickest part). The obturator foramen is likely absent (Fig. 8G).

Femur. The femur of CCMGE 17-44/13328 is slender with proximal and distal ends only slightly expanded (Fig. 8A). Its proximodistal length comprises 0.74 of the humeral proximodistal length (0.67 in the holotype CMN 40608). The femur of CCMGE 17-44/13328 is very similar to that of the holotype, possessing flattened ventral process terminating proximal to the mid-point, and thereby being more prominent than that of *A. lundi* (Roberts *et al*., 2014). The dorsal process is less pronounced than the ventral process and shifted to the anterior edge of the femur. There are two distal facets, which are concave and poorly demarcated, forming a common distal groove for the epipodial elements (Fig. 8D). The fibular facet is slightly inclined posterodistally, whereas the tibial facet faces nearly distally.

Measurements: See Tables S1 and S2 in Zverkov & Prilepskaya, documents.

Ontogenetic changes and variation in Arthropterygius chrisorum

Thanks to new specimens of juveniles and young adults, we can now make some observations on the ontogenetic changes of *Arthropterygius chrisorum*.

In general, changes in morphological proportions during growth of *A. chrisorum* are consistent with those observed in other ichthyosaurs (Huene, 1922; McGowan, 1973b; Deeming *et al*., 1993). Having largely incomplete specimens (Fig. 9) we are unable to assess the growth of the whole skull and the whole body, thereby we compared selected cranial and postcranial elements (Fig. 10). The growth of elements of the skull base and occiput of *A. chrisorum* is more or less isometric compared to each other. The same concerns the growth of elements of the appendicular skeleton (Fig. 10A). At the same time, the growth rates differ between the skeletal regions.

Relative anteroposterior length of the basisphenoid and the humerus is among the few ratios that could be calculated for *A. chrisorum* in order to compare the growth of the cranial and postcranial

skeleton. In juvenile CCMGE 3-16/13328 this ratio is 0.58, in young adult CCMG E 17-44/13328 – 0.42, and in mature individual CMN 40608 – 0.35; thus we observe typical negative allometry. It is not surprising that the growth of the cranial elements is negatively allometric relative to the growth of the appendicular elements. Interesting is that growth of the appendicular skeleton is positively allometric relative to that of the axial skeleton (Fig. 10A), whereas for *Ichthyosaurus* and *Stenopterygius* this reported as being isometric (McGowan, 1973b).

Judging from the available cranial elements, the general morphology and proportions of the occipital region have not undergone sufficient changes with age. Despite differences in size CCMGE 3-16/13328, CCMGE 17-44/13328 and PMO 222,669 have a characteristic shape of the quadrate condyle: it is dorsoventrally high with a V-shaped ventral margin of the articular boss. Furthermore, the quadrate do not develop the anterior protrusion with age. In all specimens of *Arthropterygius chrisorum,* the basisphenoid is trapezoidal in ventral outline, being mediolaterally wider anteriorly than posteriorly. The juvenile CCMGE 3-16/13328 has a narrower anterior profile when compared to those of adults CCMGE 17-44/13328, PMO 222,669 and CMN 40608 (Fig. 10B, C, D, E), supporting observations of Kear & Zammit (2014) on *Platypterygius australis*. The only marked difference of the basisphenoids is the relative position of the posterior foramen for the internal carotid arteries, which is still exposed ventrally in juvenile CCMGE 3-16/13328, but already separated by a grown shelf in young adults PMO 222,669 and CCMGE 17-44/13328 (Fig. 10B, C, D).

The coracoids of juvenile CCMGE3-16/13328 are more rounded in outline compared to those of adults (Fig. 10W, X, Y). This is primarily due to less developed anteromedial process and not yet developed posterior protrusion. It is interesting that there are no marked differences in humeral morphology between the juvenile and adults. The marked change is the angle between the radial facet and facet for the anterior accessory epipodial element that became less pronounced with age (Fig. 10M–Q). The absence of marked ontogenetic changes in relative size and shape of the humeral distal facets supports their diagnostic value; thereby the features related to humeral distal facets can be used to diagnose species of *Artropterygius* irrespective of osteological maturity.

All the specimens of *Arthropterygius chrisorum* have concave humeral distal facets and convex proximal articular facets of the epipodial element. A tendency for deepening of humeral distal facets with age could be observed, however, it is non-uniform. Although the old adult CMN 40608

has very deeply concave facets (Maxwell, 2010), comparable in size SGM 1502 has less concave facets and consequently should have had less convex proximal surfaces of the epipodial elements. Considering this variation and the fact that after the publication of Maxwell (2010) humerus-epipodial peg-and-socket articulation was reported for other ophthalmosaurids (Zverkov *et al.,* 2015), we have to assume that 'proximal surface of zeugopodial elements angular in outline for articulation with humerus' (Maxwell, 2010: 404) cannot be further considered as a diagnostic character of *Arthropterygius*.

Arthropterygius hoybergeti (Druckenmiller, Hurum, Knutsen & Narkem, 2012) comb. nov.

(Figs 11–14)

v*2012 *Palvennia hoybergeti* Druckenmiller, Hurum, Knutsen & Narkem: 326, figs 12–21

Holotype: SVB 1451, a nearly complete skull, atlas/axis complex and fragmentary vertebra, right clavicle, fragments of left and right scapulae, proximal and distal portions of a humerus, limb elements and several disarticulated dorsal ribs.

Referred specimens: YKM 63548, a slab containing a series of 19 presacral vertebrae with articulated neural arches and ribs, right humerus, a cast of the left humerus with associated radius, ulna and intermedium (original forelimb was lost because of pyrite decay); UPM 2442, left humerus.

Emended diagnosis. A moderately large ophthalmosaurid (up to 4 meters) distinguished from other species of *Arthropterygius* by the following unique character combination: basisphenoid longer anteroposteriorly than mediolaterally wide, with the widest part in the region of basipterygoid processes; posterior foramen for internal carotid arteries opening on the posteroventral edge of the basisphenoid and forming a notch as in *A. lundi* and unlike *A. chrisorum*; small basioccipital facet of the opisthotic (large in other known species of *Arthropterygius*); relatively large teeth with circular in cross-section roots and robust ridged crowns as in *A. chrisorum* but unlike gracile subtly ridged crowns of *A. lundi*; slightly anteroposteriorly elongated proximal end of the humerus (as in *A. chrisorum* and *Undorosaurus gorodischensis*); well developed plate-like trochanter dorsalis and deltopectoral crest (unlike in

other species of *Arthropterygius*); anterodistal facet for the anterior accessory epipodial element sufficiently smaller than the radial facet, being thus relatively smaller than that in *A. lundi* and *A. chrisorum*, ventral skew between the radial and ulnar facets is nearly absent, however, the ulnar facet is nonetheless markedly shorter dorsoventrally than the radial facet.

Occurrence: *Arthropterygius hoybergeti* is known from the Slottsmøya Member of the Agardhfjellet Formation of Svalbard (type locality), where it was found most likely within the *Dorsoplanites ilovaiskii* Ammonite Biozone (lower Middle Volgian). Two specimens from the Volga Region (both found on the right bank of the Volga River near Gorodischi Village, Ulyanovsk Region) referred here to as *A. hoybergeti* are corresponding to *Dorsoplanites panderi* Ammonite Biozone of Promza Formation.

Description

Here we provide some new observations on the holotype SVB 1451, which had been described in detail by Druckenmiller *et al*. (2012); thereby we discuss only some misinterpretations of Druckenmiller *et al*. (2012) and provide some additional information, not reported before.

Nasal. The nasal of SVB 1451 bears a well-pronounced lamella, a 'wing', overhanging the dorsal border of the naris.

Parietal. The parietal has a very short but robust medial symphysis and well-pronounced notch posterior to it (Fig. 11A). The element posseses a relatively elongated and slender supratemporal process (Fig. 11A).

Squamosal. Although reported as absent, the squamosal of SVB 1451 (Fig. 11B) was mentioned by Druckenmiller *et al*. (2012) as a "small rib-like element" of unclear identity, and even figured (Druckenmiller *et al*., 2012: 327, fig. 16E, F).

Quadrate. Both quadrates of SVB 1451 are preserved, but only partially exposed, so that dorsal portion of the right quadrate and ventral portion of the left quadrate are available for observations. The occipital lamella of the quadrate is extremely well developed (Fig. 12O). The articular condyle is relatively weak; the articular boss is larger than the surangular boss and protrudes ventrally. There is a pronounced angular protrusion of the quadrate (absent in *A. chrisorum*).

Basisphenoid. The basisphenoid of SVB 1451 could be observed in ventral and dorsal views (Figs 11A; 12B). It is longer anteroposteriorly than mediolaterally wide. The widest part is the region of basipterygoid processes that are directed anterolaterally. A posterior foramen for the internal carotid arteries opens on the posteroventral edge of the basisphenoid and forms a notch as in *A. lundi* and unlike *A. chrisorum* (Fig. 12B).

Opisthotic. The opisthotic was not described for SVB 1451 by Druckenmiller *et al*. (2012), neither by Delsett *et al.* (2018), however, both opisthotics are well-preserved. The paraoccipital process of the opisthotic is short and robust, which is a common condition for ophthalmosaurids except for *Ophthalmosaurus* and *Acamptonectes* (Fischer *et al*., 2012). The facet for the supratemporal is oval in outline, being dorsoventrally compressed (Fig. 12I). The lateral muscular ridge is well developed (Fig. 12D, I). The stapedial facet is somewhat triangular in outline and bisected by a straight mediolateral canal for either VII or for IX nerve, as was interpreted by Kirton (1983) (see also Kear, 2005; Moon & Kirton, 2016). The facet for the basioccipital is relatively small and quadrant in outline with convex margin directed dorsolaterally, it is sufficiently smaller than the stapedial facet (Fig. 12C). The impression of semicircular canals of the otic capsule is V-shaped (Fig. 12G, H). Both impressions of the horizontal semicircular canal and posterior vertical semicircular canal are nearly equal in length, unlike in *Undorosaurus gorodischensis* and *Acamptonectes densus*, in which horizontal semicircular canal impression is markedly longer (Fischer *et al*., 2012; Zverkov & Efimov, in press). The impression housing the posterior ampulla, utriculus and the sacculus is expanded (Fig. 12G).

Exoccipital. Both exoccipitals are preserved in SVB 1451, however, right element was misidentified as left and figured upside down in the original description (Druckenmiller *et al*., 2012). The statement that ‘there is no evidence of any foramina for cranial nerves perforating the element’ (Druckenmiller *et al*., 2012: 331) is not correct and resulted from the state of preservation, as was also suggested by Delsett *et al.* (2018: 23). At least one hypoglossal foramen could be seen on the lateral side of the left exoccipital, although, indeed, columnar morphology with the reduced base of the occipital foot make the reduction of a number of hypoglossal foramina expected.

Stapes. Although the left stapes of SVB 1451 is still in situ, mostly covered by other elements (Fig. 11A), the isolated right stapes was misidentified as left and figured upside down in the original description (Druckenmiller *et al*., 2012; fig. 19). This misinterpretation has already been corrected by Delsett *et al.* (2018). The hyoid process of the stapes is relatively well developed and helps for correct spatial orientation of the element (Fig. 12L). The basisphenoid and basioccipital facets are clearly demarcated; dorsal to them there is an extensive facet for the opisthotic (Fig. 12J). Given that the stapedial facet of the basioccipital is directed anteriorly, and that there is some extent of stapedial curvature, the stapes, when articulated, was strongly rotated anteroventrally (Fig. 12A). This condition is very unusual for ophthalmosaurids but probably was typical for ichthyosaurs of *Arthropterygius* clade, as all of them have anteriorly directed stapedial facet of the basioccipital. The configuration of the articulated occipital region of *A. hoybergeti* was strongly protruding posteriorly, somewhat 'vaulted', which is probably a result of a strong reduction of the postorbital region.

Articular. The articular of SVB 1451 was recently described by Delsett *et al.* (2018: 8). It is roughly trapezoid in outline, only slightly longer anteroposteriorly than dorsoventrally high (Fig. S4 in Zverkov & Prilepskaya, documents). It is very similar to that of *A. chrisorum* (Maxwell 2010).

Dentition. The teeth of *A. hoybergeti* are relatively large. The crowns are robust, conical, ranging from straight to slightly recurved. The enamel ornamentation is composed of numerous tightly packed ridges, which are semicircular in cross-section (Fig. 13A). The ridges seem to extend to the apex of the crown and arranged around its entire circumference. The apicobasal length of the largest crown is *c*. 14 mm in apicobasal length and 9 mm in diameter at the base.

Vertebral column. There is no line of fusion of atlas and axis contra Druckenmiller *et al*. (2012: 334). An incomplete anterior presacral ('cervical') centrum is preserved and has characteristic oval outline slightly tapering ventrally (Fig. S05).

Clavicle. The right clavicle is nearly complete but badly preserved (11A), it is very robust and similar to those of *A. chrisorum* and *A. lundi*, thus typical of the genus.

Scapula. The preserved scapular dorsal rami are slightly curved and mediolaterally compressed having an oval cross-section of the shaft (Fig. 14B, C).

Humerus. A number of fragments of the right humerus are preserved (however, some of these fragments could belong to the left humerus). Most important are proximal and distal portions. The shape of the preserved proximal portion of the right humerus indicates that it was anteroposteriorly elongate and has a pronounced plate-like deltopectoral crest (Fig. 14D, E). The anterodistal fragment of the humerus demonstrates that it was dorsoventrally thick distally. A facet for the anterior accessory element is relatively small and triangular in outline (Fig. 14F; S7A in Zverkov & Prilepskaya, documents). Complete humeri of referred specimens allow to depict all the details of humeral morphology: in addition to plate-like deltopectoral crest, there was well-developed and plate-like dorsal process (Fig. 14H, I, K–M, Q). The radial facet is the thickest part of the distal humerus, which gradually flattens posteriorly to more elongated ulnar facet (Fig. 14J, N). There is no marked ventral skew between the radial and ulnar facets compared to that in *A. chrisorum* and *A. lundi*, however, the decrease in thickness between the radial and ulnar facets is apparent (Fig. 14J).

Epipodial and autopodial elements. Several epipodial and autopodial elements are preserved in SVB 1451, including the complete anterior accessory epipodial element, radius and intermedium as well as fragmental ulna (Fig. 14F). While not included in the original description (Druckenmiller *et al*., 2012), the elements were recently mentioned and figured by Delsett *et al*. (2018), however, with some misidentifications (anterior accessory epipodial element was misidentified as a pisiform; distal carpal 3 is identified with no grounds, whereas an element identified as the radiale herein was considered to be a metacarpal). YKM 63548 has articulated radius, ulna and intermedium (Fig. 14Q). The anterior accessory epipodial element present in SVB 1451 is semicircular in dorsal view, it strongly tapers along the anterior margin, which is nearly straight, but still not involved in perichondral ossification (Fig. 14F). The radius is typically pentagonal in dorsal view and has a strongly convex proximal articular surface. The ulna is somewhat hexagonal, it lacks perichondral ossification along the posterior edge; distally it bears three nearly equal facets for the intermedium, ulnare and the pisiform (Fig. 14Q). The intermedium is somewhat diamond-shaped in dorsal view, wedging between the radius and ulna and bearing two distal facets, evidently for distal carpals three and four (Fig. 14F, Q). The autopodial elements are circular in outline and were loosely arranged in the limb as in *Ophthalmosaurus icenicus* (see Moon & Kirton, 2016) and other species of *Arthropterygius*.

Remarks

We suppose that the fact that Delsett *et al*. (2018) referred *Arthropterygius chrisorum* PMO 222.669 to as *Palvennia hoybergeti* leaves no questions regarding why we identify '*Palvennia*' *hoybergeti* as a species within *Arthropterygius.* Indeed, both *A. chrisorum* and *A. hoybergeti* have very similar, although not identical, cranial anatomy and the main differences of the two species are related to the morphology and proportions of their appendicular skeleton. The following diagnostic features of the genus *Arthropterygius* present in the holotype of *Palvennia hoybergeti* (SVB 1451): (1) strongly ventrally bowed jugal; (2) wide supratemporal anteromedial tongue covering the postfrontal; (3) relatively gracile quadrate with a 'weak' condyle; (4) extracondylar area of the basioccipital wide in lateral view and practically unseen in posterior view; (5) stapedial and opisthotic facets of the basioccipital shifted anteriorly and poorly visible in lateral view; (6) basisphenoid with foramen for the internal carotid arteries opening posteriorly; (7) basioccipital facet of the basisphenoid facing posterodorsally, occupying in dorsal view area equal or even larger than that of dorsal plateau; (8) wide and extremely robust clavicles.

The specimens referred herein to as *A. hoybergeti* lack cranial remains, whereas the holotype lacks most of the postcranium resulting in poor overlap between these specimens. This could call into question our decision to refer UPM 2442 and YKM 63548 to *A. hoybergeti*, however, we suggest that this is a reasonable assumption. Despite the minute difference in size, the humeri of UPM 2442 and YKM 63548 are very similar one to another and bear diagnostic features of *Arthrthropterygius*: three concave distal articular facets for the preaxial accessory element, radius, and ulna; ulnar facet: radial facet dorsoventral width ratio *c.* 0.8; dorsoventrally compressed posterior edge of the humerus. Furthermore, YKM 63548 preserves epipodial elements and intermedium that are greatly consistent with those of other *Arthropterygius* species: ulna is larger than radius and lacks the posterior perichondral ossification; intermedium bears two nearly equal distal facets. At the same time, these humeri are distinct from humeri of *A. chrisorum* and *A. lundi* in absence of pronounced ventral skew between the radial and ulnar facet and in relatively small size of the facet for the anterior accessory epipodial element. Thus, UPM 2442 and YKM 63548 belong to *Arthropterygius*, but represent a species different from *A. chrisorum* and *A. lundi*. Although the humerus of *A. hoybergeti* is fragmented it also

~~demonstrates~~ relatively small facet for anterior accessory epipodial element and well developed plate-like deltopectoral crest, ~~not characteristic for~~ other species of *Arthropterygiu*s except ~~for a 'species' represented by~~ UPM 2442 and YKM 63548, hence ~~our decision to~~ consider UPM 2442 and YKM 63548 as belonging to *A. hoybergeti.*

Measurements. See Druckenmiller *et al*. (2012).

***Arthropterygius lundi* (Roberts, Druckenmiller, Sætre, Hurum, 2014) comb. nov.**

(Figs 13D, C, 15–17, 18F, S8)

v*2014 *Janusaurus lundi* Roberts *et al*.: 4, figs 3–14.

v.2015 *Arthropterygius sp.*, Zverkov, Arkhangelsky, Pardo Pérez, Beznosov: 84, figs. 3–7.

2016 Janusaurus lundi Roberts *et al*.; Delsett *et al*.: figs 6b, 9, 10b–d.

2017 Janusaurus lundi Roberts *et al*.; Delsett *et al*.: fig. 12J, K.

Holotype: PMO 222.654, an incomplete skeleton (for details see Roberts *et al*. 2014).

Referred specimens: SGM 1502 (for details see Zverkov *et al*. 2015); SGM 1731-01–15, 10 anterior presacral vertebrae with articulated neural arches; scapulae; left coracoid; left humerus with articulated epipodial and proximal autopodial elements.

Emended diagnosis: A medium sized ophthalmosaurid (3–4 meters long) diagnosed relative to other species of *Arthropterygius* by the following unique characters (including autapomorphies, marked with '*') and character combination: extremely gracile and constricted stapedial shaft*; basisphenoid trapezoid in ventral view with widest part in the region of basipterygid processes; posterior foramen for internal carotid arteries opening on the posteroventral edge of the basisphenoid and forming a notch as in *A. hoybergeti* and unlike *A. chrisorum*; large basioccipital facet on the opisthotic (reduced in *A. hoybergeti*); small teeth with gracile crowns and poorly pronounced ridges (relatively large teeth with ridged crowns in *A. hoybergeti*, although teeth are unknown for other species of *Arthropterygius*); interclavicle with pointed lateral extremities and deep trough on the dorsal surface of posterior median stem*; isometric

proximal end of the humerus with nearly equal dorsoventral and anteroposterior length (as in *Ophthalmosaurus icenicus, Undorosaurus nessovi* and *U. trautscholdi*); reduced dorsal process and deltopectoral crest; strongly dorsoventally flattened posterior and distal parts of the humerus; anterodistal facet for the anterior accessory epipodial element nearly as long, but not as wide as the radial facet, being thus relatively smaller than that of *A. chrisorum* (this facet is sufficiently smaller in *A. hoybergeti*), ventral skew between the radial and ulnar facets is pronounced in a lesser degree than in the type species, but stronger than in *A. hoybergeti*; ?strongly expanded dorsal portion of the ilium with distinct anterodorsal process (could be a generic feature).

Occurrence: *Artropterygius lundi* is recognized in the European Russia and Svalbard. Everywhere it is found in the early Middle Volgian: Slottsmøya Member of the Agardhfjellet Formation in Svalbard (type locality), *Pavlovia rugosa* to *Dorsoplanites ilovaiskii* ammonite biozones; Paromes Formation in Timan-Pechora Basin and Promza Formation of the Volga Region, all these finds correspond to *Dorsoplanites panderi* Ammonite Biozone.

Description

Here we provide some new observations on the holotype (PMO 222.654) and description of SGM 1731-01–15. Description of SGM 1502 was given in Zverkov *et al*. (2015).

Skull. Several sutures in the holotype skull are reinterpreted herein (Fig. 15). The postfrontal medial contact with the supratemporal was imprecisely traced by Roberts *et al*. (2014) likely because of poor preservation. In fact, similarly to other species of *Arthropterygius* the supratemporal of PMO 222.654 forms an anteromedial tongue covering the postfrontal (Fig. 15A, B). The parietal of *A. lundi* has a typical morphology of *Arthropterygius* with a very short medial symphysis and well-pronounced notch posterior to it (Fig. 15A, B). The anterior portion of the parietal has likely contributed to a presumably large parietal foramen that was restricted by the frontals anterolaterally (Fig. 15). A ventral exposure of the parietal allows adding that the supratemporal process is relatively slender (Fig. 15C, D).

Squamosal. A squamosal was ‘presumed to have been absent in PMO 222.654’ (Roberts *et al*., (2014: 7), on the basis that ‘the region in which this element is usually present is well preserved in the specimen’ (Roberts *et al*., (2014: 7), however, as in case of other specimens from Svalbard this assumption is likely misleading (Zverkov & Efimov, in press). In the postorbital region of

PMO 222.654, there is an anteroposteriorly elongated depression along the ventral margin of the supratemporal ~~and continuing anteriorly to postfrontal~~ (Fig. 15A). Furthermore, the surface of the postorbital in this region is roughened. The depression has exact the same configuration as that of *A. hoybergeti* (SVB 1451) and presumably represents the facet of squamosal, thereby we conclude that there was a squamosal in *A. lundi* similar in morphology to that of *A. hoybergeti.* As this element is delicate and poorly attached to the rest of postorbital bar, it is not surprising that it was detached and in some cases missing in a number of specimens from Svalbard, including PMO 222.654.

Quadratojugal. Considering the slenderness and small size of the quadratojugal, as well as the configuration of its articulation with the quadrate, it is likely that in life this element was largely obscured in lateral view and exposed mostly posteriorly.

Quadrate. Judging from its exposed portions, the quadrate of PMO 222.654 has relatively 'weak' condyle and a shallow notch of the quadrate foramen; its occipital lamella presumed to be reduced (Fig. 15C, D). The dorsoventral height of the quadrate of PMO 222.654 is *c.* 105 mm. The facet for quadratojugal is located on the inner surface of the quadrate as in *A. chrisorum* (Fig. 15C, D; see Fig. 3J, L, O, P for comparison). Nearly the entire posteromedial surface of the quadrate is occupied by an extensive contact with the pterygoid, and only small region in its dorsal part has contact with the supratemporal (Fig. 15C, D). Evidently, there was no supratemporal-stapes contact.

Basisphenoid. The basisphenoid of PMO 222.654 is mostly hidden in the matrix and covered by other elements, thereby the only significant observation that could be made to the moment is that the facet for the basioccipital was strongly shifted dorsally, a condition typical of *Arthropterygius*. The basisphenoid was described in detail for SGM 1502 that is here referred to as *A. lundi* (see Zverkov *et al*., 2015).

Opisthotic. Although it was not reported by Roberts *et al*. (2014), the nearly complete right opisthotic is present in the holotype (PMO 222.654). The paraoccipital process of the opisthotic is relatively short and very robust. The facet for the supratemporal is triangular in outline (Fig. 16E). The lateral muscular ridge is well developed. The stapedial facet is roughly trapezoidal in outline (Fig. 16D). The facet for the basioccipital is quadrant in outline with convex margin

directed dorsolaterally (Fig. 16B); it is as large as the stapedial facet. A V-shaped impression formed by two smooth-floored semicircular canals of the otic capsule is deep. Impressions of the horizontal semicircular canal and posterior vertical semicircular canal are nearly equal in length as in *A. hoybergeti*. The posterior vertical semicircular canal impression is only slightly wider. The impression housing the posterior ampulla, utriculus and the sacculus is expanded, especially in its anteroventral part, to where sacculus impression continues (Fig. 16F, G).

Dentition. The dentition of *A. lundi* is weak compared to that of *A. chrisorum* (PMO 222.669) and *A. hoybergeti* (SVB 1451). The crowns are slender and their enamel is subtly ridged (Fig. 13B, C). An estimated crown height is less than 9 mm in PMO 222.654, as calculated by Roberts *et al.* (2014: 15). The largest crown of SGM 1502 is 10 mm high and has 5 mm in basal diameter.

Axial and appendicular skeleton. Not much could be added to the thorough description of the axial and appendicular skeleton of *Arthropterygius lundi* made by Roberts *et al*. (2014). Among the interesting traits not mentioned by the aforementioned authors are the extensive circular facet on the clavicle that formed a firm articulation with the acromial process of the scapula (Fig. 17D, E) and, typical of the genus, pronounced angle close to 90 degrees between the articulated coracoids (Fig. 17Q). A ‘foramen’ located on the ventral surface of the interclavicle of PMO 222.654, is likely an artefact of preservation, ~~but~~ not an autapomorphic trait as was supposed by Roberts *et al*. (2014). The interclavicular trough is very deep unlike in other species of *Arthropterygius* and in other ophthalmosaurids in general, thereby we support the statement of Roberts *et al*. (2014) that this could be considered as an autapomorphy. A bulge in the middle of the interclavicle posterior median stem is present in PMO 222.654 (Fig. 17F, G), supporting our assumption that this is a characteristic trait of *Arthropterygius*.

The well-preserved coracoid and scapula of SGM 1731-01–15 demonstrate a typical morphology of *Arthropterygius* (Fig. 17A–C). The coracoid is slightly longer anteroposteriorly than wide mediolaterally; it bears a prominent anteromedial process, laterally limited by an extensive anterior notch. The posterior portion of the coracoid is strongly compressed and forms a convex protrusion posteriorly (Fig. 17A). The scapula has a well-developed acromial process, nearly equal coracoid facet and glenoid contribution (the latter is slightly shorter) and typical mediolaterally compressed, oval in cross-section scapular shaft (Fig. 17B, C).

Humerus. Although coracoid and scapula do not bear any specific traits in *A. lundi*, the humerus does. Having humeri nearly identical to that of PMO 222.654, both SGM 1502 and SGM 1731-01–15 fit greatly to complement the hypodigm. The humerus of *Arthropterygius lundi* has a characteristic isometric proximal end as high dorsoventrally as long anteroposteriorly, and strongly flattened distal end and posterior portion of the shaft (Fig. 17H–L, N–P). The dorsal process and deltopectoral crest of the humerus are relatively poorly developed. The ventral skew between the radial and ulnar facets is pronounced in a lesser degree than in the type species, but stronger than in *A. hoybergeti*.

Epipodial and autopodial elements. The epipodial and autopodial elements in SGM 1731-01–15 and PMO 222.654 are virtually identical. The anterior accessory epipodial element is circular in dorsal view. The radius has a typical pentagonal shape in dorsal view. The ulna is markedly larger than the radius, it is somewhat hexagonal, lacking a perichondral ossification along its posterior edge. Distally ulna bears three nearly equal facets for the intermedium, ulnare and the pisiform (Fig. 17M, N). The intermedium is diamond-shaped in dorsal view, having equal contacts with the radius and ulna and bearing two distal facets, evidently for distal carpals three and four. The autopodial elements are mostly circular in outline and were loosely packed as in *Ophthalmosaurus icenicus* (see e.g. Moon & Kirton, 2016) and other species of *Arthropterygius*. Of certain interest are two small ossicles that are semicircular in outline, having perichondral ossification along one of the edges (Fig. 17N). These are probably the pisiform and an element of a postaxial accessory 6th digit.

Measurements. See Roberts *et al.* (2014), Zverkov *et al.* (2015) and Table S3 in Zverkov & Prilepskaya, documents.

***Arthropterygius volgensis* (Kasansky, 1903) comb. nov.**

(Figs 18, 19, 20E)

v*1903 *Ichthyosaurus volgensis* Kasansky: 29, Tabs I, II.

1910 Ophthalmosaurus sp.; Bogolubov: 472 [*pars*].

2000 Otschevia ?volgensis; Arkhangelsky: 550.

2000 ?*Ophthalmosaurus* sp.; Storrs *et al*.:197 [*pars*].

2008 Undorosaurinae gen. indet.; Arkhangelsky: 253 [*pars*].

Holotype: KSU 982/P-213, incomplete skeleton of a juvenile represented by cranial remains (including basisphenoid, opisthotics, quadrates, parietals, right supratemporal and articular), three posterior caudal and tailfin vertebrae; neural arches and rib fragments, coracoids; fragments of the interclavicle, scapula and clavicles, distal portion of the femur.

Diagnosis: *Arthropterygius volgensis* could be diagnosed relative to other species of *Arthropterygius* by the following characters: gracile articular condyle of the quadrate, less high dorsoventrally and less obtuse posteriorly, do not forming a pronounced ventral angle; and square ventral outline of the basisphenoid with posterior end of the element mediolaterally wider than the anterior end, due to a pronounced reduction of the basipterygoid processes.

Occurrence: *Arthropterygius volgensis* is known from only the type locality to the moment: the mouth of the Berezoviy Dol Ravine near Novaya Racheika Village, Syzran District, Samara Region. Upper Jurassic, Middle Volgian, *Dorsoplanites panderi* Ammonite Biozone.

Description

Skull

Supratemporal. A posterodorsal portion of the right supratemporal is preserved (for the figure see Kasansky 1903, Tab.1 fig. 10). The medial ramus is massive and mediolaterally short, it bears a concave facet for articulation with the parietal.

Parietal. The parietal is well preserved and similar to that of other *Arthropterygius* species. It possess a relatively elongated and slender supratemporal process (Fig. 18P). The posterodorsal surface of the supratemporal processes is rugose with the central ridge that contributed to a somewhat peg-and-socket articulation with the supratemporal (Fig. 18P). The medial articular

facet is anteroposteriorly shortened; its surface is deeply ridged for a strong interdigitating articulation with the contralateral parietal. Posterior to the facet is a pronounced notch of finished ossification (Fig. 18P, S). Anteriorly, the parietal bears rugose facets for articulation with the frontal and postfrontal. Ventral surface of the element is divided into two areas: the deep and extensive impression of the cerebral hemisphere occupy more than a half of the anterior ventral surface (Fig. 18R, ich); posteriorly situated optic lobe impression, which is roughly circular in outline, occupies the rest of the element (Fig. 18R, iop). The dorsal surface of the parietal is convex and nearly horizontal along the midline in lateral view. There was no sagittal eminence.

Quadrate. The articular condyle of the quadrate is relatively reduced and dorsoventrally low compared to that of *A. chrisorum*. The articular and surangular bosses of the condyle are nearly equal in size (Fig. 18O, N). The articular boss is only slightly more pronounced ventrally, however its ventral margin is gradually curved, but not V-shaped as in *A. chrisorum*. The facet for the quadratojugal is a small depression on the dorsal surface of the condyle (Fig. 18N). The quadrate foramen is shallow due to a reduction of the articular condyle and the occipital lamella (Fig. 18L). The occipital and pterygoid lamellae are slightly demarcated one from another forming an angle of c. 145 degrees. A circular depression of the stapedial facet is located in the middle of the medial surface (Fig. 18L).

Basisphenoid. The basisphenoid is square in ventral view: its posterior and anterior ends are nearly equal in mediolateral length (Fig. 18A). The basipterygoid processes are reduced and faced anterolaterally. The basioccipital facet is a broad hexagonal irregularly pitted surface that faces posterodorsally. A pentagonal dorsal plateau is mediolaterally wide. The stapedial facet is oblique and relatively small (Fig. 18C). The anterior wall is high and vertical, even on the lateral sides. The dorsum sellae, located in the middle of the anterior surface, is smoothly bordered from the rest of the anterior wall (Fig. 18D). The impressions of a cartilaginous continuation of the crista trabecularis are well-pronounced (Fig. 18D). The posterior foramen for the internal carotid arteries opens posteroventrally, forming a medial notch of the posteroventral edge of the basisphenoid, as is CCMGE 3-16/13328, which may be due to the immaturity of these individuals.

Opisthotic. The paraoccipital process of the opisthotic is shortened and robust, however, this could be regarded as an immature condition as was discussed by Kear & Zammit (2014). The

facet for the supratemporal is triangular in outline (Fig. 18H). The lateral muscular ridge is well pronounced. The trapezoid in outline stapedial facet is larger than the facet for the basioccipital, which is quadrant in outline with convex margin directed dorsolaterally (Fig. 18F, K). The stapedial facet bears a deep straight mediolateral groove either for VII or for IX nerve in its middle (Fig. 18K). The impressions for the semicircular canals of the otic capsule are deep and nearly equal in length as in other species of *Arthropterygius*. The impression of the posterior vertical semicircular canal is wider than that of the horizontal semicircular canal. The impression housing the posterior ampulla and the sacculus is expanded (Fig. 18J).

Articular. The articular is anteroposteriorly elongated and trapezoid in outline (Fig. 18T, U). It is highly similar to that of *Arthropterygius lundi* (Roberts *et al*., 2014), being more anteroposteriorly elongated than in *A. chrisorum* and *A. hoybergeti* (Fig. S4 in Zverkov & Prilepskaya, documents; Maxwell, 2010).

Axial skeleton. The detailed description and measurements of the vertebral column (which is nowadays missing) were provided by Kasansky (1903).

Pectoral girdle. The preserved middle fragments of clavicles (Fig. 19H) demonstrate morphology common of ophthalmosaurids: these are anteroposteriorly thin and dorsoventrally high elements, curving in dorsolateral direction. The clavicles are dorsoventrally high as in other species of *Arthropterygius*. The interclavicle (Fig. 19H, I) is a relatively large element, being approximately 2/3 of the coracoid length. Its posterior median stem is shaft-like, ventrally convex and dorsally bearing a shallow trough. The scapula is incompletely preserved in two fragments. The acromial process of the scapula is large and flattened, anteroventrally curving at the anterior edge (Fig. 19G). The scapular shaft is mediolaterally compressed, as in other species of *Arthropterygius* and ophthalmosaurines *Ophthalmosaurus icenicus* and *Acamptonectes densus* (Fischer *et al*., 2012; Moon & Kirton, 2016). Both coracoids are well preserved, they are rounded in general outlines; however, their anteroposterior length slightly exceeds mediolateral width. The ventral surface of the element is slightly saddle-shaped (Fig. 19B), whereas the dorsal surface is nearly flat (Fig. 19A). The scapular facet is demarcated by an obtuse angle (160 degrees) from the glenoid contribution. The medial symphysis is dorsoventrally thin, extending along anterior two-thirds of the coracoid, as in *A. chrisorum* and *A. lundi* (Roberts *et al*., 2014). The angle between articulated coracoids is close to 90 degrees (Fig. 19E).

Femur. The only distal portion of the right femur is preserved (Fig. 19J–M). Its distal facets are poorly ossified and slightly demarcated, thus it is even hard to say, whether two or three distal facets are present (Fig. 19J, K, M). The ventral process, located in the middle of the ventral surface is more prominent than the anteriorly shifted dorsal process (Fig. 19L).

Remarks. Kasansky originally incorrectly identified the femur as a humerus, at the same time two broken pedicles of the neural arches were misidentified as femora (Kasansky, 1903).

The holotype and only known specimen KSU 982/P-213 is a juvenile individual, thereby the value of features used as diagnostic could be questioned. Indeed, a number of observed traits could be interpreted as juvenile conditions: reduced occipital lamella of the quadrate, minimally developed basipterygoid processes and short paroccipital process of the opisthotic (see Kear & Zammit, 2014). However, a series of specimens of different age classes available now for *Arthropterygius chrisorum* allows advocating some of our conclusions. Although the relative development of the basipterygoid processes of the basisphenoid during the ontogeny is supported by our observations, we state that the general ventral (or dorsal) outline of the basisphenoid is stable between all the age classes. Kear & Zammit stated that in the *in utero P. australis* 'the basipterygoid processes are minimally developed, giving the basisphenoid a much narrower anterior profile when compared with those of adults' (Kear & Zammit, 2014: 77). Based on this, they concluded that for characters dealing with a shape of basipterygoid processes, i.e. Maxwell (2010: char. 11) and Fischer *et al*. (2011: char. 17; 2012: char. 16), foetal individual scores differently than mature ones. However, this is not a fully justifiable observation, as in fact both foetal and mature *P. australis*, regardless the state of development of basipterygoid processes, preserve generally 'pentagonal' (or, it is better to say, trapezoidal) ventral outline of the basisphenoid with anterior region markedly wider than the posterior part. This is clearly seen from the fig. 5m of Kear & Zammit (2014). In contrast, taxa with 'square' ventral outline of the basisphenoid always have the same width of anterior and posterior basisphenoid (NGZ pers. obs.). All specimens of *Arthropterygius chrisorum* have basisphenoid that is mediolaterally wider anteriorly than posteriorly. Indeed, the juvenile CCMGE 3-16/13328 has narrower anterior profile when compared with those of adults CCMGE 17-44/13328 and CMN 40608 (Fig. 20), supporting the observation of Kear & Zammit (2014); still the anterior region of the basisphenoid of juvenile CCMGE 3-16/13328 is wider than the posterior region (Fig. 20A). In contrast, the posterior region of the basisphenoid of KSU 982/P-213 is wider

than the anterior region (Fig. 20E); although CCMGE 3-16/13328 and KSU 982/P-213 represent close ontogenetic stages (basisphenoid and quadrate of KSU 982/P-213 are slightly smaller, whereas coracoid is bigger than those of CCMGE 3-16/13328). Another marked difference of CCMGE 3-16/13328 and KSU 982/P-213 is the shape of the condyle of their quadrates. Whereas CCMGE 3-16/13328, CCMGE 17-44/13328 and PMO 222.669, regardless differences in size, have similar shape of the condyle, KSU 982/P-213 differs in having less dorsoventrally high condyle with gradually curving (not V-shaped) ventral margin. This allows suggesting that the shape of the quadrate could also be regarded as interspecifically and ontogenetically stable feature. Thereby we conclude that at the current state of knowledge, *A. volgensis* should be regarded as a distinct valid species of *Arthropterygius* rather than a synonym of other known species of the genus or a nomen dubium.

Measurements. See Kasansky (1903) and Table S4 in Zverkov & Prilepskaya, documents.

Phylogenetic analysis

Method. For the phylogenetic analysis, we used recent matrix focused on ophthalmosaurids, presented by Zverkov & Efimov (in press). One unit, '*Keilhauia nui*', was removed, and other two, *Arthropterygius volgensis* and *A. chrisorum* PMO 222.669 were added to the dataset. The scores for species of *Arthropterygius* were extended and partially changed based on new data (see supplemental materials for details). Six new characters related to the morphology of the supratemporal, parietal, quadrate, coracoid and humerus were added to the dataset (for details see Tab. S10 in Zverkov & Prilepskaya, documents). The new characters were coded from the literature for taxa that we have not personally examined (Tab. S11 in Zverkov & Prilepskaya, documents; Gilmore, 1905; Broili, 1907; Andrews, 1910; Fraas, 1913; Sollas, 1916; Romer, 1968; McGowan, 1972, 1973a; Johnson, 1979; Kirton, 1983; Wade, 1984, 1990; Godefroit, 1993; Fernández, 1994, 1997, 1999, 2007a; Bardet & Fernández, 2000; Maisch & Matzke, 2000; McGowan & Motani, 2003; Kear, 2005; Motani, 2005; Maxwell & Caldwell, 2006; Druckenmiller & Maxwell, 2010; Kolb & Sander, 2009; Zammit, Norris & Kear, 2010; Fischer *et al.,* 2011, 2012, 2014a,b; Maxwell, Fernandez & Schoch, 2012; Fernández & Talevi, 2014;

Marek *et al*., 2015; Paparella *et al*., 2017). The analysis was performed using TNT 1.5 (Goloboff *et al*., 2016), applying traditional search with 10000 replicates and tree bisection and reconnection (TBR) with 100 trees saved per replication. ~~The RAM allocation was extended to 1024 megabytes (`mxram 1024`) and the memory to 10 000 trees (`hold 10000`).~~ Decay indices (Bremer support, 'suboptimal' = 5) and resampling methods to estimate the robustness of nodes (standard bootstrapping and jackknifing, 1000 iterations) were also computed in TNT 1.5.

In order to eliminate problematic 'wildcard' taxa, we used an *a posteriori* approach of Pol & Escapa (2009) that is directly implemented in TNT 1.5 (`pcrprune`). The two taxa (*Athabascasaurus bitumineus* Druckenmiller & Maxwell, 2010 and *Platypterygius platydactulus* Broili, 1907) were identified as unstable and pruned from the second analysis. The pruned dataset was analysed using the exact same procedures as was used for the full dataset.

Results

Our analysis of the full dataset recovered ten most parsimonious trees of 310 steps with the consistency index (CI) = 0.416 and retention index (RI) = 0.662. The strict consensus (length of 321 steps; CI = 0.402; RI = 0.642) is relatively well resolved, however, supports for relationships within Ophthalmosauridae are still low (Fig. 19A). Despite the modifications of the original matrix, the recovered topology is nearly identical to that of Zverkov & Efimov (in press), except for minute changes in relations of derived-most platypterygiines that are even more badly resolved. A clade that includes species of *Arthropterygius* ('A' in Figure 18) is recovered as the sister group to Platypterygiinae (Fig. 19A). Sister relations of *Arthropterygius* and platypterygiines are supported by two synapomorphies: 'T'-shaped prootic osseous labyrinth (49.0→49.1) and absence of the obturator foramen in the ischiopubis (98.1→98.2).

Only two most parsimonious trees (length of 300 steps, CI = 430, RI = 662) were recovered by the pruned analysis. In the strict consensus tree (length of 302 steps, CI = 425, RI = 656; Fig. 19B), Platypterygiinae is relatively better resolved. Surprisingly, *Caypullisaurus* is found as a sister, not to *Grendelius*, but to *Leninia* (based on two non-unique synapomorphies: presence of prefrontal dorsomedial expansion (16.0→16.1), and squared sqamosal (34.1→34.0). However, the relations of derived platypterygiines is not a focus of the current paper. ~~Of our special interest~~

~~is that~~ *Arthropterygius* clade is recovered as a sister group to ophthalmosaurines, these two from a clade with low support, ~~but sharing~~ three synapomorphies (presence of the lateral 'wing' of the nasal (14.0→14.1); absence of supratemporal-postorbital contact (27.1→27.0); and circular shape of the basioccipital condyle (43.1→43.0).

The *Arthropterygius* clade is supported by nine unambiguous synapomorphies: posterior position of the foramen for internal carotid arteries (unique, 40.1→40.2); dorsally facing basioccipital facet of the basisphenoid (non-unique, 41.0→41.1); raised opisthotic facet of the basioccipital (non-unique, 46.0→46.1); anteriorly shifted stapedial and opisthotic facets of the basioccipital (unique, 47.0→47.1); gracile stapedial shaft (non-unique, 52.0→52.1); robust clavicles (unique, 78.0→78.1), ulnar facet/radial facet ratio less than ~~0,83~~ (unique, 84.0→84.1); weak quadrate condyle (non-unique, 110.0→110.1); angle between the articulated coracoids less than 110 degrees (unique, 111.0/1→111.2).

In both the full and pruned analyses the *Arthropterygius* clade has very high Bremer support values (4 and 5), Bootstrap and Jackknife (more than 80), thus being the most well-supported clade in our analyses (Fig. 19). The result is of high importance for our taxonomic decision, as it leaves no substantial reasons to consider taxa within the *Arthropterygius* clade as representatives of separate genera.

Multivariate analysis of ophthalmosaurid humeral morphology

One of the most peculiar skeletal elements of *Arthropterygius* is its humerus that bears a number of diagnostic features and could be easily recognized among humeri of other ophthalmosaurids. In order to highlight this, we provide the following principal component analysis (PCA) of ophthalmosaurid humeral morphology.

Method. To compare humeri of ophthalmosaurids we gathered a series of metrics and ratios that collectively summarize morphology of the humerus (Tabs S6, S7 in Zverkov & Prilepskaya, documents). The metrics are: proximodistal length of the humerus, anteroposterior width of

humeral proximal and distal ends, thickness of humeral proximal end; dorsoventral width of humeral distal end; anteroposterior width at midshaft, anteroposterior and dorsoventral width of the distal facets, and the angle between the ulnar and radial facets (for details see Fig. S1 in Zverkov & Prilepskaya, documents). Based on the metrics the following ratios were calculated (Tab. S7 in Zverkov & Prilepskaya, documents):

(1) Humeral proximal expansion: anteroposterior width of humeral proximal end divided by the humeral proximodistal length.
(2) Humeral distal expansion: anteroposterior width of humeral distal end divided by the humeral proximodistal length.
(3) Humeral stoutness: humeral minimal anteroposterior width at diaphysis divided by the humeral proximodistal length.
(4) Humeral proximodistal proportionality: anteroposterior width of humeral proximal end divided by the same measurement of its distal end. The character based on this ratio is used in current phylogenetic analyses and distinguish ophthalmosaurids, which commonly have nearly equal proximal and distal humeral ends or proximal end slightly wider than the distal end see e.g. Fischer *et al*. (2011: Character 32).
(5) Isometry of the humeral proximal end (or 'anteroposterior elongation' of the humeral proximal end): anteroposterior width of humeral proximal end divided by the thickness of humeral proximal end (see Fig. S1 in Zverkov & Prilepskaya, documents). This ratio has extremely high value in '*Grendelius*' *zhuravlevi* (2.587) for which strongly compressed humeral proximal end is considered as autapomorphic (Zverkov, Arkhangelsky & Stenshin, 2015); the standard values for ophthalmosaurids are 1.8–1.5; for taxa with 'isometric' humeral proximal end this value could be close to one (e. g. *Undorosaurus nessovi*, and *Platypterygius platydactylus* see Tab S7 in Zverkov & Prilepskaya, documents).
(6) Humeral distal compression: anteroposterior width of humeral distal end relative to the maximal dorsoventral width of humeral distal end.
(7) Relative anteroposterior width of facet for preaxial accessory epipodial element and radial facet.
(8) Relative anteroposterior width of ulnar and radial facets. As well as for ratio 4, there is a character based on similar ratios in current phylogenetic analyses, see e.g. Motani (1999: Character 52) and Moon (2017: Character 209). However, the referred character use 'relative

size' of ulnar and radial facets, which is not always clear as ulnar facet could be longer than radial facet but the same time, less wide dorsoventrally (as in most specimens of *Arthropterygius*). In this regard, it is better to consider separately relative anteroposterior width of ulnar and radial facets and relative dorsoventral width of ulnar and radial facets.
(9) Relative dorsoventral width of ulnar and radial facets.

The dataset is resolved at the specimen level with left and right humeri considered separately in order to reveal the existing humeral asymmetry within an individual and to assess its possible effects on the results. Data (see Tabs S6, S7 in Zverkov & Prilepskaya, documents) were collected based on personal observations of NGZ and completed by measurements and in rare cases analysis of pictures of the following references: Broili, 1907; Nace, 1939; Wade, 1984; Delair, 1986; McGowan, 1972; Arkhangelsky, 1998; Kolb & Sander, 2009; Maxwell, 2010; Maxwell & Kear, 2010; Moon & Kirton, 2016. Only humeri with all documented ratios were considered, in rare cases, we completed our dataset by approximate ratios estimated based on oblique views (the case of *B. extremus* and *P. platydactylus*) or proportionally translated from other conspecific individuals (the case of *P. americanus*). The final dataset consisted of 39 humeri belonging to 29 individuals and ten variables (Tab. S8 in Zverkov & Prilepskaya, documents). The ratios and angle between the ulnar and radial facets (in rad) were used as variables for the PCA. Data were scaled to equal variance by subtracting the mean value for each variable and then dividing each variable by the standard deviation. We then created a distance matrix with these data (Tab. S8 in Zverkov & Prilepskaya, documents). The dataset was analysed in PAST v. 3.20 (Hammer *et al.,* 2001).

Results

The first four axes describe over 81% of the total variance (33.8%, 20.7%, 16.8% and 10.5% respectively). All variables showed low loadings on PC1 (>-0.50; <0.50); among them better pronounced are humeral distal expansion (variable 2: 0.46), relative size of *faae* (variable 7: 0.41) and humeral stoutness (variable 3: 0.34), as well as relative dorsoventral width of ulnar and radial facets (variable 9: -0.39) and an angle between these facets (variable 10: -0.36). For the PC2 highest positive loadings are shown by variables 1 (0.59), 4 (0.50), 5 (0.47) and 3 (0.35)

thereby PC2 characterise humeral proximal expansion, humeral proximodistal proportionality, humeral stoutness and isometry of the humeral proximal end. PC3 depicts humeral distal compression (variable 6: 0.53) and an angle between the ulnar and radial facets (10: 0.47) and in lesser degree proportions of the humeral proximal end (variable 5: 0.38) and proximodistal proportionality (variable 4: -0.31). PC4 is responsible for relative size and shape of humeral distal facets: relative anteroposterior width of ulnar and radial facets (8: 0.62); relative dorsoventral width of these facets (9: 0.35) and relative anteroposterior width of *faae* and the radial facet (7: -0.50). The distribution of variable loadings could be found in Tab. S9 (Zverkov & Prilepskaya, documents).

Considering low sampling for most of the taxa in our analysis, it is hard to say with confidence if the absence of marked morphospace overlap between ophthalmosaurid taxa is a true condition, or it is biased by the sampling. Whether or not, it is clear that some ophthalmosaurids are well separated, e.g. *Brachypterygius*-*Grendelius* cluster (low values on PC1 and high values on PC3) and *Arthropterygius* cluster (high values on PC1, low values on PC4) see Figure 22.

Our PCA (Fig. 22) demonstrate a relatively wide morphospace occupation for species of *Arthropterygius*, which is mostly due to *Arthropterygius hoybergeti*, having humeri that are morphologically closer to 'standard' ophthalmosaurid condition and thereby falling closer to other ophthalmosaurids, in particular, *Undorosaurus gorodischensis* and *Platypterygius hercynicus*. *A. lundi* is separated by positive values of the PC4 (Fig. 22C) and along with *A. chrisorum* demonstrate high values on PC1.

Species of *Undorosaurus* could also be potentially distinguished based on humeral morphology (Fig. 22A, D). *Undorosaurus gorodischensis* morphospace is separated from other species of *Undorosaurus* by the second principal component axis, as *U. nessovi* and *U. trautscholdi* demonstrate high negative values on PC2. In general morphology, *U. gorodischensis* have anteroposteriorly elongated humeral proximal end, that is of roughly oval outline, whereas *U. nessovi* and *U. trautscholdi* are characterized by a nearly circular outline of the humeral proximal end, which is depicted by PC2 partially responsible for humeral proximal expansion.

Several derived Cretaceous platypterygiines, added to our analysis, occupy different parts of the morphospace also demonstrating the potential of humeral morphology for distinguishing Cretaceous ichthyosaurs.

The interesting result of our analysis is that in some ophthtalmosaurid individuals left and right humeri can fall wider to each other than to humeri of other specimens of the species and even to other species and genera, indicating the presence of a pronounced humeral asymmetry in ophthalmosaurids. The most outstanding specimen with humeral asymmetry in our analysis is *Platypterygius hercynicus*. The asymmetry could only partially be explained by artefacts of preservation and/or pathologies, but, considering its presence in practically all the specimens with both humeri preserved, it is likely a natural condition.

Discussion

Variation in humeral morphology interspecific or infraspecific?

As in case of *Undorosaurus* (Zverkov & Efimov, in press) and *Grendelius* (Zverkov, Arkhangelsky & Stenshin, 2015), species of *Arthropterygius* could be potentially distinguished based exclusively on humeral morphology, which was already demonstrated above. Especially valuable is the outline of the humeral proximal end – each of these genera has species with anteroposteriorly elongated humeral proximal ends (*Grendelius zhuravlevi*, *Undorosaurus gorodischensis*, *Arthropterygius chrisorum*) and those with isometric proximal ends (*G. alexeevi*, *U. nessovi*, *U. trautscholdi*, *A. lundi*). We cannot exclude the possibility that some of these species may actually represent males and females, thus demonstrating sexual dimorphism, differing in limb morphology in a way, similar to that hypothesized for Triassic ichthyopterygians *Chaohusaurus* and *Shastasaurus* (Shang & Li, 2013; Motani *et al.,* 2018). However, given other existing differences (especially cranial) between the discussed species, and considering that in some genera more than one species with either elongated or isometric humeral proximal end could be present, it is impossible to say, which of the species are representing sexual morphs of the same species and which of them are morphs of other species. Thereby, in the current state of knowledge, we prefer to retain all the 'morphs' as separate species.

Palaeobiogeographic implication of *Arthropterygus*

After the discovery of *Arthropterygius* in Argentina (Fernández & Maxwell, 2012), this taxon, even being known from a couple of specimens, has already raised a question regarding the cosmopolitan distribution of ichthyosaurs (Fernández & Maxwell, 2012; Zverkov *et al*., 2015). New discoveries further support the idea that most of ophthalmosaurids have had a widespread distribution.

For the analysis of dispersal routes of Late Jurassic ichthyosaurs the data on connections between the basins is of principal importance. According to palaeogeographic reconstructions, based primarily on invertebrates, the Middle Russian Sea and European basins were connected by the Brest (Pripyat) Strait until the beginning of the middle Volgian *Virgatites virgatus* Chron. This is determined by identical sequences of virgatitid ammonites in the Polish and Middle Russian seas (Fig. 23; Sasonova & Sasonov, 1967; Mesezhnikov & Zakharov, 1974; Rogov *et al.,* 2008; Rogov, 2012, 2013a). After the closure of the Brest Strait in the early *Virgatites virgatus* Chron, the Middle Russian Sea became isolated from the west and south until the beginning of the Cretaceous (Fig. 23; Sasonova & Sasonov, 1967; Baraboshkin, 1999, 2003). In the north, the Middle Russian Sea was connected with other Arctic basins via the Mezen-Pechora Strait (Sasonova & Sasonov, 1967). This connection was restricted during the middle part of the middle Volgian, but intense from the end of the middle Volgian, as ammonites of the *Virgatites virgatus* and contemporary *Dorsoplanites maximus* ammonite biozones are markedly different, whereas ammonite faunas of the *Epivirgatites nikitini* Ammonite Biozone and its correlatives are showing numerous common elements in the Arctic (Rogov, 2010; Kiselev & Rogov, 2018). Furthermore, during the Kimmeridgian and Volgian Arctic seas and seas of Northwestern Europe were connected by the Norwegian-Greenland Seaway (Mesezhnikov & Zakharov, 1974; Mutterlose *et al.,* 2003; Rogov, 2012). Judging from the data on the distribution of ammonites, immigration through the Norwegian-Greenland Seaway was limited in the Kimmeridgian (Rogov, 2012), but in the early Volgian the situation has changed significantly, and this time interval in the Panboreal Superrealm is characterized by nearly identical successions of Pectinatitinae ammonites from northern France to the Lena river basin in Siberia (Rogov & Zakharov, 2009). The similarity between ammonite faunas of the Anglo-Paris Basin with those of Arctic persisted in the early stages of the middle Volgian, but later a significant differentiation

of ammonite communities began, and only for the late Volgian it is possible to identify the resumption of active faunal exchange between the NW Europe and the Middle Russian Sea, particularly noticeable at the end of the late Volgian (early Berriasian, *Volgidiscus lamplughi* Chron) (Rogov, 2013b, 2014; Kiselev *et al*., 2018).

For the Kimmeridgian – early middle Volgian (early Tithonian with its bipartite division) time interval we can observe a high similarity of ichthyosaurs of the Middle Russian Sea and seas of Northwestern Europe: both these basins are inhabited by small-sized ichthyosaurs of *Nannopterygius* clade and moderate to large representatives of the genus *Grendelius* (Fig. 23). Currently, these ichthyosaurs are not found elsewhere in contemporaneous deposits. Furthermore, for this time bin there are rare but widespread finds of *Ophthalmosaurus* in England, France, Russia, Mexico and ?Argentina (Bardet et al., 1997; Etches & Clarke, 1999; Buchy & López Oliva, 2009; Fernández & Maxwell, 2012; Moon & Kirton, 2016; Arkhangelsky *et al*., 2018).

Arthropterygius seem to be very common ichthyosaurs for this time bin: *Arthropterygius chrisorum* is found in Arctic Canada, Svalbard and Volga Region, thus indicating a wide distribution of this species across the Arctic basins and Middle Russian Sea. The same concerns *Arthropterygius hoybergeti* and *A. lundi*, which are both known from Svalbard and Volga Region. Additionally *A. lundi* is known from the Timan-Pechora, thus unambiguously demonstrating that the Mezen-Pechora Strait was used as a passage during this time interval. Discovery of *Arthropterygius* sp. in the Tithonian of Argentina indicate that representatives of the genus could distribute through the Arctic, and then to the South along the Paleopacific coast of the American continent to the Neuquen Basin (Fernández & Maxwell, 2012; Zverkov *et al*., 2015). Similar migration route was assumed for the Late Kimmeridgian ammonite *Zenostephanus* (Rogov & Poulton, 2015). The Hispanic corridor connecting the Paleopacific and Tethys basins is less possible dispersal route for *Arthropterygius*, as among numerous ichthyosaur specimens from the Kimmeridgian and Tithonian of Western Europe (e.g. in Kimmeridge Clay and Solnhofen formations) there are still no diagnostic remains of *Arthropterygius*. In this regard, the Brest Strait and the Norwegian-Greenland Seaway ~~are also~~ unlikely were used as dispersal passages by *Arthropterygius* spp. However, a discovery of *Arthropterygius* in Western Europe could challenge this hypothesis.

After the closure of the Brest Strait *Grendelius* disappeared in the Middle Russian Sea, probably replaced by similar in size and apparently occupying the same ecological niche *Undorosaurus*. At the same time, representatives of *Nannopterygius* clade remained abundant in the Middle Russian Sea, and considering recent discoveries existed also at Svalbard (Fig. 23; Delsett *et al*., 2018: 35). It has recently been demonstrated that *Undorosaurus* first appeared in the Polish Sea in the early Middle Volgian and likely distributed to the Middle Russian Sea using the Brest Strait. After the closure of the Brest Strait in the *Virgatites virgatus* Chron *Undorosaurus* dispersed in the Middle Russian Sea and produced several species (see Zverkov & Efimov, in press). During the *Virgatites virgatus–Epivirgatites nikitini* chrons, *Undorosaurus gorodishensis* reached high latitudes of Svalbard, unambiguously demonstrating the exchange of herpetofauna between the Middle Russian Sea and Arctic basins.

Arthropterygius are currently unknown in the Middle Russian Sea from the *Virgatites virgatus* Chron, but they still existed at high latitudes during the late Volgian and Ryazanian (latest Tithonian and Berriassian), thus being among the few ichthyosaur taxa that are recognized in the Berriassian.

To conclude our palaeobiogeographic observations: for the Kimmeridgian – early Middle Volgian time bin we recognize three ichthyosaur taxa that unite the Middle Russian Sea and basins of Western Europe *(Ophthalmosaurus icenicus*, representatives of *Grendelius*, and *Nannopterygius* clade). At the same time, these ichthyosaurs are not yet found in the Arctic, except for possible *Nannopterygius* clade ichthyosaur PMO 222.658 recently reported from Svalbard by Delsett *et al.* (2018: 35). At the same time, three species of *Arthropterygius* demonstrate close relations of the Middle Russian Sea and Arctic basins. From the Middle Volgian *Virgatitus virgatus* Chron the unifying element of the Middle Russian Sea and Arctic basins is *Undorosaurus gorodischensis*, while *Arthropterygius chrisorum* occurs only at high latitudes. Interestingly, no ichthyosaur genera are yet to be found in all the three basins, giving reason to suggest the existence of concurrence between Late Jurassic ophthalmosaurids resulting in limitation of their aerials.

Significance of the new finds and further perspectives in the study of ophthalmosaurids

The Beriassian fossil record of marine tetrapods is scarce and patterns of faunal turnover during the Jurassic–Cretaceous transitional interval are non-uniform (e.g. Benson *et al*., 2010; 2013; Benson & Druckenmiller, 2014; Tennant *et al.,* 2017; Zverkov *et al*., 2018). It has already been suggested that ichthyosaurs survived the Jurassic–Cretaceous transition relatively unscathed (Fischer *et al*., 2012, 2013). However, Berriassian ichthyosaur record is still poor (Fernández & Aguirre-Urreta, 2005; Fernández, 2007a; Ensom *et al*., 2009; Fischer *et al*., 2012; Green & Lomax, 2014; Delsett *et al.,* 2017). As was demonstrated above '*Keilhauia nui*' from the Berriassian of Svalbard is a *nomen dubium*, thus only one Berriassian ichthyosaur, *Caypullisaurus bonapartei* from the Neuquen Basin of Argentina, could hitherto have been recognized at the species level (Fernández, 2007a), demonstrating that this Tithonian species sucsessfully crossed the Jurassic–Cretaceous boundary. In this regard, discovery of *Arthropterygius chrisorum* in the Berriassian of Franz Joseph Land provides the second ophthalmosaurid species that unambiguously crossed the Jurassic–Cretaceous boundary, further argument that this transition had minimal (if some) effect on ichthyosaurs.

A discrete character of the fossil record of ophthalmosaurids (see e.g. Cleary *et al*., 2015) has led to certain problems in the study of this group. The only more or less thoroughly investigated ophthalmosaurids to date are Callovian *Ophthalmosaurus icenicus* (Andrews, 1910; Appleby, 1956; Kirton, 1983; Moon & Kirton, 2016) and Albian *Platypterygius australus* (Wade, 1984, 1991; Kear, 2005; Zammit, Norris & Kear, 2010; Kear & Zammit, 2014). Other ophthalmosaurids are incomparably poorly known either due to a small sample size or because of fragmented and/or poor preservation. In such conditions, it is hardly possible to develop a strong phylogenetic hypothesis for ophthalmosaurids. The continuing replenishment of the ophthalmosaurid taxon list by new poorly known and difficult to compare (but having withal a number of autapomorphies) taxa do not make this task easier. The fair attempt to consider all the known ophthalmosaurid taxa and all the proposed phylogenetic characters results in the extremely poorly resolved Ophthalmosauridae (Moon 2017).

Recently Massare & Lomax (2018) demonstrated the effect of large sample sizes on the identification of taxonomically distinct morphological characters in *Ichthyosaurus*. This is what is actually needed for ophthalmosaurids~~: to have larger sample sizes for as many taxa as possible~~. In this regard, Late Jurassic to Early Cretaceous formations of Arctic, considering the abundance

and exceptional preservation of marine reptiles (Delsett *et al*., 2016; NGZ pers. obs.), have great perspectives for collection of a large sample size, comparable to those of the Lias Group and Posidonia Shale lagerstaetten of Western Europe.

Acknowledgements

We thank organizers and participants of the expedition in Franz Joseph Land: N.N. Sobolev, E.A. Korago, E.O. Petrov, S.V. Yudin, P.V. Rekant, A.V. Shmanyak, P.O. Sobolev (all from VSEGEI), N.Yu. Matushkin and N.E. Mikhaltsov (A.A. Trofimuk Institute of Petroleum Geology and Geophysics SB RAS), D.E. Cherepanov (Rosneft Oil Company), very special thanks to V.B. Ershova (Saint Petersburg State University) and A.V. Prokopiev (Diamond and Precious Metal Geology Institute SB RAS). Many thanks to M.A. Rogov (GIN) who managed to second NGZ to Franz-Joseph Land and provided valuable consultations on the stratigraphy and palaeobiogeography of the Boreal Upper Jurassic and Lower Cretaceous. Thanks a lot to T. Poulton for consultations on stratigraphy of Arctic Canada and discussion on the stratigraphic position of CMN 40608. Erin Maxwell (Staatliches Museum für Naturkunde Stuttgart) is thanked for discussion on *Arthropterygius* and for providing valuable photographs of CMN 40608. Jordan Mallon (CMN) is thanked for providing additional photographs of CMN 40608. J.H. Hurum, M.-L. Knudsen Funke, B. Funke, V.S. Engelschiøn and L.L. Delsett are thanked for hospitality and valuable assistance during NGZ work with PMO collections 27–30 September 2017 and 7–8 November 2018. We thank I.A. Starodubtseva (SGM), V.V. Silantiev and M.N. Urazaeva (KSU), I.M. Stenshin (UPM) and O.V. Borodina (YKM) for the opportunity to study materials under their care and kind assistance during NGZ visits. Thanks to the technical support of the Artec 3D company, our research is provided with high-quality 3D models. We thank the Willi Hennig Society for their sponsorship making TNT available for researchers free of pay.

References

Andrews CW. 1910. *A descriptive catalogue of the Marine Reptiles of the Oxford Clay, part I.* British Museum of Natural History, London, 205 pp, 10 pls.

Appleby RM. 1956. The osteology and taxonomy of the fossil reptile *Ophthalmosaurus*. *Proceedings of the Zoological Society of London* **126**:403–447.

Angst D, Buffetaut E, Tabouelle J, Tong H. 2010. An ichthyosaur skull from the Late Jurassic of Svalbard. *Bulletin de la Société Géologique de France* **181**(5):453–458.

Arkhangelsky MS. 1997. On a new ichthyosaurian genus from the Lower Volgian substage of the Saratov, Volga Region. *Paleontological Journal* **31**:87–90.

Arkhangelsky MS. 1998. On the ichthyosaurian fossils from the Volgian stage of the Saratov Region. *Paleontological Journal* **32**:192–196.

Arkhangelsky MS. 2000. On the ichthyosaur *Otschevia* from the Volgian stage of the Volga region. *Paleontological Journal* **34**:549–552.

Arkhangelsky MS. 2001a. The historical sequence of Jurassic and Cretaceous ichthyosaurs. *Paleontological Journal* **35**:521–524.

Arkhangelsky MS. 2001b. On a new ichthyosaur of the genus *Otschevia* from the Volgian Stage of the Volga Region near Ulyanovsk. *Paleontological Journal* **35**:629–634.

Arkhangelsky MS. 2008. Subclass Ichthyopterygia. In Ivakhnenko MF, Kurochkin EN (eds). *Fossil vertebrates of Russia and neighboring countries. Fossil reptiles and birds. Part 1.* GEOS, Moscow. 244–262 [In Russian]

Arkhangelsky MS, Zverkov NG, Spasskaya OS, Evgrafov AV. 2018. On the first reliable record of the ichthyosaur *Ophthalmosaurus icenicus* Seeley in the Oxfordian–Kimmeridgian beds of European Russia. *Paleontological Journal* **52**:49–57 DOI 10.1134/S0031030118010033

Baraboshkin EJ. 1999 Berriasian–Valanginian (Early Cretaceous) sea-ways of the Russian Platform basin and the problem of Boreal/Tethyan correlation. *Geologica Carpathica* **50(1)**: 5–20.

Baraboshkin EYu. 2003. Early Cretaceous straits of the Russian Platform. *Bylleten MOIP. Otdel geologicheskiy* **78(4)**:35–48 [In Russian].

Bardet N, **Fernández M.** 2000. A new ichthyosaur from the Upper Jurassic lithographic limestones of Bavaria. *Journal of Paleontology* **74**:503–511 DOI 10.1017/S0022336000031760

Bardet N, Duffaud S, Martin M, Mazin J-M, Pereda-Suberbiola X, Vidier J-P. 1997. Découverte de l'ichythyosaure *Ophthalmosaurus* dans le Tithonien (Jurassique supérieur) du Boulonnais, Nord de la France. *Neues Jahrbuch für Geologie und Paläontologie, Abhandlungen* **205**:339–354.

Bauer F. 1898. Die Ichthyosaurier des oberen weissen Jura. *Palaeontographica* **44**:283–328.

Baur G. 1887. Uber den Ursprung der Extremitaten der Ichthyopterygia. *Jahresberichte und Mitteilungen des Oberrheinischen Geologischen Vereins* **20**:17–20.

Benson RBJ, Butler RJ, Lindgren J, **Smith AS.** 2010. Mesozoic marine tetrapod diversity: mass extinctions and temporal heterogeneity in geological megabiases affecting vertebrates. *Proceedings of the Royal Society B* **277**:829–834 DOI 10.1098/rspb.2009.1845

Benson RBJ, Druckenmiller PS. 2014. Faunal turnover of marine tetrapods during the Jurassic-Cretaceous transition. *Biological Reviews* **89**(1):1–23 DOI 10.1111/brv.12038

Benson RBJ, Mannion PD, Butler RJ, Goswami A, Evans SE. 2013. Cretaceous tetrapod fossil record sampling and faunal turnover: implications for biogeography and the rise of modern clades. *Palaeogeography, Palaeoclimatology, Palaeoecology* **372**:88–107 DOI 10.1016/j.palaeo.2012.10.028

Bogolubov NN. 1910. On Portlandian ichthyosaurs. *Bulletin de l'Academie Imperiale des Sciences de St.-Petersbourg* **4(6)**:469–476. [In Russian]

Blainville HMD. 1835. Description de quelques especes de reptiles de la Californie, precedee de l'analyse d'un systeme general d'erpetologie et d'amphibiologie. *Nouvelles annals du Muséum d'Histoire naturelle, Paris* **4**:233–296.

Broili F. 1907. Ein neuer Ichthyosaurus aus der norddeutschen Kreide. *Palaeontographica* **54,** 139–162.

Buchy M-C. 2010. First record of *Ophthalmosaurus* (Reptilia: Ichthyosauria) from the Tithonian (Upper Jurassic) of Mexico. *Journal of Paleontology* **84**(1):149–155.

Buchy M-C, López Oliva JG. 2009. Occurrence of a second ichthyosaur genus (Reptilia: Ichthyosauria) in the Late Jurassic Gulf of Mexico. *Boletin de la Sociedad Geologica Mexicana* **61**(2):233–238.

Cleary TJ, Moon BC, Dunhill AM, Benton MJ, Ruta M. 2015. The fossil record of ichthyosaurs, completeness metrics and sampling biases. *Palaeontology* **58**:521–536 DOI 10.1111/pala.12158

Etches S, Clarke J. 1999. Steve Etches Kimmeridge Collection IllustratedCatalogue. Privately printed, Chandler's Ford, Hants.

Deeming DC, Halstead LB, Manabe M, Unwin DM. 1993. An ichthyosaur embryo from the Lower Lias (Jurassic: Hettangian) of Somerset, England, with comments on the reproductive biology of ichthyosaurs. *Modern Geology* **18**:423–442.

Delair JB. 1959. The Mesozoic reptiles of Dorset. Part Three: conclusion. *Proceedings of the Dorset Natural History and Archaeological Society* **81**:59–85.

Delair JB. 1986. Some little known Jurassic ichthyosaurs from Dorset. *Proceedings of the Dorset Natural History and Archaeological Society* **107**:127–134**.**

Delsett LL, Novis LK, Roberts AJ, Koevoets MJ, Hammer Ø, Druckenmiller PS, Hurum JH. 2016. The Slottsmoya marine reptile Lagerstatte: depositional environments, taphonomy and diagenesis. *Geological Society, London, Special Publications* **434**(1):165–188 DOI 10.1144/SP434.2

Delsett LL, Roberts AJ, Druckenmiller PS, Hurum JH. 2017. A new ophthalmosaurid (Ichthyosauria) from Svalbard, Norway, and evolution of the ichthyopterygian pelvic girdle. *PLoS ONE* **12**(1):e0169971 DOI:10.1371/journal.pone.0169971

Delsett LL, Druckenmiller PS, Roberts AJ, Hurum JH. 2018. A new specimen of *Palvennia hoybergeti*: implications for cranial and pectoral girdle anatomy in ophthalmosaurid ichthyosaurs. *PeerJ* **6:**e5776 DOI:10.7717/peerj.5776

Druckenmiller PS, Maxwell EE. 2010. A new Lower Cretaceous (lower Albian) ichthyosaur genus from the Clearwater Formation, Alberta, Canada. *Canadian Journal of Earth Sciences* **47**:1037–1053. DOI 10.1139/E10-028

Druckenmiller PS, Hurum J, Knutsen EM, Nakrem HA. 2012. Two new ophthalmosaurids (Reptilia: Ichthyosauria) from the Agardhfjellet Formation (Upper Jurassic: Volgian/Tithonian), Svalbard, Norway. *Norwegian Journal of Geology* **92**:311–339. https://njg.geologi.no/images/NJG_articles/NJG_2_3_2012_17_Druckenmiller_etal_Pr.pdf

Efimov VM. 1997. A new genus of ichthyosaurs from the Late Cretaceous of the Ulyanovsk Volga Region. *Paleontological Journal* **31**:422–426.

Efimov VM. 1998. An ichthyosaur, *Otschevia pseudoscythica* gen. et sp. nov. from the Upper Jurassic strata of the Ulyanovsk region. *Paleontological Journal* **32**:187–191.

Efimov VM. 1999*a*. Ichthyosaurs of a new genus *Yasykovia* from the Upper Jurassic strata of European Russia. *Paleontological Journal* **33**:92–100.

Efimov VM. 1999*b*. A new family of ichthyosaurs, the Undorosauridae fam. nov. from the Volgian stage of the European part of Russia. *Paleontological Journal* **33**:174–181.

Embry AF. 1994. Uppermost Triassic, Jurassic, and lowermost Cretaceous stratigraphy, Melville Island area, Arctic Canada. In Christie RL, McMillan NJ (eds), *The Geology of Melville Island, Arctic Canada*. Geological Survey of Canada Bulletin 450:139–159 DOI 10.4095/194013

Ensom PC, Clements RG, Feist-Burkhardt S, Milner AR, Chitolie J, Jeffery PA, Jones C. 2009. The age and identity of an ichthyosaur reputedly from the Purbeck Limestone Group, Lower Cretaceous, Dorset, southern England. *Cretaceous Research* **30**:699–709 DOI 10.1016/j.cretres.2008.12.005

Fernández M. 1994. A new long-snouted ichthyosaur from the early Bajocian of Neuquén basin (Argentina). *Ameghiniana* **31:**291–297.

Fernández M. 1997. A new ichthyosaur from the Tithonian (Late Jurassic) of the Neuquen Basin (Argentina). *Journal of Paleontology* **71**:479–484.

Fernández M.S. 1999. A new ichthyosaur from the Los Molles Formation (Early Bajocian), Neuquen Basin, Argentina. *Journal of Paleontology* **73**(4):677–681.

Fernández MS. 2000. Late Jurassic ichthyosaurs from the Neuquén Basin, Argentina. *Historical Biology* **14**:133–136 DOI 10.1080/10292380009380561

Fernández M, Aguirre-Urreta MB. 2005. Revision of *Platypterygius hauthali* von Huene, 1927 (Ichthyosauria, Ophthalmosauridae) from the Early Cretaceous of Patagonia, Argentina. *Journal of Vertebrate Paleontology* **25**:583–587 DOI 10.1671/0272-4634(2005)025[0583:ROPHVH]2.0.CO;2

Fernández MS. 2007a. Redescription and phylogenetic position of *Caypullisaurus* (Ichthyosauria:Ophthalmosauridae). *Journal of Paleontology* **81**:368–375.

Fernández MS. 2007b. Chapter 11. Ichthyosauria. In: Gasparini Z, Salgado L, Coria RA, eds. *Patagonian Mesozoic reptiles*. Indiana University Press, Bloomington and Indianapolis:271–291.

Fernández MS, Maxwell EE. 2012. The genus *Arthropterygius* Maxwell (Ichthyosauria: Ophthalmosauridae) in the Late Jurassic of the Neuquen Basin, Argentina. *Geobios* **45**:535–540 DOI 10.1016/j.geobios.2012.02.001

Fernández M, Talevi M. 2014. Ophthalmosaurian (Ichthyosauria) records from the Aalenian–Bajocian of Patagonia (Argentina): an overview. *Geological Magazine* **151**:49–59 DOI 10.1017/S0016756813000058

Fischer V. 2012. New data on the ichthyosaur *Platypterygius hercynicus* and its implications for the validity of the genus. *Acta Palaeontologica Polonica* **57** 123–134 DOI 10.4202/app.2011.0007

Fischer V, Masure E, Arkhangelsky MS, Godefroit P. 2011. A new Barremian (Early Cretaceous) ichthyosaur from Western Russia. *Journal of Vertebrate Paleontology* **31**:1010–1025 DOI 10.1080/02724634.2011.595464

Fischer V, Maisch MW, Naish D, Kosma R, Liston J, Joger U, Krüger FJ, Pardo Pérez J, Tainsh J, Appleby RM. 2012. New ophthalmosaurid ichthyosaurs from the European Lower Cretaceous demonstrate extensive ichthyosaur survival across the Jurassic–Cretaceous boundary. *PLOS ONE* **7(1):**e29234. DOI:10.1371/journal.pone.0029234

Fischer V, Appleby RM, Naish D, Liston J, Riding JB, Brindley S, Godefroit P. 2013. A basal thunnosaurian from Iraq reveals disparate phylogenetic origins for Cretaceous ichthyosaurs. *Biology Letters* **9**:20130021. DOI:10.1098/rsbl.2013.0021

Fischer V, Arkhangelsky MS, Uspensky GN, Stenshin IM, Godefroit P. 2014a. A new Lower Cretaceous ichthyosaur from Russia reveals skull shape conservatism within Ophthalmosaurinae. *Geological Magazine* **151**:60–70 DOI 10.1017/S0016756812000994

Fischer V, Bardet N, Guiomar M, Godefroit P. 2014b. High diversity in Cretaceous ichthyosaurs from Europe prior to their extinction. *PLOS ONE*, **9**(1), e84709. DOI:10.1371/journal.pone.0084709

Fraas EE. 1913. Ein unverdrückter Ichthyosaurus-Schädel. *Jahreshefte des Vereins für vaterländische Naturkunde in Württemberg* **69**:1–12.

Gasparini Z, Spalletti L, de la Fuente MS. 1997. Tithonian marine reptilesof the Western Neuquén Basin, Argentina. Facies and palaeoenvironments. *Geobios*, **30**:701–712 DOI 10.1016/S0016-6995(97)80158-1

Gasparini Z, Fernández MS, de La Fuente MS, Herrera Y, Codorniú L, Garrido A. 2015. Reptiles from lithographic limestones of the Los Catutos member (Middle–Upper Tithonian), Neuquén Province, Argentina: an essay on its taxonomic composition and preservation in an environmental and geographic context. *Ameghiniana* **52**(1):1–28 DOI 10.5710/AMGH.14.08.2014.2738

Gilmore CW. 1905. Osteology of *Baptanodon* (Marsh). *Memoirs of the Carnegie Museum*, **II**:77–129.

Godefroit P. 1993. Les grands ichthyosaures sinémuriens d'Arlon. *Bulletin de l'Institut Royal des Sciences Naturelles de Belgique Sciences de la Terre* **63**:25–71.

Goloboff P, Catalano S. 2016. TNT, version 1.5, with a full implementation of phylogenetic morphometrics. *Cladistics* DOI. 10.1111/cla.12160

Grange DR, Storrs GW, Carpenter S, Etches S. 1996. An important marine vertebrate-bearing locality from the Lower Kimmeridge Clay (Upper Jurassic) of Westbury, Wiltshire. *Proceedings of the Geologists' Association* **107**:107–116.

Green JP, Lomax DR. 2014. An ichthyosaur (Reptilia: Ichthyosauria) specimen from the Lower Cretaceous (Berriasian) Spilsby Sandstone Formation of Nettleton, Lincolnshire, UK. *Proceedings of the Geologists' Association* **125**:432–436 DOI 10.1016/j.pgeola.2014.08.007

Hammer Ø, Harper DAT, Ryan PD. 2001. PAST: Paleontological Statistics Software Package for Education and Data Analysis. *Palaeontologia Electronica* **4**(1): DOI. http://palaeo-electronica.org/2001_1/past/issue1_01.htm

Huene Fvon. 1922. *Die Ichthyosaurier des Lias und ihre Zusammenhänge*. *Monographien zur Geologie und Paläontologie, 1*. Verlag von Gebruder Borntraeger, Berlin, 114 pp.

Hulke JW. 1871. Note on an *Ichthyosaurus* (*I. enthekiodon*) from Kimmeridge Bay, Dorset. *Quarterly Journal of the Geological Society of London* **27**:440–441.

Jeletzky JA. 1965. Upper Volgian (Latest Jurassic) ammonites and Buchias of Arctic Canada. *Geological Survey of Canada, Bulletin* 128:1–51.

Jeletzky JA. 1973. Biochronology of the marine boreal latest Jurassic, Berriasian and Valanginian in Canada. In: Casey R, Rawson PF, eds. *The Boreal Lower Cretaceous*. Geological Journal Special Issue 5: 41–80.

Johnson R. 1979. The osteology of the pectoral complex of *Stenopterygius* Jaekel (Reptilia: Ichthyosauria). *Neues Jahrbuch für Geologie und Paläontologie, Abhandlungen* **159**:41–86.

Kabanov KA. 1959. [Burial of Jurassic and Cretaceous reptiles in the region of Ulyanovsk.] *Izvestiya Kazanskogo Filiala AN SSSR, Seriya Geologicheskikh Nauk* **7**:211–214. [In Russian].

Kasansky P. 1903. Ueber die Ichthyosaurus-Knochen aus dem Sysranischem Kreise des Gouvernement Simbirsk. *Trudy Obshchestva estestvoispytatelej pri Imperatorskom Kazanskom Universitete* [*Proceedings of the Naturalists Society, Kazan Imperial University*] **37**(3):1–33. [In Russian].

Kosteva NN. 2005. Stratigraphy of the Jurassic–Cretaceous deposits of Franz Joseph Land Archipeago. *Arctica i Antarctica* [*Arctic and Antarctic*] **4**(38):16–32. [In Russian].

Kravets VS, Mesezhnikov MS, Slonimsky GA. 1976. Structure of the Jurassic – Lower Cretaceous deposits in the basin of Pechora River. *Trudy VNIGRI* **388**:27–41. [In Russian].

Kear BP. Cranial morphology of *Platypterygius longmani* Wade, 1990 (Reptilia: Ichthyosauria) from the Lower Cretaceous of Australia. *Zoological Journal of the Linnean Society* **145**: 583–622 DOI 10.1111/j.1096-3642.2005.00199.x

Kirton AM. 1983. *A review of British Upper Jurassic ichthyosaurs*. Ph.D. thesis, University of Newcastle-upon-Tyne. 239 p. (pdf available at EThOS: https://ethos.bl.uk/OrderDetails.do?uin=uk.bl.ethos.344855).

Kiselev DN, Rogov MA. 2018. Ammonites and stratigraphy of the terminal part of the Middle Volgian substage (Upper Jurassic; *Epivirgatites nikitini* Zone and its equivalents) of the Panboreal Realm: 2. *Titanites* and *Glaucolithites*. *Stratigraphy and Geological Correlation*, **26**(1), 18–66 DOI 10.1134/S0869593818010057

Kiselev DN, Rogov MA, Zakharov VA. 2018. The *Volgidiscus singularis* Zone of the terminal horizons of the Volgian Stage of European Russia and its significance for interregional correlation and paleogeography. *Stratigraphy and Geological Correlation* **26**(2):206–233 DOI 10.1134/S0869593818020053

Kolb C, Sander PM. 2009. Redescription of the ichthyosaur *Platypterygius hercynicus* (Kuhn 1946) from the Lower Cretaceous of Salzgitter (Lower Saxony, Germany). *Palaeontographica. Abteilung A (Paläozoologie, Stratigraphie)* **288**:151–192.

Kuhn O. 1946. Ein skelett von *Ichthyosaurus hercynicus* n. sp. aus dem Aptien von Gitter. *Berichte der Naturforschenden Gesellschaft Bamb* **29**:69–82.

Maisch MW, Matzke AT. 2000.The Ichthyosauria. *Stuttgarter Beiträge zur Naturkde. Serie B (Geologie und Paläontologie)* **298**:1–159.

Mansell-Pleydell JC. 1890. Memoir upon a new ichthyopterygian from the Kimmeridge Clay of Gillingham, Dorset, *Ophthalmosaurus pleydelli*. *Proceedings of the Dorset Natural History and Antiquarian Field Club* **11**:7–15.

Marek R, Moon BC, Williams M, Benton MJ. 2015. The skull and endocranium of a Lower Jurassic ichthyosaur based on digital reconstructions. *Palaeontology* **58**:723–742 DOI 10.1111/pala.12174

Massare JA, Lomax DR. 2018. Hindfins of *Ichthyosaurus*: effects of large sample size on 'distinct' morphological characters. *Geological Magazine*. [In press] DOI:10.1017/S0016756818000146

Maxwell EE. 2010. Generic reassignment of an ichthyosaur from the Queen Elizabeth Islands, Northwest Territories, Canada. *Journal of Vertebrate Paleontology* **2**(30):403–415 DOI 10.1080/02724631003617944

Maxwell EE, Caldwell MW. 2006a. A new genus of ichthyosaur from the Lower Cretaceous of Western Canada. *Palaeontology* **49**:1043–1052 DOI 10.1111/j.1475-4983.2006.00589.x

Maxwell EE, Kear BP. 2010. Postcranial anatomy of *Platypterygius americanus* (Reptilia: Ichthyosauria) from the Cretaceous of Wyoming. *Journal of Vertebrate Paleontology* **30:**1059–1068 DOI 10.1080/02724634.2010.483546

Maxwell E, Fernandez MS, Schoch RR. 2012. First diagnostic marine reptile remains from the Aalenian (Middle Jurassic): a new ichthyosaur from southwestern Germany. *PLoS ONE*, **7**(8):e41692. DOI:10.1371/journal.pone.0041692

McGowan C. 1972. The systematics of Cretaceous ichthyosaurs with particular reference to the material from North America. *Contributions to Geology, University of Wyoming* **11:**9–29.

McGowan C. 1973a. The cranial morphology of the Lower Liassic latipinnate ichthyosaurs of England. *Bulletin of the British Museum (Natural History), Geology* **24**:1–109.

McGowan C. 1973b. Differential growth in three ichthyosaurs: *Ichthyosaurus communis*, *I. breviceps*, and *Stenopterygius quadriscissus* (Reptilia, Ichthyosauria). *Life Sciences Contributions, Royal Ontario Museum* **93**:1–21. DOI 10.5962/bhl.title.52086

McGowan C. 1976. The description and phenetic relationships of a new ichthyosaur genus from the Upper Jurassic of England. *Canadian Journal of Earth Sciences* **13**:668–683. DOI 10.1139/e76-070

McGowan C. 1997. The taxonomic status of the late Jurassic ichthyosaur *Grendelius mordax*: a preliminary report. *Journal of Vertebrate Palaeontology* **17**:428–430. DOI 10.1080/02724634.1997.10010986

McGowan C, Motani R. 2003. *Handbook of Paleoherpetology, Part 8, Ichthyopterygia.* Verlag Dr. Friedrich Pfeil, Munich, 175 pp.

Mitta VV, Alekseev AS, Shik SM eds. 2012. *Unified regional stratigraphic scheme of the Jurassic of East European Platform*. PIN RAS – VNIGNI, Moscow: 64 p. + 14 tables. [In Russian].

Mesezhnikov MS, Zakharov VA 1974. Volgian paleozoogeography of the North of Eurasia. In: Dagis AS, Zakharov VA eds. *Mesozoic Palaeobiogeography of North Eurasia*. Novosibirsk, Nauka:87–100. [in Russian]

Meyer Hvon. 1864. *Ichthyosaurus leptospondylus* Wag.? aus dem lithostratigraphischen Schiefer von Eichstätt. *Palaeontographica* **11:**222–225.

Moon BC. 2017. A new phylogeny of ichthyosaurs (Reptilia: Diapsida). *Journal of Systematic Palaeontology* DOI 10.1080/14772019.2017.1394922

Moon BC, Kirton AM. 2016. *Ichthyosaurs of the British Middle and Upper Jurassic. Part 1, Ophthalmosaurus.* Monograph of the Palaeontographical Society, London: 84 pp., 30 pls. DOI 10.1080/02693445.2016.11963958

Motani R. 2005. True skull roof configuration of *Ichthyosaurus* and *Stenopterygius* and its implications. *Journal of Vertebrate Paleontology* **35**:338–342 DOI 10.1671/0272-4634(2005)025[0338:TSRCOI]2.0.CO;2

Motani R, Huang J, Jiang D-Y, Tintori A, Rieppel O, You H, Hu Y-Ch, Zhang R. 2018. Separating sexual dimorphism from other morphological variation in a specimen complex of fossil marine reptiles (Reptilia, Ichthyosauriformes, *Chaohusaurus*). *Scientific Reports* **8**: 14978. DOI 10.1038/s41598-018-33302-4

Mutterlose J, Brumsack H, Flogel S, Hay W, Klein C, Langrock U, Lipinski M, Ricken W, Soding E, Stein R, Swientek O. 2003. The Greenland-Norwegian Seaway: A key area for understanding Late Jurassic to Early Cretaceous paleoenvironments. *Paleoceanography* **18**(1): 1–26.

Nace RL. 1939. A new ichthyosaur from the Upper Cretaceous Mowry Formation of Wyoming. *American Journal of Science* **237**:673–686 DOI 10.2475/ajs.237.9.673

Paparella I, Maxwell E, Cipriani A, Roncacè S, Caldwell M. 2017. The first ophthalmosaurid ichthyosaur from the Upper Jurassic of the Umbrian–Marchean Apennines (Marche, Central Italy). *Geological Magazine* **154(4)**:837–858 DOI 10.1017/S0016756816000455

Pol D, Escapa IH. 2009. Unstable taxa in cladistics analysis: identification and the assessment of relevant characters. *Cladistics* **25**:515–527. DOI 10.1111/j.1096-0031.2009.00258.x

Poulton TP. 1994. Jurassic stratigraphy and fossil occurrences - Melville, Prince Patrick, and Borden Islands. In: Christie RL, McMillan NJ, eds. *The Geology of Melville Island*, *Arctic Canada.* Geological Survey of Canada, Bulletin 450:161–193 DOI 10.4095/194013

Roberts AJ, Druckenmiller PS, Sætre GP, Hurum JH. 2014. A new upper Jurassic ophthalmosaurid ichthyosaur from the Slottsmoya Member, Agardhfjellet Formation of Central Spitsbergen. *PLoS ONE*, **9**(8), e103152 DOI 10.1371/journal.pone.0103152

Rogov MA. 2010. New data on ammonites and stratigraphy of the Volgian Stage in Spitzbergen. *Stratigraphy and Geological Correlation* **18**:505–531 DOI 10.1134/S0869593810050047

Rogov MA. 2012. Latitudinal gradient of taxonomic richness of ammonites in the Kimmeridgian–Volgian in the northern hemisphere. *Paleontological Journal* **46**(2):148–156 DOI 10.1134/S0031030112020104

Rogov MA. 2013a. Ammonites and Infrazonal Subdivision of the Dorsoplanites panderi Zone (Volgian Stage, Upper Jurassic) of the European Part of Russia. *Doklady Earth Sciences* **451**(2):803–808.

Rogov MA. 2013b. The end-Jurassic extinction. In *Extinction, Grzimek's Animal Life Encyclopedia*, Gale/Cengage Learning, Detroit: 487–495.

Rogov MA. 2014. *Khetoceras* (Craspeditidae, Ammonoidea) - a new genus from the Volgian Stage of Northern Middle Siberia, and parallel evolution of Late Volgian Boreal ammonites. *Paleontological Journal* **48**:457–464 DOI 10.1134/S0031030114050086

Rogov MA, Poulton TP. 2015. Aulacostephanid ammonites from the Kimmeridgian (Upper Jurassic) of British Columbia (western Canada) and their significance for correlation and palaeobiogeography. *Bulletin of Geosciences* **90**:7–20 DOI 10.3140/bull.geosci.1501

Rogov M, Zakharov V. 2009. Ammonite- and bivalve-based biostratigraphy and Panboreal correlation of the Volgian Stage. *Science in China, Series D, Earth Sciences* **52**:1890–1909.

Rogov M, Zakharov V. Kiselev D. 2008. Molluscan immigrations via biogeographical ecotone of the Middle Russian Sea during the Jurassic. *Volumina Jurassica* VI:143-152.

Rogov M, Zverkov N, Zakharov V, Ershova V. 2016. New biostratigraphic data on the Upper Jurassic – Lower Cretaceous of Franz Joseph Land. In: Alekseev AS. ed. Paleostrat-2016. Annual meeting of the Paleontological Section of the Soc. Natur. Moscow, January 26-27, 2016. Program and abstracts. Paleontological Instute, Moscow:70–71

Romer AS. 1968. An ichthyosaur skull from the Cretaceous of Wyoming. *Contributions to Geology*, *University of Wyoming* **7**:27–41.

Russell DA. 1994. Jurassic marine reptiles from Cape Grassy, Melville Island, Arctic Canada. In Christie RL, McMillan NJ eds. *The Geology of Melville Island, Arctic Canada*. Geological Survey of Canada Bulletin 450: 195–201 DOI 10.4095/194013

Sasonova IG, Sasonov NT. 1967. *Paleogeography of the Russian Platform during Jurassic and Early Cretaceous time*. Nedra, Moscow, 260 p. [In Russian].

Sauvage HE. 1911. Les ichtyosauriens des formations jurassiques du Boulonnais. *Bulletin de la Société Académique de l'Arrondissement de Boulogne-sur-Mer* **9**:424–445.

Shang Q, Li C. 2013. The sexual dimorphism of *Shastasaurus tangae* (Reptilia: Ichthyosauria) from the Triassic Guanling Biota, China. *Vertebrata PalAsiatica* **51**(4):253–264.

Sollas WJ. 1916. The skull of Ichthyosaurus, studied in serial sections. *Philosophical Transactions of the Royal Society of London, Series B* **208:** 63–126.

Storrs GW, Arkhangel'skii MS, Efimov VM. 2000. Mesozoic marine reptiles of Russia and other former Soviet republics. In: Benton M, Shishkin MA, Unwin DM, Kurochkin EN (eds). *The age of dinosaurs in Russia and Mongolia*. Cambridge University Press, Cambridge: 187–210.

Tennant JP, Mannion PD, Upchurch P, Sutton MD, Price GD. 2017. Biotic and environmental dynamics through the Late Jurassic- Early Cretaceous transition: evidence for protracted faunal and ecological turnover. *Biological Reviews* **92**(2):776–814 DOI 10.1111/brv.12255

Wade M. 1984. *Platypterygius australis*, an Australian Cretaceous ichthyosaur. *Lethaia* **17**: 99–113 DOI 10.1111/j.1502-3931.1984.tb01713.x

Wade M. 1990. A review of the Australian Cretaceous longipinnate ichthyosaur *Platypterygius* (Ichthyosauria, Ichthyopterygia). *Memoirs of the Queensland Museum* **28**:115–137. biostor.org/reference/109670

Wagner A. 1852. Neu-aufgefundene Saurier-Ueberreste aus den lithographischen Schiefern und dem obern Jurakalk. *Abhandlungen der Mathematischen-Physikalischen Classe der* Königlich Bayerischen Akademie der Wissenschaften **6**:663–710.

Wagner A. 1853. Die Characteristic einer neuen Art von *Ichthyosaurus* aus den lithographischen Schiefern und eines Zahnes von *Polyptychodon* aus dom Gründsandstein von Kelheim. *Bulletin der königliche Akademie der Wissenschaft, Gelehrte Anzeigen* **3**:25–35.

Yakovleva SP ed. 1993. *Unified stratigraphical scheme of the Jurassic deposits of the Russian Platform*. Saint-Petersburg. 28 sheets, 71 pp. [In Russian].

Zakharov VA. 1987. The bivalve *Buchia* and the Jurassic-Cretaceous Boundary in the Boreal Province. *Cretaceous Research* **8**:141–153 DOI 10.1016/0195-6671(87)90018-8

Zakharov VA, Rogov MA., Dzyuba OS, Žák K, Košťák M, Pruner P, Skupien P, Chadima M, Mazuch M, Nikitenko BL. 2014. Palaeoenvironments and palaeoceanography changes across the Jurassic/Cretaceous boundary in the Arctic Realm: Case study of the Nordvik section (north Siberia, Russia). *Polar Research* 33:e19714 DOI 10.3402/polar.v33.19714

Zammit M, Norris RM, Kear BP. 2010. The Australian Cretaceous ichthyosaur *Platypterygius australis*: a description and review of postcranial remains. *Journal of Vertebrate Paleontology* **30**:1726–1735 DOI 10.1080/02724634.2010.521930.

Zverkov NG, Arkhangelsky MS, Pardo Perez JM, Beznosov PA. 2015. On the Upper Jurassic ichthyosaur remains from the Russian North. *Proceedings of the Zoological Institute RAS* **319**:81–97 https://www.zin.ru/journals/trudyzin/doc/vol_319_1/TZ_319_1_Zverkov.pdf

Zverkov NG, Arkhangelsky MS, Stenshin IM. 2015. A review of Russian Upper Jurassic ichthyosaurs with an intermedium/humeral contact: Reassessing *Grendelius* McGowan, 1976. *Proceedings of the Zoological Institute RAS* **319**:558–588 https://www.zin.ru/journals/trudyzin/doc/vol_319_4/TZ_319_4_Zverkov.pdf

Zverkov NG, Fischer V, Madzia D, Benson RBJ. 2018. Increased pliosaurid dental disparity across the Jurassic–Cretaceous transition. *Palaeontology* **61**(6): 825–846.

Zverkov NG, Efimov VM. 2018. Revision of *Undorosaurus* Efimov, 1999b, a mysterious Late Jurassic ichthyosaur of the Boreal Realm. *Journal of Systematic Palaeontology*, [Accepted] DOI 10.108014772019.2018.1515793

Zverkov NG, **Prilepskaya NE.** 2019. A prevalence of *Arthropterygius* (Ichthyosauria: Ophrhalmosauridae) in the Late Jurassic – early Early Cretaceous of the Boreal Realm. figshare. Dataset. DOI 10.6084/m9.figshare.7406522 [will be activated upon acceptance]

Temporary links for review process:

Appendix 1 - https://figshare.com/s/86060e131038fe382ed6

Character-taxon matrix - https://figshare.com/s/3cccf2a076d5a68e9127

Appendix 3 Skeletal elements of juvenile *Arthropterygius chrisorum* CCMGE 3-16/13328 - https://figshare.com/s/9deb1ae8565441499385

Appendix 4 Skeletal elements of young adult *Arthropterygius chrisorum* CCMGE 17-44/13328 – https://figshare.com/s/18191adbeef7d2ffa2d7

Figure 1

Maps showing the discovery sites of *Arthropterygius* in Russia and globally.

(A) Map of Franz-Joseph Land with localities on Berghaus Island (1), and on Wilczek Land (2). (B) Map of a part of Timan-Pechora Basin, with the locality near Porozhsk Village (3). (C) Map of the middle Volga Region with the locatities near Gorodischi Village (4), Kashpir Village (5), and Novaya Racheyka Village (6). (M) The locality on Melville Island, Arctic Canada. (S) Localities on Svalbard, Norway.

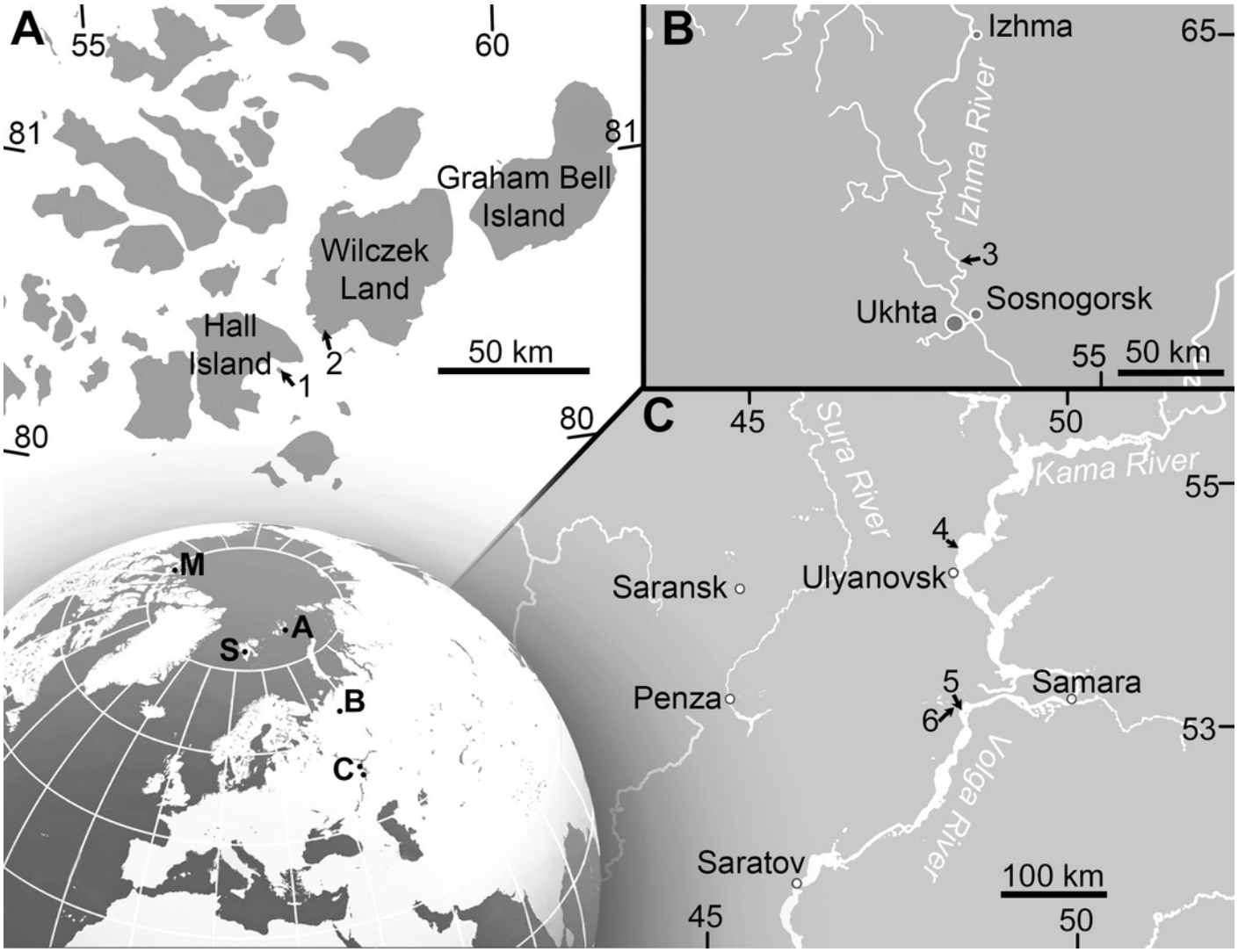

Figure 2

Cranial remains of *Arthropterygius chrisorum* CCMGE 17-44/13328 (A–J) and PMO 222.669 (L, M).

(A, B) Right postfrontal in ventral (A) and dorsal (B) views. (C) Left lateral view on articulated postfrontal, prefrontal and nasal. (D) Left prefrontal in ventral view. (E, F) Right prefrontal in ventral (E) and dorsal (F) views. (G, H) left nasal in dorsal (G) and ventral (H) views. (I, J) Right jugal in medial (I) and lateral (J) views. (K) Cranial reconstruction, showing the depicted elements (colored). (L, M) oblique dorsal view and interpretation of sutures of the skull roof of PMO 222.669. Abbreviations: ffr, facet for the frontal; fnas, facet of the nasal; fpo, facet for the postorbital; fpref, facet for the prefrontal; fqj, facet for the quadratojugal; fsut, facet for the supratemporal; lw, lateral wing of the nasal lamella; nas, nasal; par, parietal; pf, parietal foramen; pref, prefrontal; sut, supratemporal. Both scale bars represent 10 cm.

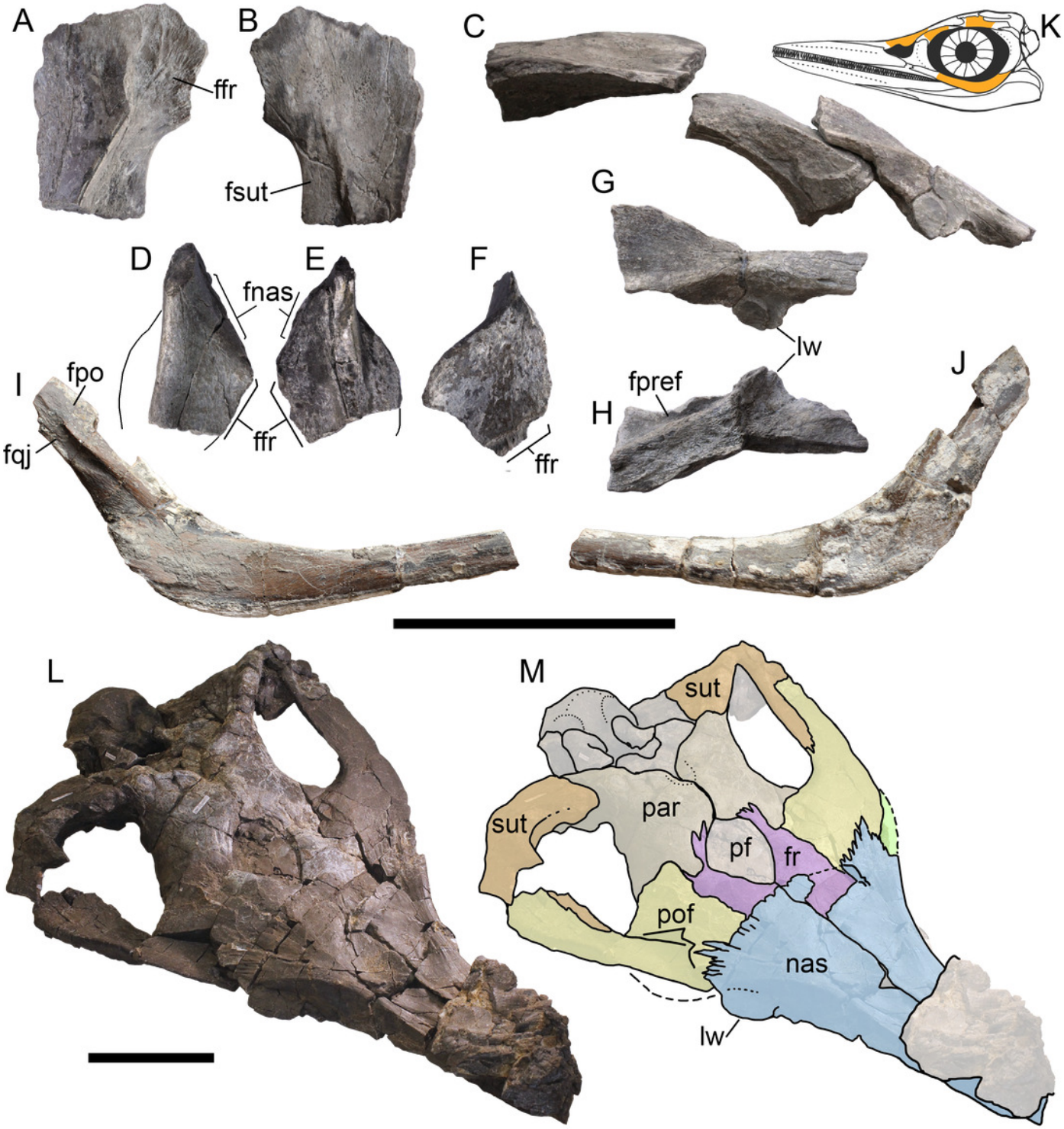
A
ffr
B
fsut
C
K
G
lw
D
E
fnas
ffr
F
ffr
I
fpo
fqj
H
fpref
J
L
M
sut
sut
par
pf
fr
pof
nas
lw

Figure 3

Cranial elements of *Arthropterygius chrisorum* CCMGE 3-16/13328 and 17-44/13328.

(A – I) Basisphenoids of CCMGE 17-44/13328 (A–D) and CCMGE 3-16/13328 (E–I) in ventral (A, E), dorsal (B, F), anterior (C, H) and lateral (D, G) views, and sagittal section of the basisphenoid (I). (J–Q) Left quadrates of CCMGE 17-44/13328(J–M) and CCMGE 3-16/13328 (N–Q) in posteromedial (J, O), anterolateral (K, Q), posterolateral (L, P) and ventral (M, N) views. (R) Supratemporal process of the right parietal of CCMGE 3-16/13328 in dorsal view. (S) Articulated fragments of the right supratemporal and parietal of CCMGE 3-16/13328 in posterior view. (T, V) Medial ramus of the left supratemporal of CCMGE 3-16/13328 in medial (T) and posterior (V) views; U, medial ramus of the right supratemporal of CCMGE 3-16/13328 in medial view. Abbreviations: art.b, articular boss; dpl, dorsal plateau of the basisphenoid; fbo, facet for the basioccipital; fop, facet for the opisthotic; fpt, facet for the pterygoid; fqj, facet for the quadratojugal; fst, facet for the stapes; icf, foramen for the internal carotid arteries; sur.b, surangular boss; trab, facets for cartilaginous continuation of the *cristae trabeculares*; VII, groove of the palatine ramus of facial (VII) nerve. Scale bar represents 5 cm.

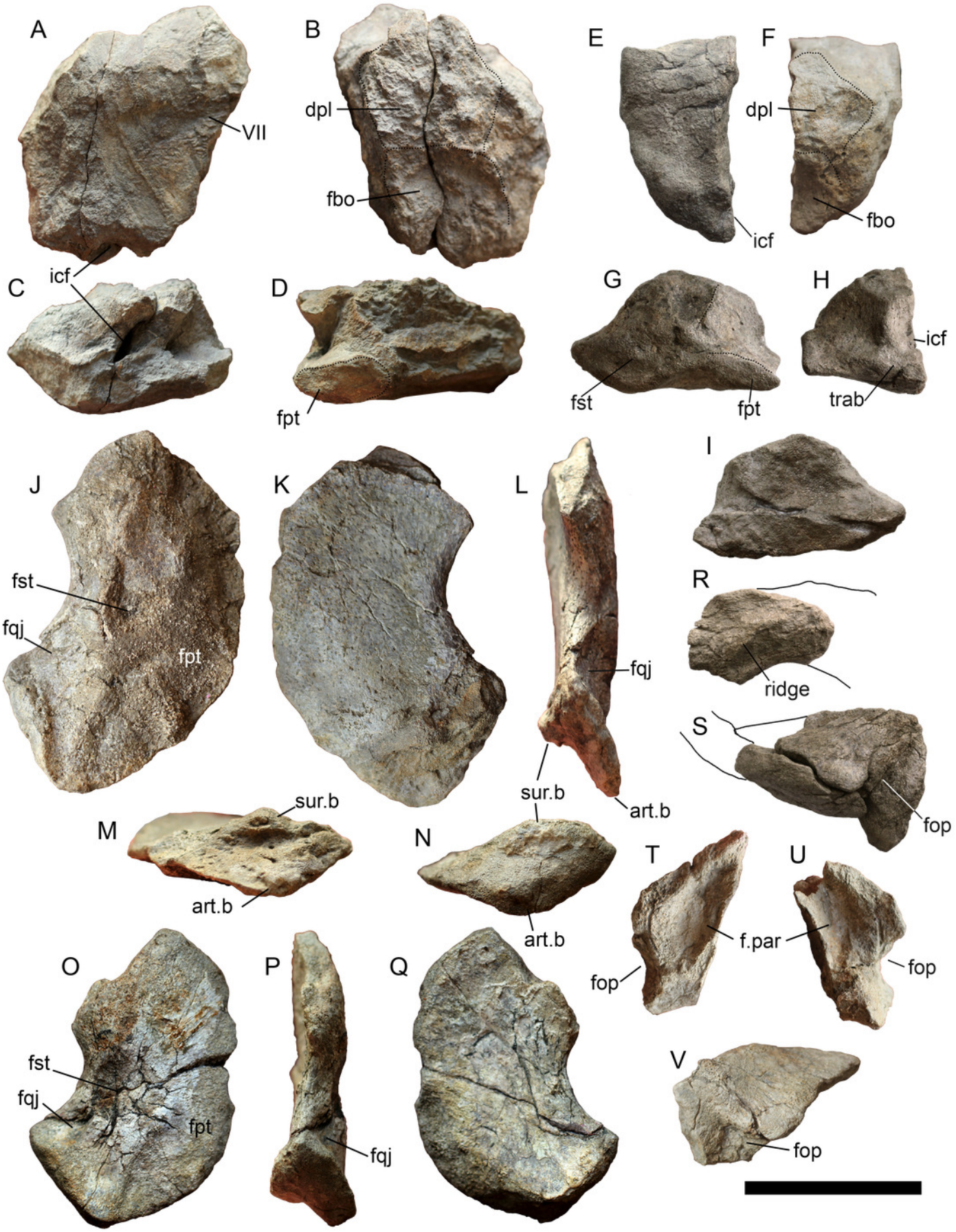
A
VII
B
dpl
fbo
E
icf
F
dpl
fbo
C
icf
D
fpt
G
fst
fpt
H
icf
trab
J
fst
fqj
fpt
K
L
fqj
sur.b
art.b
I
R
ridge
S
fop
M
sur.b
art.b
N
art.b
T
fop
U
f.par
fop
O
fst
fqj
fpt
P
fqj
Q
V
fop

Figure 4

Opisthotic, stapes and exoccipital of *Arthropterygius chrisorum* PMO 222.669.

(A) Articulated right opisthotic and stapes in posterior view. (B, C) Right opisthotic in lateral (B) and ventral (C) views. (D–F) Right stapes in dorsal (D), anterior (E) and lateral (F) views; G, right exoccipital in medial view. Abbreviations: fbo, facet for the basioccipital; fbs, facet for the basisphenoid; fst, facet for the stapes; hg, groove for transmission of hyomandibular branch of facial (VII) or glossopharyngeal (XI) nerve; mr, muscular ridge on the opisthotic. Scale bar represents 5 cm.

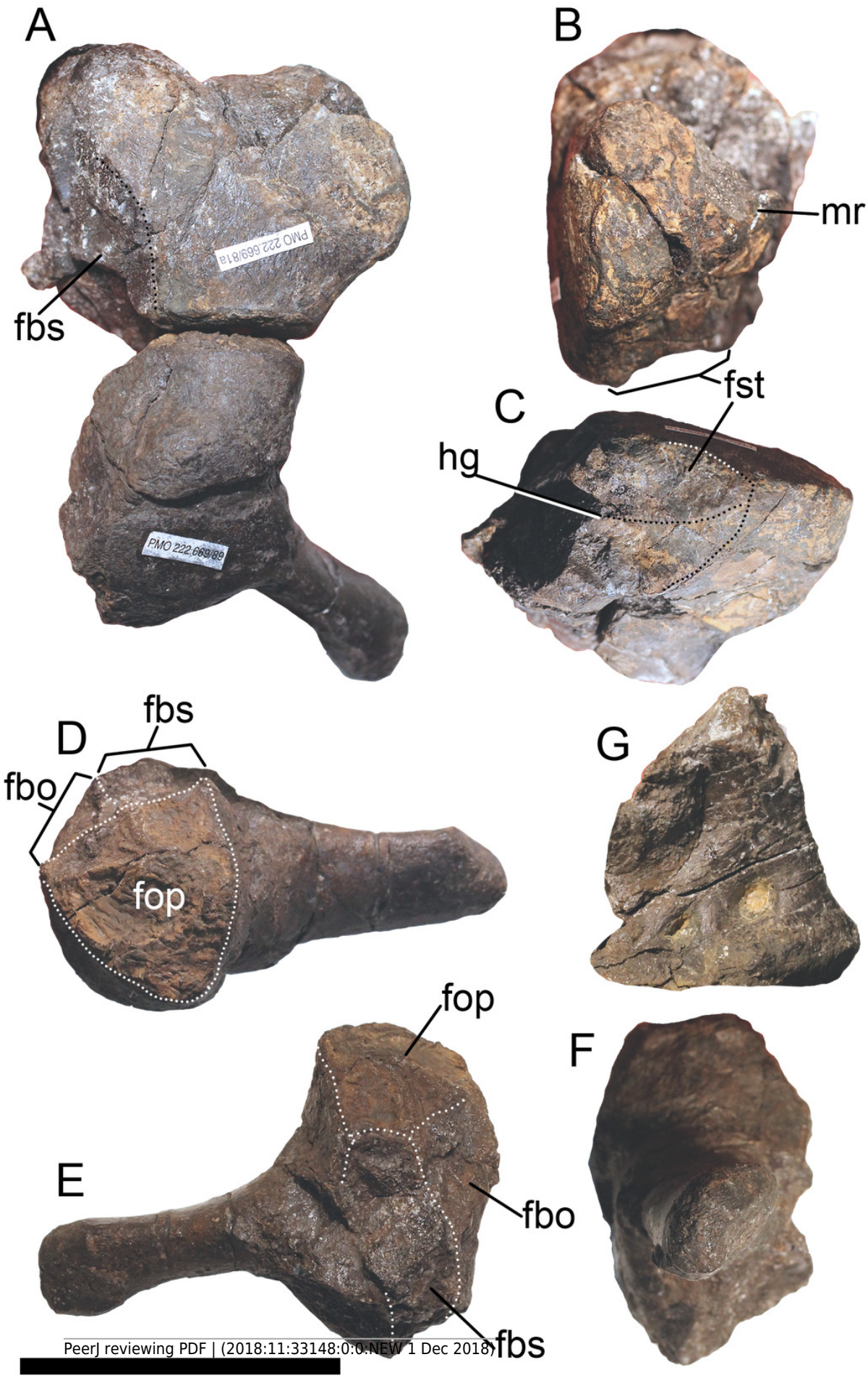
A
fbs
PMO 222.669/81a
PMO 222.669/89
B
mr
fst
C
hg
D
fbs
fbo
fop
G
E
fop
fbo
fbs
F

Figure 5

Left mandibular ramus of *Arthropterygius chrisorum* CCMGE 17-44/13328 in lateral (A) and medial (B, C) views.

Abbreviations: ang, angular; ma, muscle (*M. adductor mandibulae externus*) attachment point; pcp, paracoronoid process; pre, prearticular; spl, splenial; sur, surangular. Scale bar represents 10 cm.

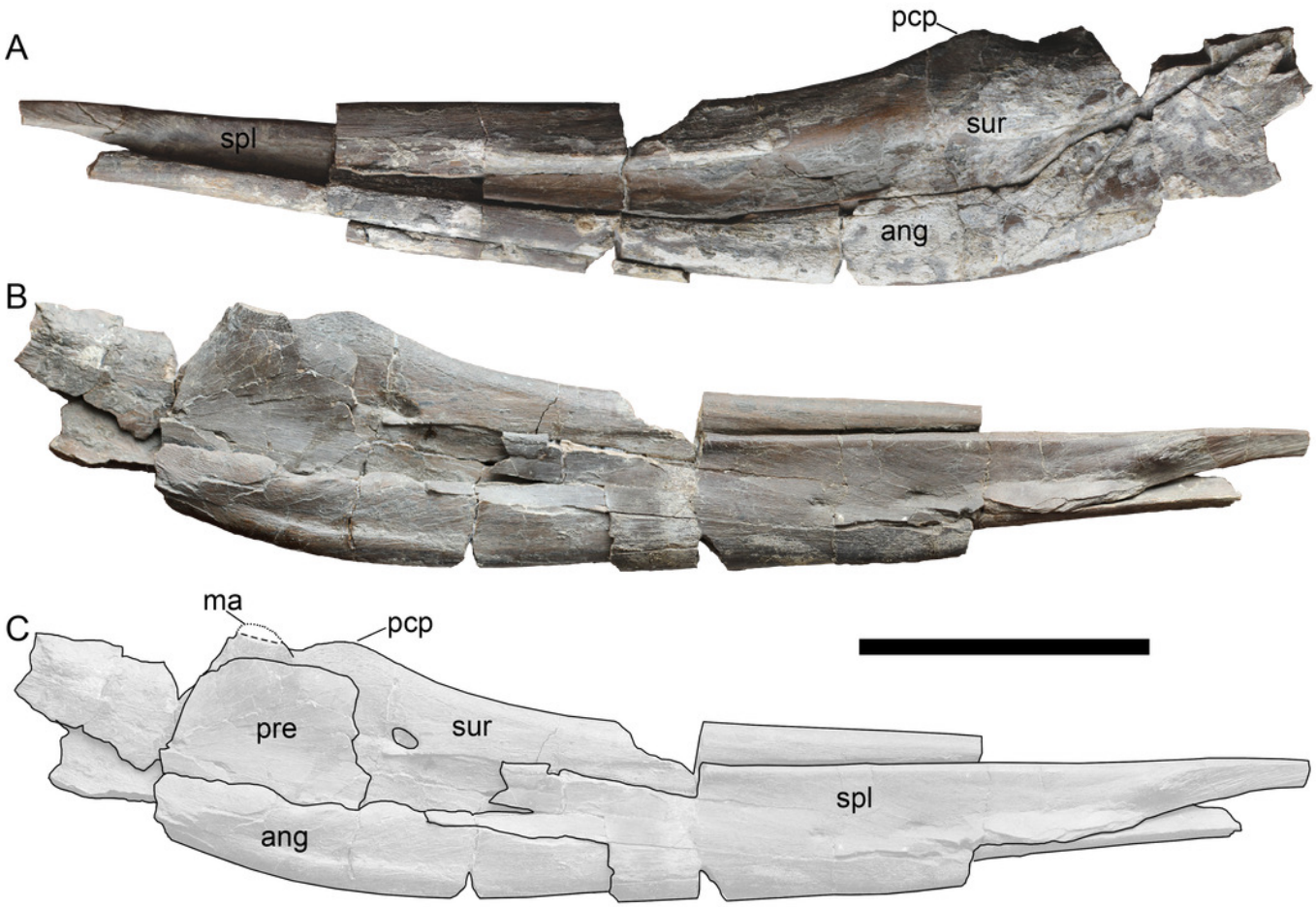

Figure 6

Selected vertebral centra of *Arthropterygius chrisorum* SGM 1573 (A–K) and CCMGE 3-16/13328 (L–A').

(A–C) Atlas-axis complex in anterior (A), right lateral (B) and posterior (C) views. (D–G, L–O) Anterior presacral vertebral centra. (H–K, P–U) Posterior presacral vertebral centra. (V–A') Caudal centra. Each centrum depicted in articular and lateral views respectively. Scale bar represents 5 cm.

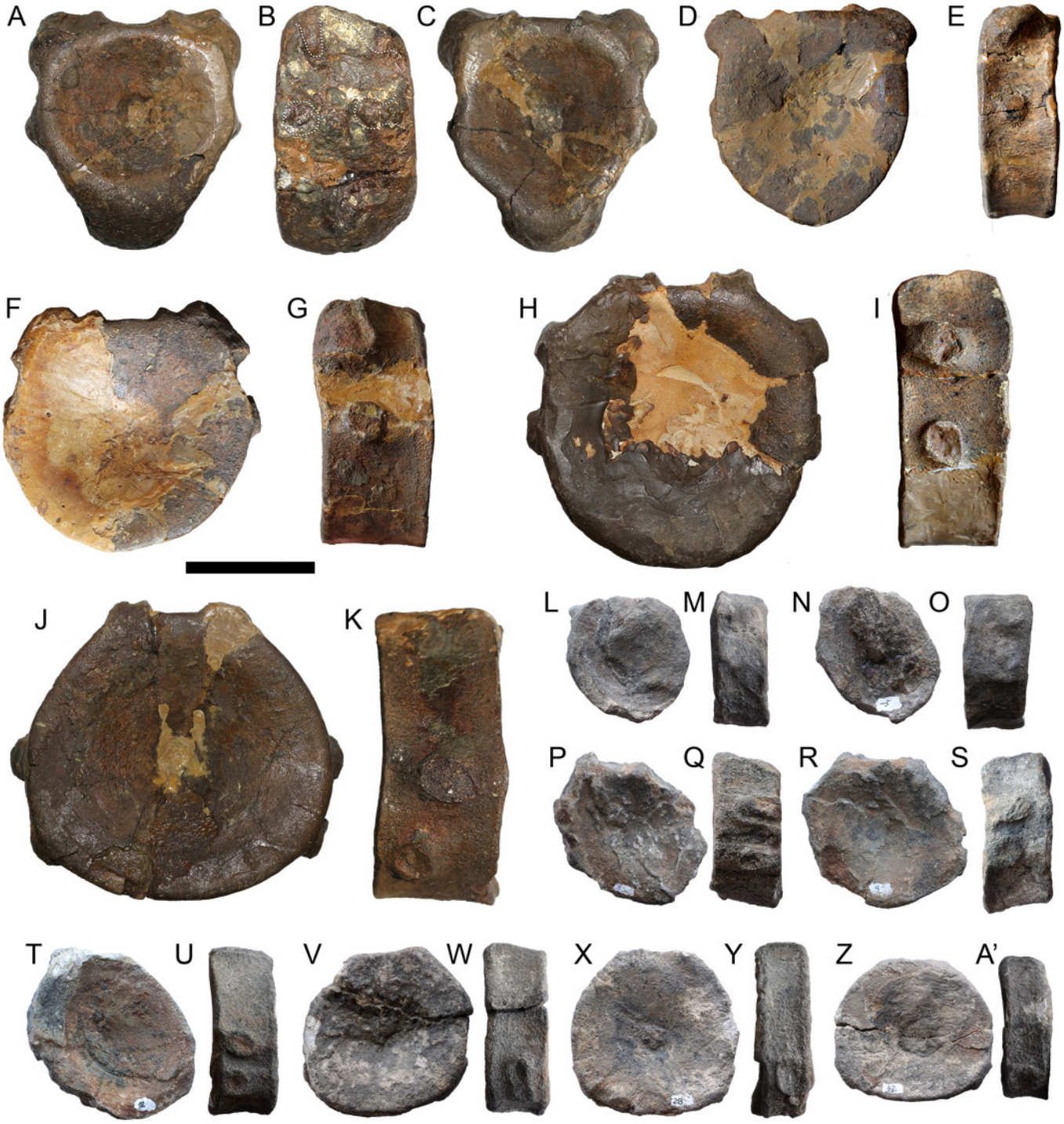
A
B
C
D
E
F
G
H
I
J
K
L
M
N
O
P
Q
R
S
T
U
V
W
X
Y
Z
A'

Figure 7

Forelimb and pectoral girdle elements of *Arthropterygius chrisorum* CCMGE 17-44/13328 (A–E, X–B’), CCMGE 3-16/13328 (F–R), and SGM 1573 (S–W, C’–E’).

(A) Right forelimb of CCMGE 17-44/13328 in ventral view. (B–F) Right humerus of CCMGE 17-44/13328 in posterior (B), dorsal (C), distal (D) and proximal (E) views. (F) right forelimb of CCMGE 3-16/13328 in dorsal view. (G–K) Right humerus of CCMGE 3-16/13328 in ventral (G), distal (H), anterior (I), posterior (J) and proximal (K) views. (J–M) Left scapula of CCMGE 3-16/13328 in lateral (J), medial (K), anterior (L) and proximal (M) views. (N) Interclavicle of CCMGE 3-16/13328; O–R,coracoids of CCMGE 3-16/13328 in anterior (O) and ventral disarticulated (P) views, lateral (R) and medial (S) views of the right coracoid. (S–W) Right humerus of SGM 1573 in dorsal (T), ventral (U), posterior (V), distal (W) and proximal (K) views. (X–Z) Right clavicle of CCMGE 17-44/13328 in anterior (Y), posterior (Z) and ventral (A’) views. (A’) Fragmentary interclavicle of CCMGE 17-44/13328 in dorsal view. (B’) Dorsal ramus of the left scapula of CCMGE 17-44/13328 in lateral view. (C’, D’) interclavicle of SGM 1573 in ventral (D’) and dorsal (E’) views. (E’) fragmentary dorsal ramus of the scapula of SGM 1573. Abbreviations: aae, anterior accessory epipodial element; acr, acromial process; amp, anteromedial process of the coracoid; atb, anterior transverse bar of the iterclavicle; dpc, deltopectoral crest; faae, facet for the anterior accessory epipodial element; fcor, facet for the coracoid; fgl, glenoid contribution; fr, facet for the radius; fsc, facet for the scapula; fu, facet for the ulna; i, intermedium; mst, bulge in the middle of the interclavicle posterior median stem; pi, pisiform; r, radius; ra, radiale; td, dorsal process; u, ulna; ul, ulnare. Scale bar represents 10 cm.


A
B
td
C
F
G
J
K
L
u
r
i
H
acr
M
fcor
fgl
I
td
acr
N
aae
r
u
pi
ra
i
D
fu
fr
faae
O
dpc
td
E
dpc
S
td
T
P
amp
Q
fsc
fgl
R
faae
fr
X
A'
Y
fsc
B'
U
V
faae
fr
fu
Z
C'
D'
atb
E'
td
W
mst
mst
dpc

Figure 8

Left femur (A–F) and partial ischiopubis (G) of *Arthropterygius chrisorum* CCMGE 17-44/13328.

Femur in ventral (A), anterior (B), proximal (C), distal (D), dorsal (E) and posterior (F) views. *Abbreviations*: dp, dorsal process of the femur; ffi, facet for the fibula; fti, facet for the tibia; vp, ventral process of the femur. Scale bar represents 5 cm.

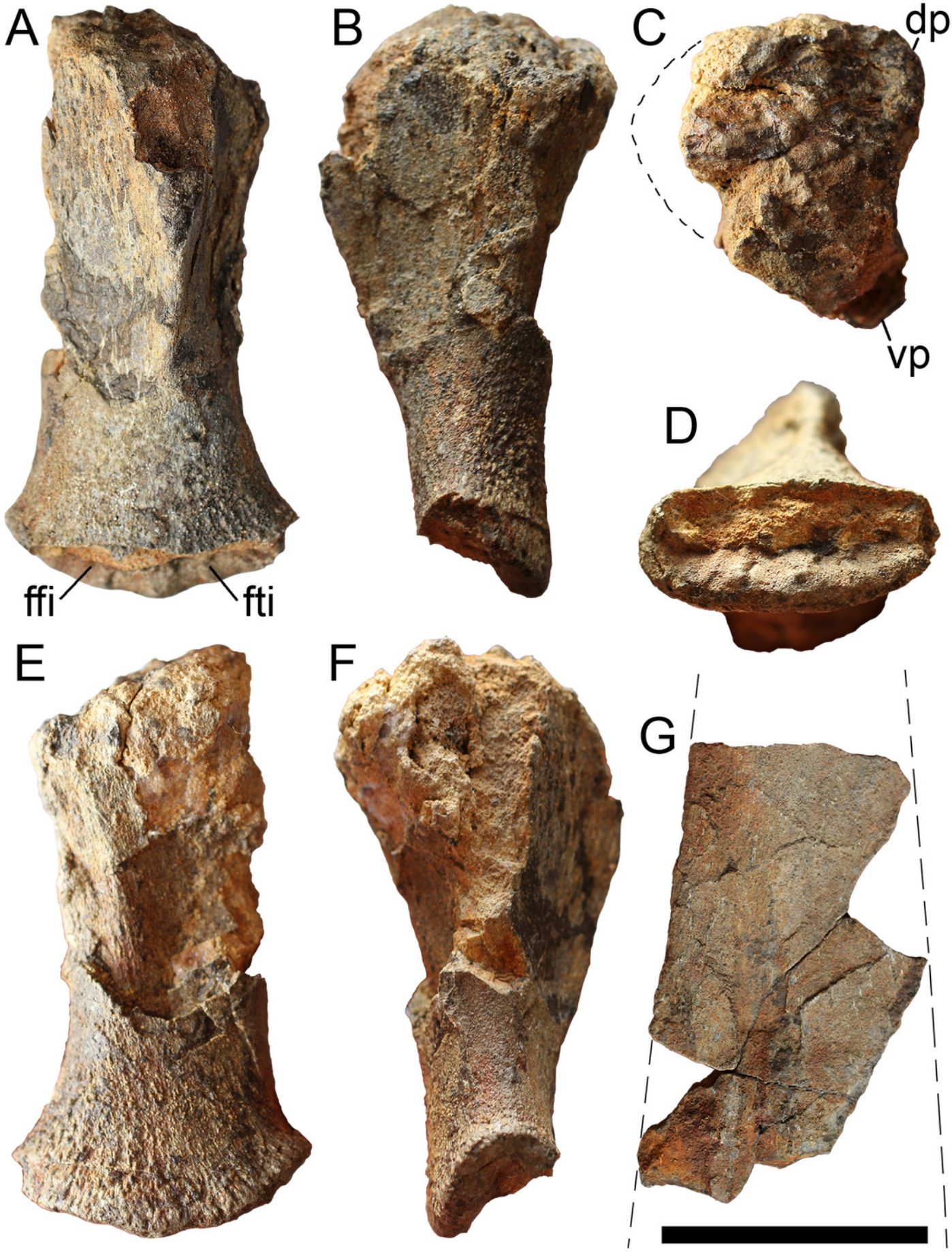
A
B
C
dp
vp
D
ffi
fti
E
F
G

Figure 9(on next page)

Skeletal reconstructions of *Arthropterygius chrisorum* old adult based on CMN 40608 and SGM 1573 (A) young adult based on CCMGE 17-44/13328 and PMO 222.669 (B) and juvenile based on CCMGE 3-16/13328 and PMO 222.655 (C).

Unknown skeletal regions are shown in grey. Scale bar equals 1 m.

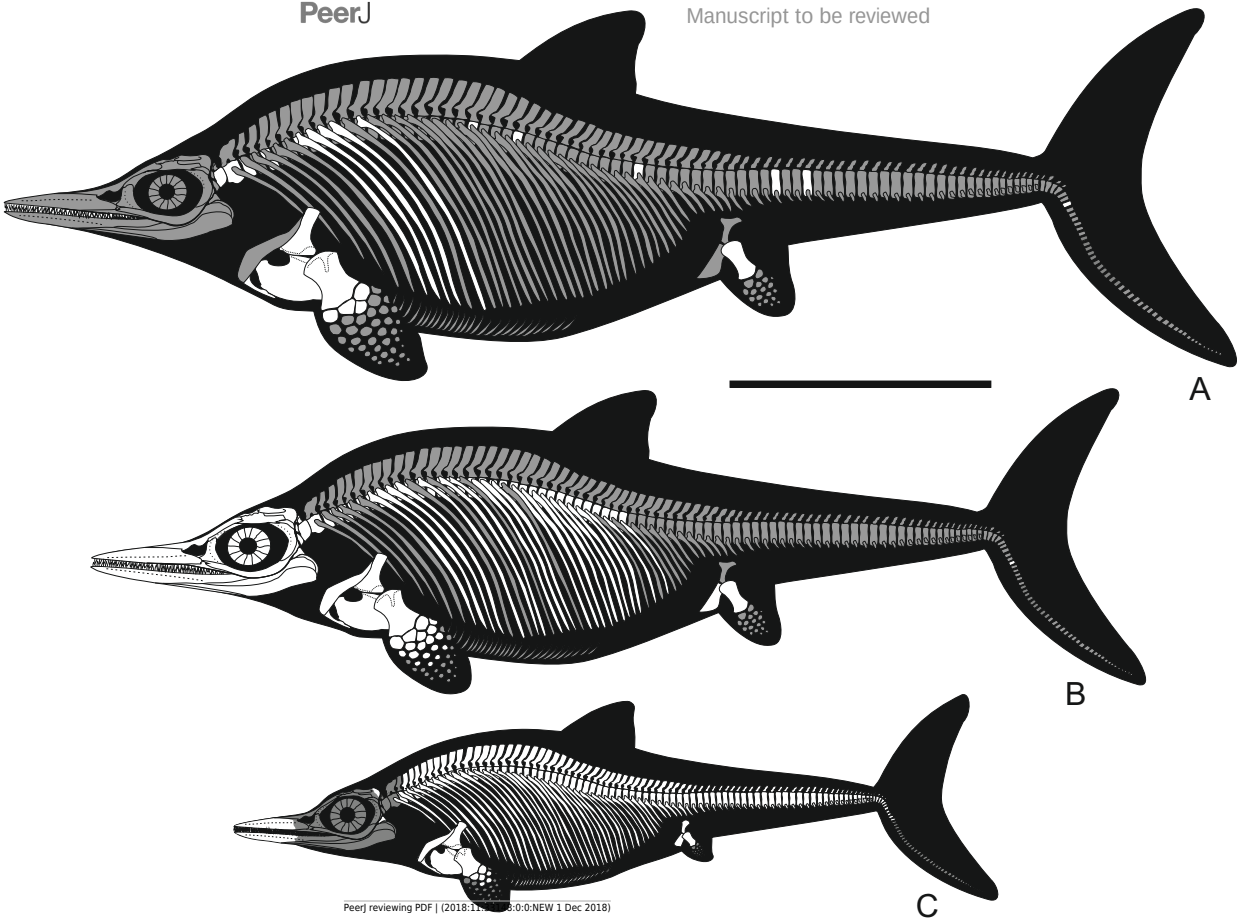
A
B
C

Figure 10(on next page)

Cranial and postcranial ontogeny of *Arthropterygius chrisorum.*

(A) simplified 'plot' showing measurements of various cranial and postcranial elements versus hypothesized ontogenetic stage of the specimen (specimens are arranged equidistantly to each other and divided onto three ontogenetic categories: juveniles, young adults and mature). (B–C) ontogenetic series of selected skeletal elements of *Arthropterygius chrisorum*, from top to bottom: basisphenoids in ventral view; quadrates in posteromedial view; humeri in proximal wiew; forelimbs in dorsal view; humeri in distal view; coracoids in ventral view; femora in ventral view; posterior presacral vertebrae in articular and lateral views. Specimens: juvenile of *A. chrisorum* CCMGE 3-16/13328 (B, F, L, N, S, W, C', D'); young adults of *A. chrisorum* CCMGE 17-44/13328 (C, G, K, O, T, A') and PMO 222.669 (D, H, J, P, U, X); large mature individuals of *A. chrisorum* CMN 40608 (E, Q, V, Y, B', E', F') and SGM 1573 (I, E', F'); juvenile of *Arthropterygius* sp. juv. cf. *A. chrisorum* PMO 222,655 (M, R, Z); E, Q, V, Y and B' are modified from Maxwell (2010). Scale bars for B–H equal 5 cm, for I–F' – 10 cm.

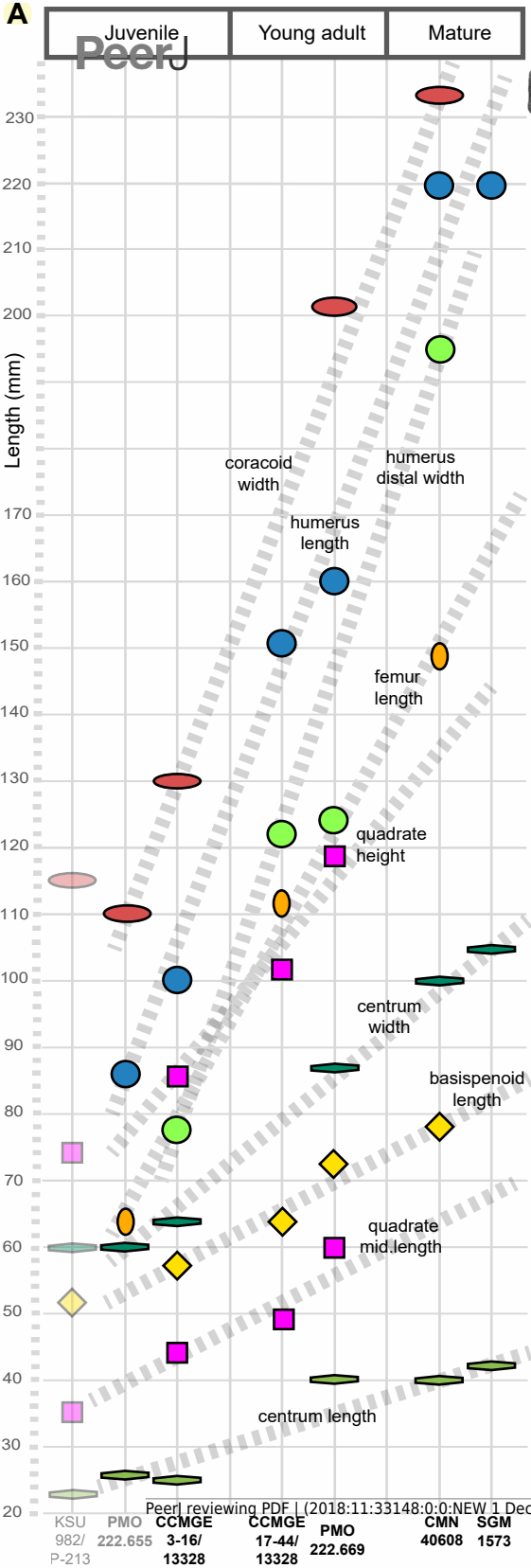

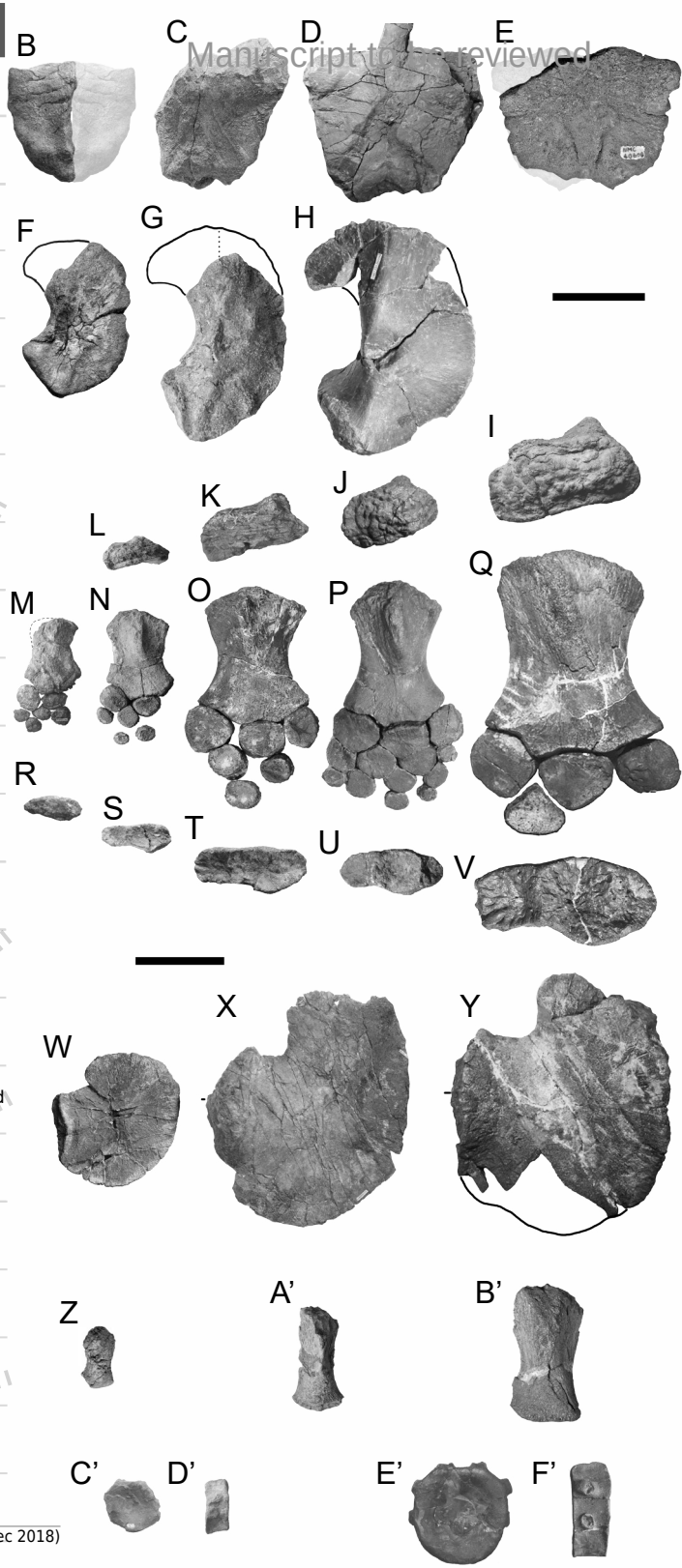

Figure 11

Skull roof (A) and postorbital region (B) of *Arthropterygius hoybergeti* SVB 1451.

Abbreviations: ex(l), left exoccipital; fbo, facet of the basisphenoid for the basioccipital; nas, nasal; op(r), right opisthotic; pf, parietal foramen; porb, postorbital; pref, prefrontal; sat, supratemporal anteromedial tongue; sq, squamosal; st(l), left stapes. Scale bars represent 10 cm.

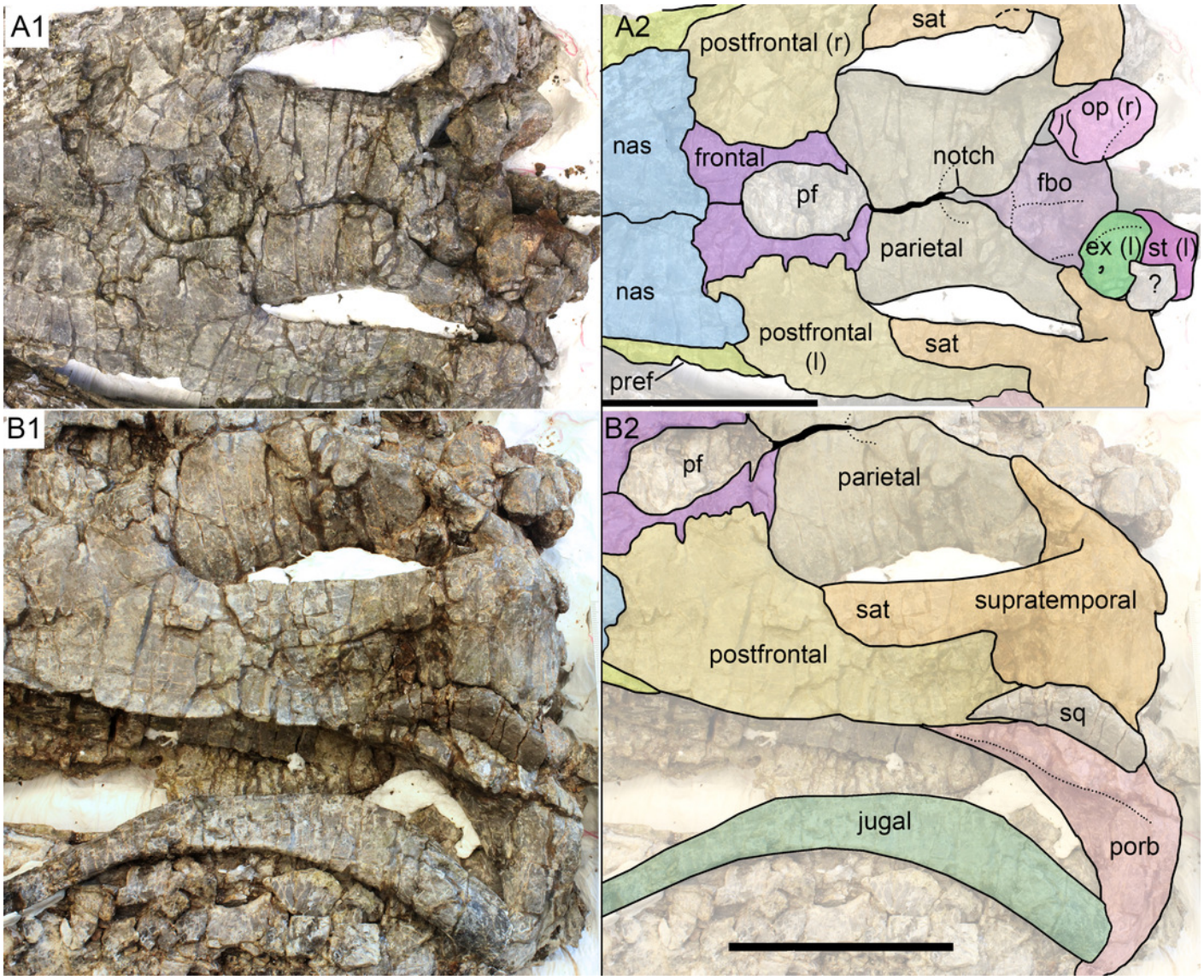

Figure 12

Occipital region elements of *Arthropterygius hoybergeti* SVB 1451.

(A) Partially reconstructed occiput in oblique posterodorsal view (left opisthotic is mirrored and mounted as right in order to complement the picture). (B) Basisphenoid in ventral view. (C–I) Left opisthotic in posterior (C), anterior (D), ventral (E), dorsal (F), medial (G, H) and lateral (I) views. (J–N) Right stapes in medial (J), distal (K), posterolateral (L), dorsal (M) and ventral (N) views. (O) Right quadrate in posteromedial view. (P) Left quadrate in ventral view. Abbreviations: am, ampulla; ap, angular protrusion of the quadrate; art.b, articular boss; bpt, basipterygoid process; fbo, facet for the basioccipital; fbs, facet for the basisphenoid; fst, facet for the stapes; hc, impression of horizontal semicircular canal; hg, groove for transmission of hyomandibular branch of facial (VII) or glossopharyngeal (XI) nerve; hy, hyoid process; icf, foramen for the internal carotid arteries; ipc, impression of posterior vertical semicircular canal; mr, muscular ridge on the opisthotic; occl, occipital lamella; sac, sacculus; sur.b, surangular boss; ut, utriculus; vf, vagus foramen. Scale bar represents 5 cm.

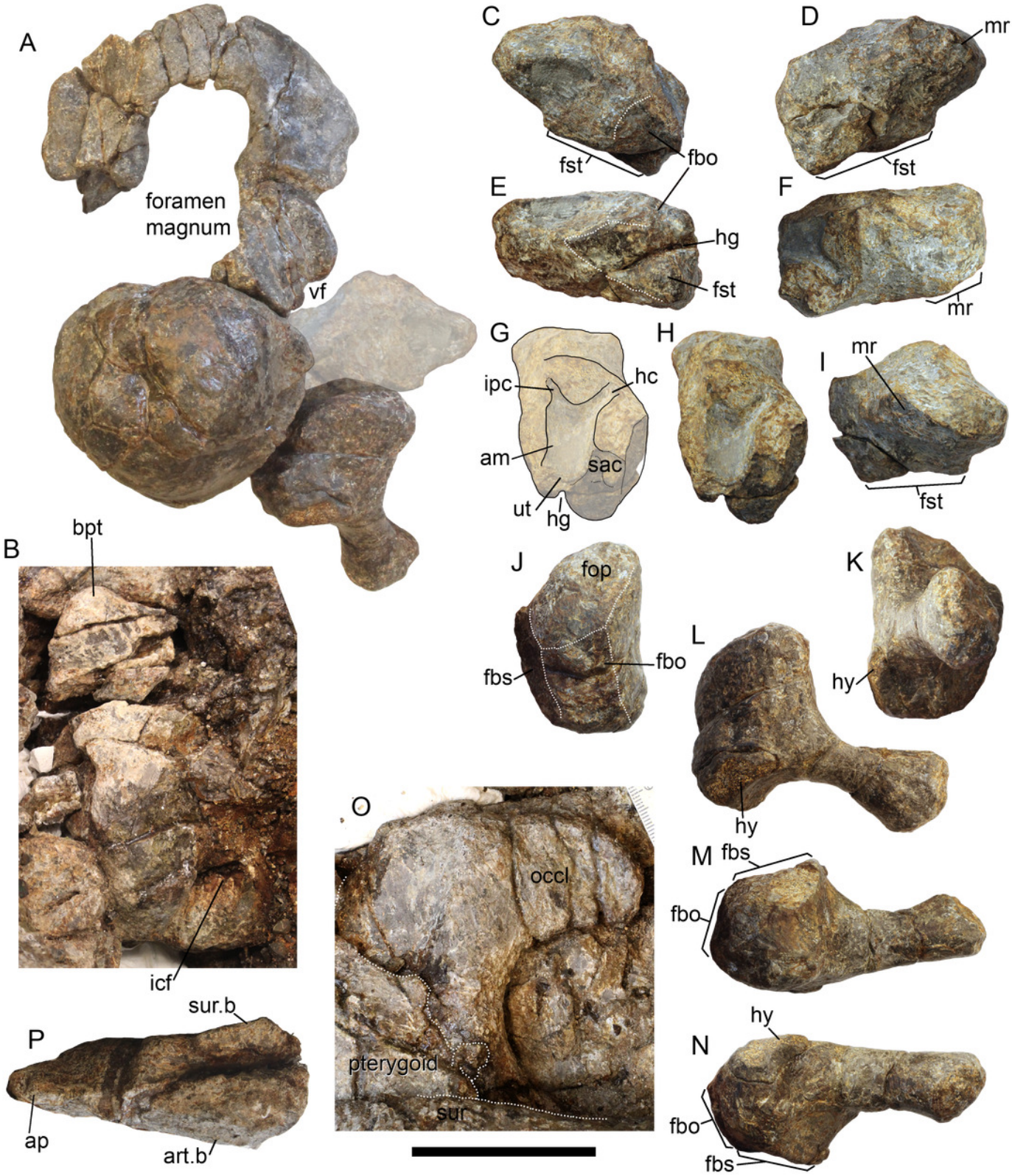
A
foramen
magnum
vf
B
bpt
icf
C
fst
fbo
D
mr
fst
E
hg
fst
F
mr
G
ipc
hc
am
sac
ut
hg
H
I
mr
fst
J
fop
fbs
fbo
K
hy
L
hy
M
fbs
fbo
N
hy
fbo
fbs
O
occl
pterygoid
sur
P
sur.b
ap
art.b

Figure 13

Teeth of *Arthropterygius hoybergeti* SVB 1451 (A) and *A. lundi* SGM 1502 (B, C).

Scale bars represent 10 mm.

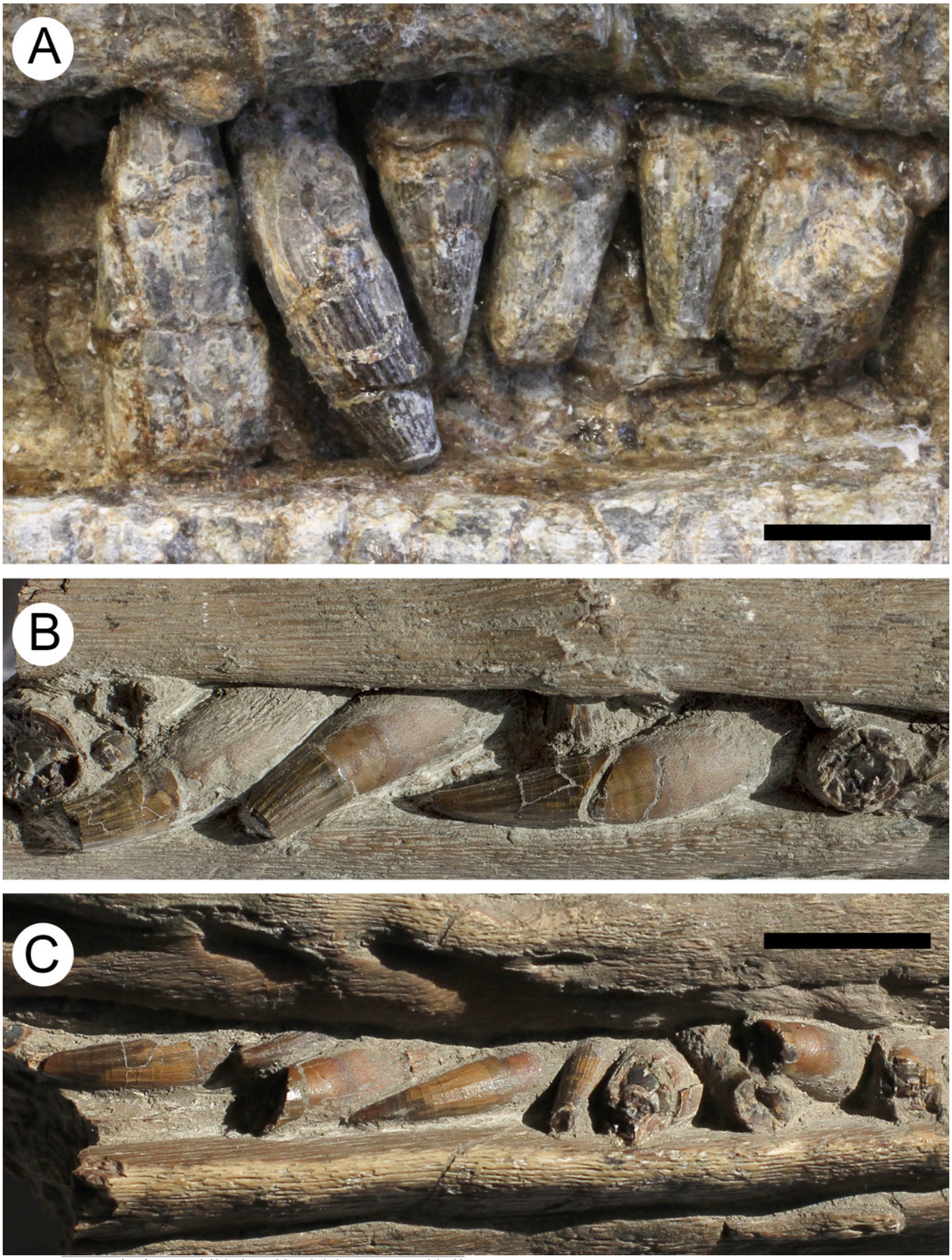
A
B
C

Figure 14

Forelimb and pectoral girdle elements of *Arthropterygius hoybergeti*.

(A) Right clavicle of SVB 1451 in external view. (B, C) Dorsal ramus of the left scapula of SVB 1451 in external view (B) and cross-section (C). (D, E) Proximal portion of the right humerus of SVB 1451 in proximal (D) and anteroventral (E) views; F, partially reconstructed forelimb of SVB 1451. (G–K) Left humerus UPM 2442 in ventral (G), posterior (H), proximal (I), distal (J) and dorsal (K) views. (L–O) Right humerus YKM 63548 in dorsal (L), posterior (M), distal (N) and proximal (O) views. (P, Q) A cast of the partial left forelimb of YKM 63548 in proximal (P) and dorsal (L) views. Abbreviations: aae, anterior accessory epipodial element; dpc, deltopectoral crest; faae, facet for the anterior accessory epipodial element; fr, facet for the radius; fu, facet for the ulna; i, intermedium; r, radius; ra, radiale; td, dorsal process; u, ulna; ul, ulnare. Scale bar represents 5 cm.


A
B
C
D
dpc
E
F
aae
r
u
?ra
i
G
dpc
fu
H
td
I
td
dpc
J
faae
fr
fu
K
td
faae
fu
L
fu
faae
M
td
N
fu
fr
P
td
dpc
O
td
dpc
Q
td
r
u
i

Figure 15

Skull of *Arthropterygius lundi* PMO 222.654 in right dorsolateral view (A) and its inner side in posteromedial view (C). Interpretations of sutures (B, D).

Abbreviations: ang, angular; ar, articular; bs, basisphenoid; fro, frontal; fst, facet for the stapes; lac, lacrimal; lw, lateral wing of the nasal lamella; ms, medial symphysis; mx, maxilla; nas, nasal; occl, occipital lamella; pf, parietal foramen; pm, premaxilla; porb, postorbital; pre, prearticular; pref, prefrontal; pt, pterygoid; sat, supratemporal anteromedial tongue; spl, splenial; sur, surangular; sut, supratemporal; q, quadrate; qj, quadratojugal. Scale bar represents 10 cm.

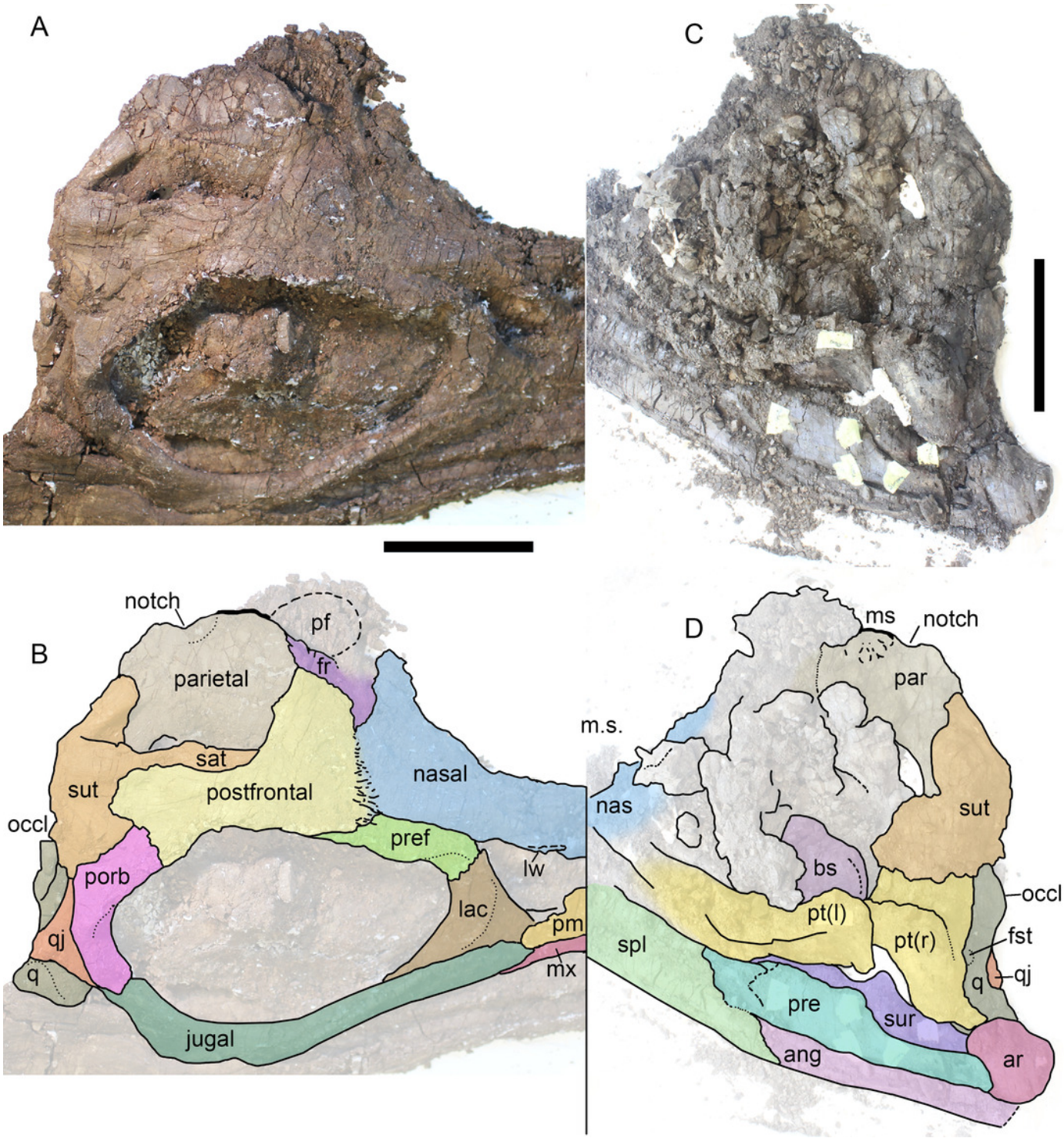
A
C
B
D
notch
pf
fr
parietal
sat
sut
postfrontal
nasal
occl
pref
porb
lw
lac
pm
qj
mx
q
jugal
ms
notch
par
m.s.
nas
sut
bs
occl
pt(l)
pt(r)
fst
spl
q
qj
pre
sur
ang
ar

Figure 16

Opisthotic and stapes of *Arthropterygius lundi* PMO 222.654.

(A–G) Opisthotic in anterior (A), posterior (B), dorsal (C), ventral (D), lateral (E) and medial (F, G) views. (H–L) Left stapes in, posterolateral (H), ventral (I), dorsal (J), distal (K) and medial (L) views. Abbreviations: am, ampulla; fbo, facet for the basioccipital; fbs, facet for the basisphenoid; fop, facet for the opisthotic; fst, facet for the stapes; hg, groove for transmission of hyomandibular branch of facial (VII) or glossopharyngeal (XI) nerve; hc, impression of horizontal semicircular canal; ipc, impression of posterior vertical semicircular canal; mr, muscular ridge on the opisthotic; sac, sacculus; ut, utriculus; vf, vagus foramen. Scale bar represents 5 cm.

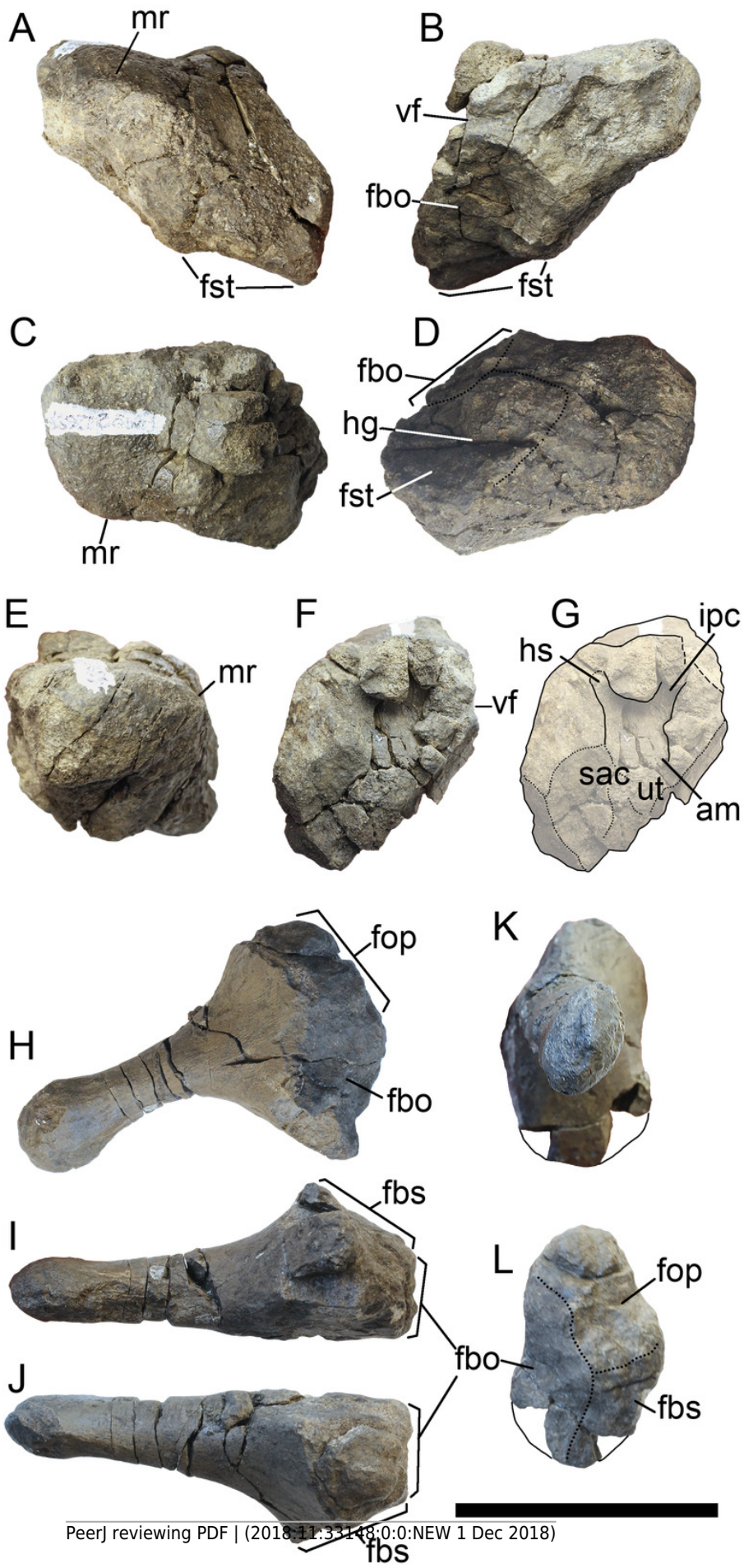
A
mr
fst
B
vf
fbo
fst
C
mr
D
fbo
hg
fst
E
mr
F
vf
G
ipc
hs
sac
ut
am
H
fop
fbo
K
I
fbs
fbo
L
fop
fbo
fbs
J
fbs

Figure 17

Forelimb and pectoral girdle elements of *Arthropterygius lundi*.

(A) Left coracoid of SGM 1731-01–15 in ventral view. (B, C) Left scapula of SGM 1731-01–15in lateral (B) and proximal (C) views. (D, E) Articulated right clavicle and scapula of PMO 222.654 in anterior (D) and posteromedial (E) views. (F, G) Interclavicle of PMO 222.654 in oblique posterolateral (F) and dorsal (G) views. (H–L) Left humerus of SGM 1731-01–15 in dorsal (H), ventral (I), anterior (J), distal (K) and proximal (L) views. (M) Articulated epipodial and autopodial elements of the left forelimb of SGM 1731-01–15. (N) Left forelimb of PMO 222.654 in dorsal view. (O, P) Left humerus of PMO 222.654 in proximal (O) and distal (P) views. (Q) Partially reconstructed pectoral girdle of PMO 222.654. Abbreviations: aae, anterior accessory epipodial element; acr, acromial process; atb, anterior transverse bar of the interclavicle; dpc, deltopectoral crest; faae, facet for the anterior accessory epipodial element; fcor, facet for the coracoid; fgl, glenoid contribution; fr, facet for the radius; fsc, facet for the scapula; fu, facet for the ulna; i, intermedium; mst, bulge in the middle of the interclavicle posterior median stem; pi, pisiform; r, radius; ra, radiale; td, dorsal process; u, ulna. Scale bars represent 10 cm.

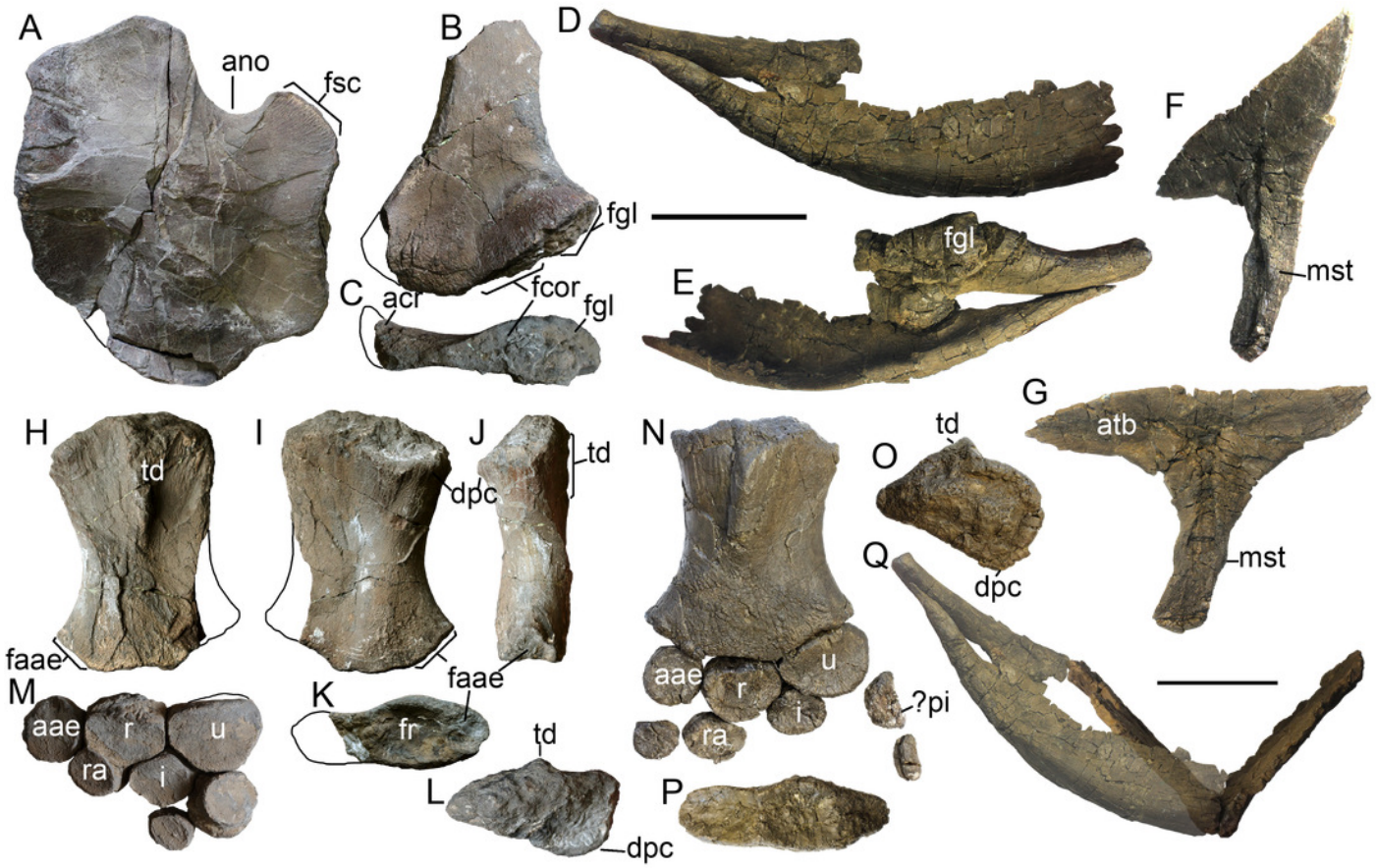
A
ano
fsc
B
fgl
C
acr
fcor
fgl
D
E
fgl
F
mst
G
atb
mst
H
td
faae
I
dpc
faae
J
td
K
fr
L
td
dpc
M
aae
r
u
ra
i
N
aae
r
u
i
ra
O
td
dpc
?pi
P
Q

Figure 18

Cranial elements of *Arthropterygius volgensis* KSU 982/P-213.

(A–E) Basisphenoid in ventral (A), dorsal (B), lateral (C), anterior (D) and posterior (E) views. (F, G, I, J) Left opisthotic in posterior (F), anterior (G), dorsal (I) and medial (J) views. (H, K) Right opisthotic in lateral (H) and ventral (K) views. (L–N) Left quadrate in posteromedial (L), anterolateral (M) and posterolateral (N) views. (O) Ventral view of the right quadrate. (P–R) Left parietal in dorsal (P), lateral (Q) and ventral (R) views; S, partial right parietal in dorsal view. (T–V) Right articular in medial (T), lateral (U) and dorsal (V) views. Abbreviations: am, ampulla; art.b, articular boss; dpl, dorsal plateau of the basisphenoid; fbo, facet for the basioccipital; ffr, facet for the frontal; fpof, facet for the postfrontal; fpt, facet for the pterygoid; fqj, facet for the quadratojugal; fst, facet for the stapes; hg, groove for transmission of hyomandibular branch of facial (VII) or glossopharyngeal (XI) nerve; hsc, impression of horizontal semicircular canal; icf, foramen for the internal carotid arteries; ich, impression of the cerebral hemisphere; iop, impression of the optic lobe; ipc, impression of posterior vertical semicircular canal; fsut, facet for the supratemporal; mr, muscular ridge on the opisthotic; occl, occipital lamella; sac, sacculus; sur.b, surangular boss; trab, facets for cartilaginous continuation of the *cristae trabeculares*; ut, utriculus; vf, vagus foramen; VII, groove of the palatine ramus of facial (VII) nerve. Scale bar represents 5 cm.

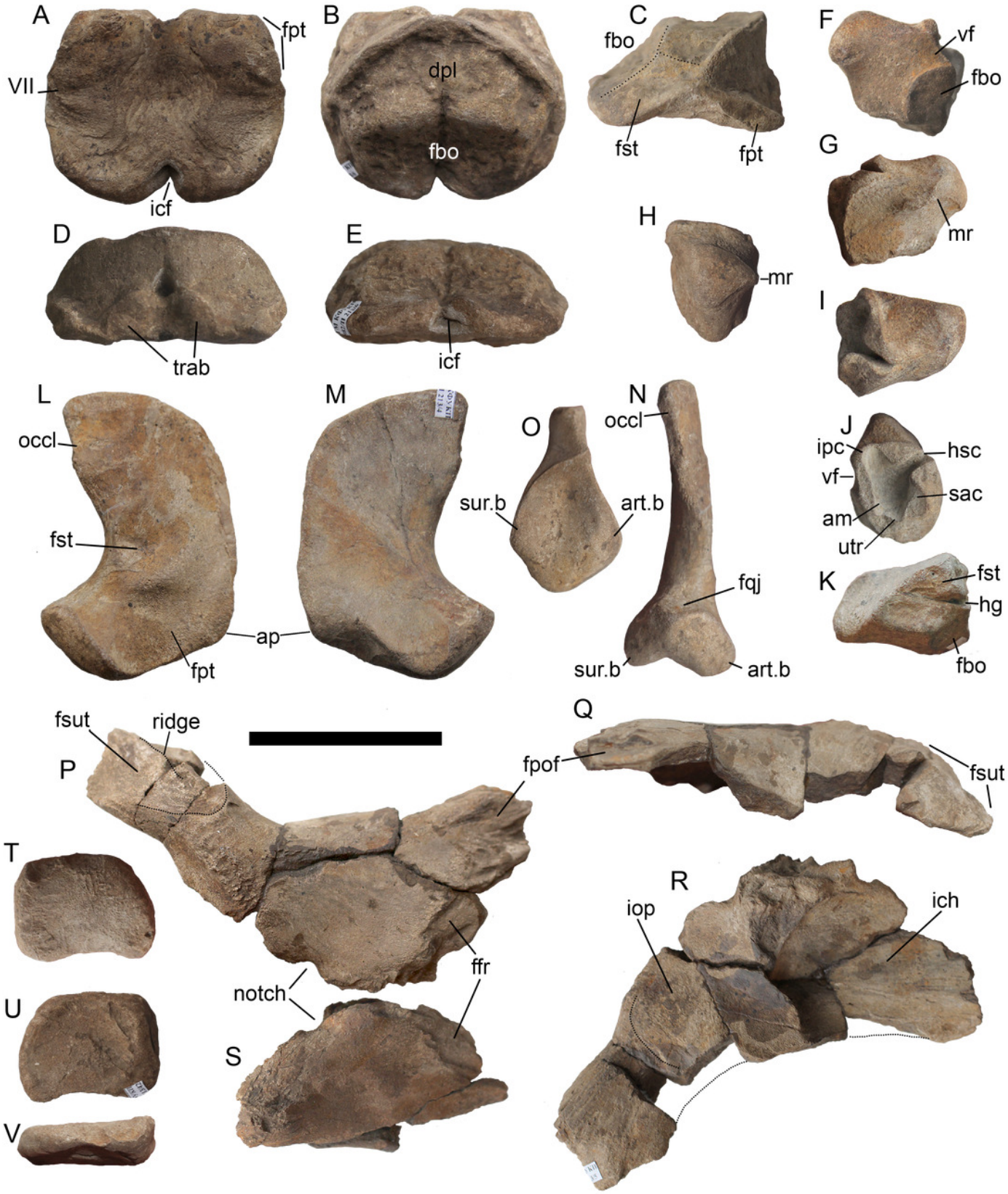
A
fpt
VII
icf
B
dpl
fbo
C
fbo
fst
fpt
F
vf
fbo
G
mr
D
trab
E
icf
H
mr
I
L
occl
fst
fpt
ap
M
O
sur.b
art.b
N
occl
fqj
sur.b
art.b
J
ipc
hsc
vf
sac
am
utr
K
fst
hg
fbo
fsut
ridge
P
fpof
Q
fsut
T
U
V
S
notch
ffr
R
iop
ich

Figure 19

Pectoral girdle elements and femur of *Arthropterygius volgensis* KSU 982/P-213.

(A) Left coracoid in dorsal view. (B–D) Right coracoid in ventral (B), dorsolateral (C) and ventromedial (D) views. (E) Articulated coracoids in anterior view. (H) Fragmentary clavicles. (F, G) Fragmentary right scapula in mediall (F) and proximal (G) views. (H, I) Interclavicle in dorsal (H) and ventral (I) views. (J–M) Right femur in ventral (J), dorsal (K), anterior (L) and distal (M) views. A portion of the right coracoid that is currently missing (B) is modified from Kasansky (1903, Tab. II, fig. 6). Abbreviations: acr, acromial process; amp, anteromedial process of the coracoid; ano, anterior notch; ffi, facet for the fibula; fgl, glenoid contribution; fsc, facet for the scapula; fti, facet for the tibia. Scale bars represent 10 cm.

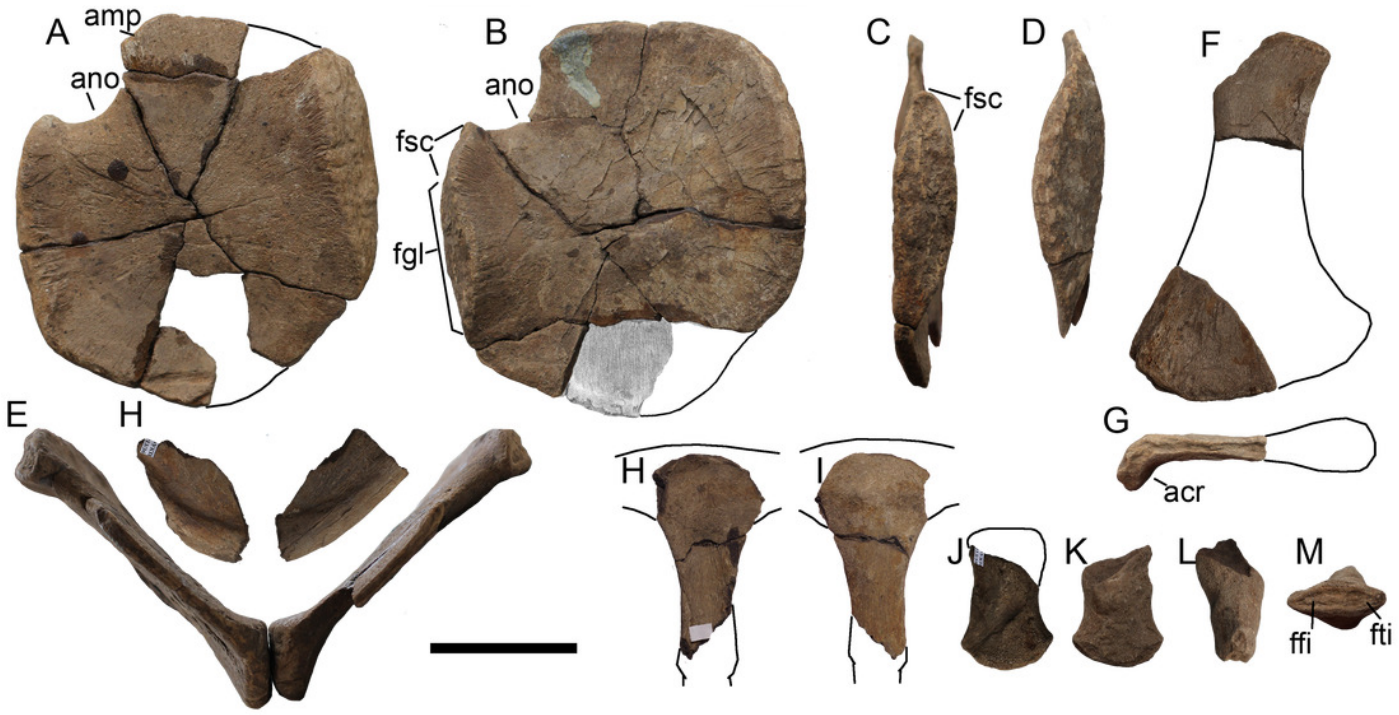

Figure 20

Comparison of basisphenoids of *Arthropterygius*.

(A) Juvenile of *A. chrisorum* CCMGE 3-16/13328. (B) Young adult of *A. chrisorum* CCMGE 17-44/13328 (take into consideration strong deformation of this specimen). (C) Young adult of *Arthropterygius* cf. *A. chrisorum* SGM 1743-2 (basipterygoid processes are slightly eroded). (D) Mature individual of *A. chrisorum* CMN 40608. (E) Juvenile of *A. volgensis* KSU 982/P-213. (F) Mature individual of *A. lundi* SGM 1502. Respective views are indicated with the same numbers: 1, anterior view; 2, ventral view; 3, dorsal view; 4, lateral view. D2 and D3 are modified from (Maxwell 2010), D1 and D4 are provided by E. Maxwell and J. Mallon (pers. comm. 2015).

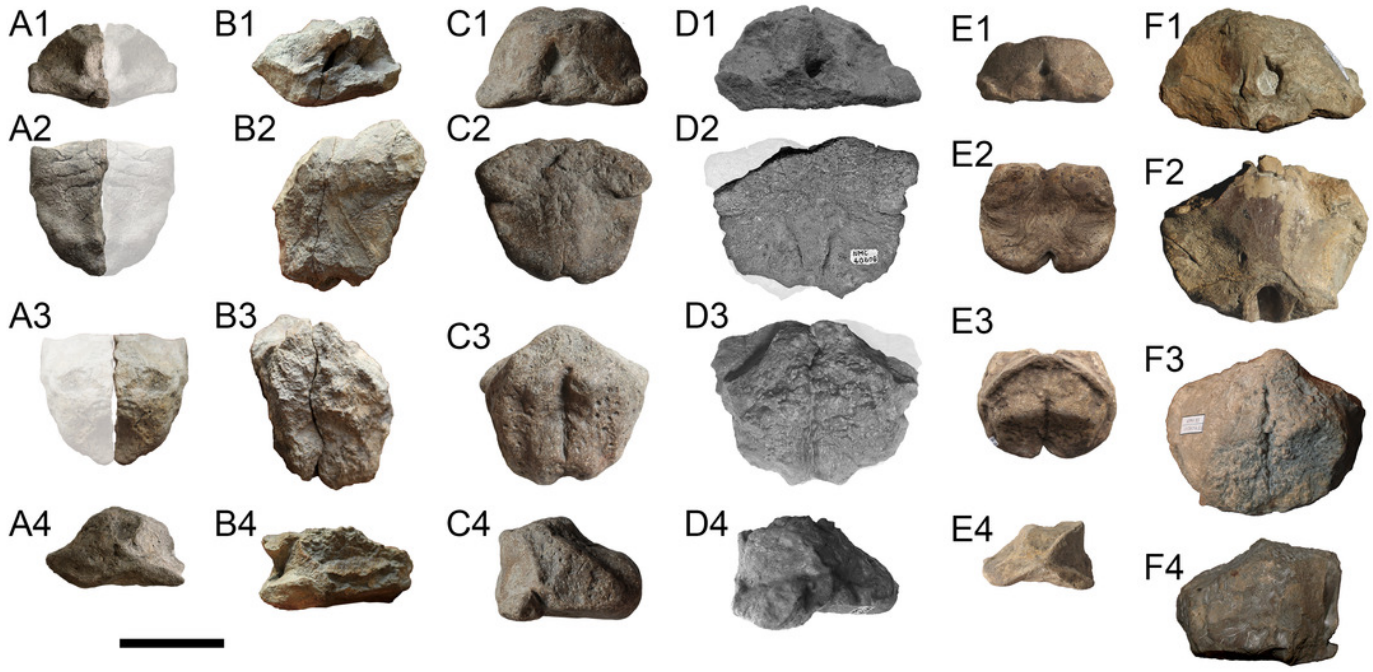

Figure 21(on next page)

Phylogenetic position of *Arthropterygius*.

(A) Strict consensus recovered from the analysis of the full dataset. (B) Strict consensus recovered from the analysis of the reduced dataset. Bremer support values > 1 are shown above the branches; bootstrap/jackknife support values of greater than 20 are indicated below the branches. *Abbreviations*: A, *Arthropterygius* clade; N, *Nannopterygius* clade; O, Ophthalmosaurinae; P, Platypterygiinae.

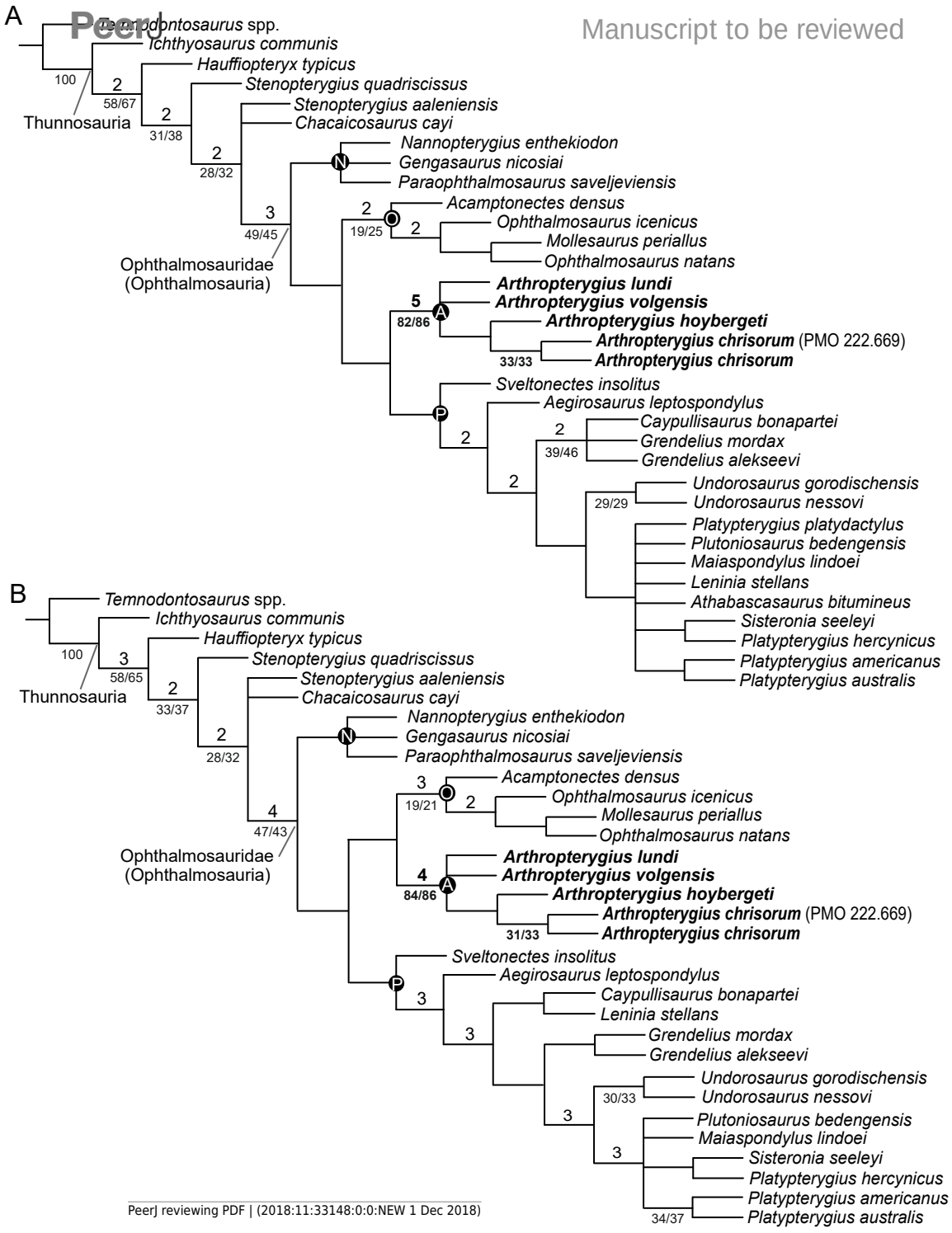
A
Temnodontosaurus spp.
Ichthyosaurus communis
Hauffiopteryx typicus
Stenopterygius quadriscissus
Stenopterygius aaleniensis
Chacaicosaurus cayi
Nannopterygius enthekiodon
Gengasaurus nicosiai
Paraophthalmosaurus saveljeviensis
Acamptonectes densus
Ophthalmosaurus icenicus
Mollesaurus periallus
Ophthalmosaurus natans
Arthropterygius lundi
Arthropterygius volgensis
Arthropterygius hoybergeti
Arthropterygius chrisorum (PMO 222.669)
Arthropterygius chrisorum
Sveltonectes insolitus
Aegirosaurus leptospondylus
Caypullisaurus bonapartei
Grendelius mordax
Grendelius alekseevi
Undorosaurus gorodischensis
Undorosaurus nessovi
Platypterygius platydactylus
Plutoniosaurus bedengensis
Maiaspondylus lindoei
Leninia stellans
Athabascasaurus bitumineus
Sisteronia seeleyi
Platypterygius hercynicus
Platypterygius americanus
Platypterygius australis
Thunnosauria
Ophthalmosauridae
(Ophthalmosauria)
100
2
58/67
2
31/38
2
28/32
3
49/45
2
19/25
2
5
82/86
33/33
2
39/46
2
29/29
B
Temnodontosaurus spp.
Ichthyosaurus communis
Hauffiopteryx typicus
Stenopterygius quadriscissus
Stenopterygius aaleniensis
Chacaicosaurus cayi
Nannopterygius enthekiodon
Gengasaurus nicosiai
Paraophthalmosaurus saveljeviensis
Acamptonectes densus
Ophthalmosaurus icenicus
Mollesaurus periallus
Ophthalmosaurus natans
Arthropterygius lundi
Arthropterygius volgensis
Arthropterygius hoybergeti
Arthropterygius chrisorum (PMO 222.669)
Arthropterygius chrisorum
Sveltonectes insolitus
Aegirosaurus leptospondylus
Caypullisaurus bonapartei
Leninia stellans
Grendelius mordax
Grendelius alekseevi
Undorosaurus gorodischensis
Undorosaurus nessovi
Plutoniosaurus bedengensis
Maiaspondylus lindoei
Sisteronia seeleyi
Platypterygius hercynicus
Platypterygius americanus
Platypterygius australis
Thunnosauria
Ophthalmosauridae
(Ophthalmosauria)
100
3
58/65
2
33/37
2
28/32
4
47/43
3
19/21
2
4
84/86
31/33
3
3
30/33
3
3
34/37

Figure 22 (on next page)

Results of Principal Component Analysis of ophthalmosaurid humeral morphology

(A) A plot of PC1-PC2. (B) A plot of PC1-PC3. (C) A plot of PC1-PC4. (D) A plot of PC2-PC3.

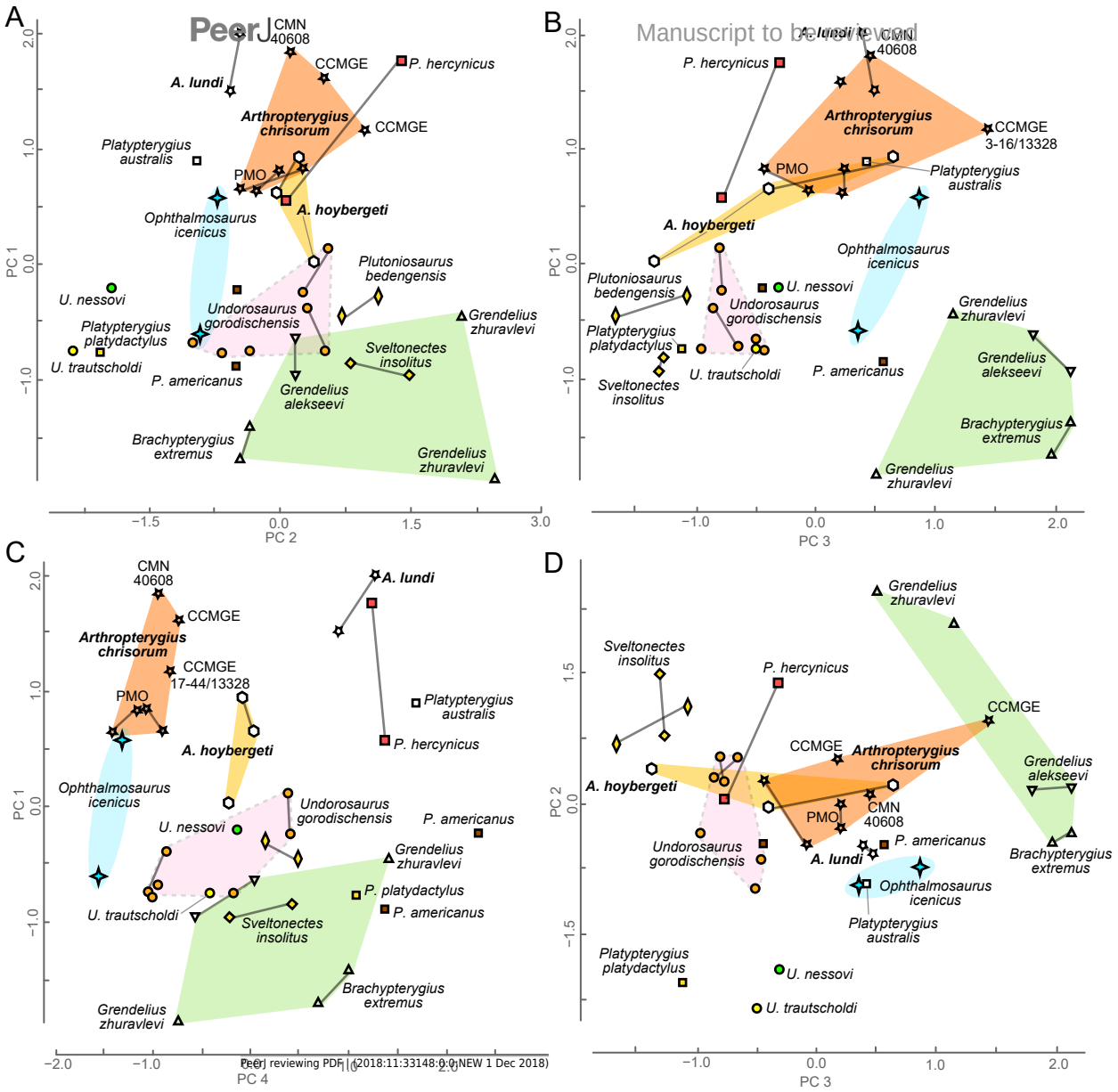

Figure 23(on next page)

Palaeogeographic maps for the Kimmeridgian – early Middle Volgian (*Dorsoplanites panderi* Chron) time interval and Middle Volgian (*Virgatites virgatus* Chron) – Late Volgian (late Tithonian to early Berriassian time interval), showing the distri

Abbreviations: N – representatives of *Nannopterygius* clade; G – possible *Grendelius*.

Reconstruction is modified from Zakharov *et al*. 2014.